Investigation of intracranial pharmacotherapy in Genetic Absence Epilepsy Rats from Strasbourg (GAERS) – a potential strategy to overcome the limitations of the standard treatment in epilepsy

Dissertation

zur Erlangung des Doktorgrades der

Mathematisch-Naturwissenschaftlichen Fakultät der

Christian-Albrechts-Universität zu Kiel

vorgelegt von

Anna-Sophia Buschhoff

Kiel, Juli 2020

Erster Gutachter: Prof. Dr. Peer Wulff
Zweite Gutachterin: Prof. Dr. Regina Scherließ

Tag der mündlichen Prüfung: 28. September 2020

I Abstract

Epilepsy is a chronic disorder of the brain and affects approximately 50 million people worldwide. It is, thus, one of the most common neurological diseases (World Health Organization, 2006). The main approach of epilepsy treatment is systemic drug application. The central nervous system (CNS), however, is a particularly challenging target for drug delivery. Systemic drug therapy is limited by the blood-brain-barrier (BBB), restricting the distribution of pharmaceuticals into the CNS. One approach to by-pass the BBB is intrathecal (IT) administration of anti-epileptic drugs with direct application of substances into the cerebrospinal fluid (CSF). This study aimed to investigate whether IT application of anticonvulsant substances is a reasonable approach to treat epilepsy. The in-depth evaluation of IT drug application was performed in the genetic absence epilepsy rats from Strasbourg (GAERS). Seizures in GAERS rats closely resemble human absence seizures and can be detected as characteristic spike-and-wave discharges (SWDs) in the electroencephalogram (EEG). To quantify seizure occurrence in GAERS and assess the efficacy of anti-epileptic therapy, automated seizure detection based on EEG recordings was implemented. With this method, seizure detection was performed with an F-score of 96 %.

The analysis of 12h and 24h recordings in untreated animals revealed circadian undulations of SWD activity with a peak of seizures between 2am and 4am. This observation was in agreement with earlier studies that showed that SWD activity depends on the vigilance level in rats (Drinkenburg et al., 1991).

By intracerebroventricular (i.c.v.) injections, drug application into the CSF was archived. To this end, a guide cannula was implanted into the right lateral ventricle. Initially, the standard anti-absence drugs, ethosuximide (ETX), and valproate (VPA) (Manning et al., 2003), were tested with this IT application approach. The treatment caused a substantial and dose-dependent reduction in SWD for both drugs and revealed that localized therapy with ETX is significantly more effective than with VPA. Additionally, the i.c.v. administration of ETX was dramatically more efficient than systemic ETX application of the same dose. The subsequent analysis of substance distributions in the brain after intracranial application suggested that the therapeutic effect was not caused by the indirect entry of ETX into brain parenchyma via the bloodstream but rather mediated by the direct entry from the CSF.

Additional experiments to explore the therapeutic efficacy of the neuropeptides Neuropeptide Y (NPY) and Somatostatin (SST) as potential alternative to standard drugs, did not reveal a robust anti-absence effect. Consequently, these neuropeptides were not considered potent substances for localized drug therapy in absence epilepsy.

II Zusammenfassung

Epilepsie ist mit etwa 50 Millionen betroffenen Menschen weltweit eine der häufigsten Funktionsstörungen des Gehirns (World Health Organization, 2006). Die neurologische Erkrankung ist gekennzeichnet durch wiederkehrende epileptische Anfälle, die häufig durch eine systemische medikamentöse Therapie behandelt werden können. Eine große Herausforderung der systemischen Therapie ist allerdings der Transport von Wirkstoffen in ihr Zielgebiet, da das zentrale Nervensystem (ZNS) durch die Blut-Hirn-Schranke geschützt wird. Durch die hohen Serumkonzentrationen, die notwendig sind, damit eine therapeutische Konzentration im Gehirn erreicht werden kann, kann es zu peripheren Nebenwirkungen kommen. Eine Möglichkeit die Blut-Hirn-Schranke zu umgehen, ist die direkte Injektion von antiepileptischen Wirkstoffen in den Liquorraum, die sogenannte intrathekale Applikation (IT-Applikation).

In der vorliegenden Arbeit wurde untersucht, ob die IT-Applikation von antiepileptischen Wirkstoffen eine mögliche Alternative zur systemischen Epilepsietherapie darstellen kann.

Hierzu wurde die lokale Applikation verschiedener Wirkstoffe in einem Modellorganismus für Abcense-Epilepsie, den *genetic absence epilepsy rats from Strasbourg* (GAERS), getestet. Die Tiere zeigen Anfälle, die sich durch Spike-Wave-Aktivität (SWD) im EEG manifestieren. Anhand der Anfallshäufigkeit der Tiere kann die Wirksamkeit einer Therapie bewertet werden. Zu diesem Zweck wurde eine automatische computerunterstützte Detektion von Anfällen implementiert.

Mittels einer Kanüle im rechten lateralen Ventrikel (intracerebroventrikulär – i.c.v.) der Tiere konnten Wirkstoffe direkt in den Liquor appliziert werden. Untersucht wurden unter anderem die Wirkstoffe erster Wahl für Absence-Epilepsie, Valproat (VPA) und Ethosuximid (ETX). Für beide Medikamente konnte eine starke konzentrationsabhängige antiepilepitische Wirkung nach i.c.v. Therapie nachgewiesen werden. Das Medikament ETX zeigte eine stärkere sowie länger anhaltende Wirkung im Vergleich zu VPA. Darüber hinaus war die lokale Therapie mit einer geringen Dosis von ETX signifikant effektiver in der Behandlung epileptischer Anfälle als die systemische Therapie mit der gleichen Medikamentendosis.

Durch Untersuchungen zur Substanzverteilungen im ZNS, konnte die Annahme bestätigt werden, dass die therapeutische Wirkung nicht durch den indirekten Eintritt von ETX in das Gehirnparenchym über den Blutkreislauf verursacht wird, sondern durch den direkten Eintritt ins Gehirn aus dem Liquor.

Des Weiteren wurden die Neuropeptide Neuropeptid Y (NPY) und Somatostatin (SST) auf ihre antiepileptische Wirkung nach i.c.v. Gabe getestet. Neuropeptide sind attraktive, potenzielle Alternativen zu den klassischen Antiepileptika, da sie als endogene Neuromodulatoren schon in sehr geringen Konzentrationen wirksam sind. Die lokale Applikation der Neuropeptide NPY und SST zeigte jedoch bei GAERS-Ratten keine antiepileptische Wirkung. Daher wurden die getesteten Neuropeptide für eine lokalisierte medikamentöse Therapie von Abcense-Epilepsie nicht weiter in Betracht gezogen.

III Contents

IV List of abbreviations

AED…… *antiepileptic drug*
AGII…… *Angiotensin II*
am…… *ante meridiem*
AP…… *anteroposterior*
BBB…… *blood-brain-barrier*
cf. …… *compare*
CNS…… *central nervous system*
CP…… *choroid plexus*
CSF…… *cerebrospinal fluid*
e.c.d. …… *epidural cup*
e.g. …… *exempli gratia*
EEG…… *electroencephalogram*
ETX…… *ethosuximide*
FG…… *fast green*
FN…… *false negative*
FP…… *false positive*
GABA…… *γ-aminobutyric acid*
GAERS…… *Genetic Absence Epilepsy Rat from Strasbourg*
h…… *hour*
HET…… *hyperexcitability test*
HPLC…… *high-performance liquid chromatography*
i.c.v. …… *intracerebroventricular*
i.e. …… *id est*
i.p. …… *intraperitoneal*
i.v. …… *intravenous*
I_h…… *h-currents*
ILAE…… *International League Against Epilepsy*
ISF…… *interstitial fluid*
I_t…… *transient Ca^{2+} current*
IT…… *intrathecal*
LV…… *lateral ventricle*

min……*minutes*
ML……*mediolateral*
NPY……*neuropeptide Y*
NREM……*non-rapid eye movement*
NRT……*reticular thalamic nucleus*
OF……*open field*
pm……*post meridiem*
REM……*rapid-eye-movement*
s……*seconds*
s.c. ……*subcutaneous*
S1……*primary somatosensory*
S2……*secondary somatosensory*
SAS……*subarachnoid space*
SEM……*standard error of the mean*
SST……*Somatostatin*
SWD……*spike-and-wave discharge*
TC……*thalamocortical neurons*
T-channels……*low-threshold T-type Ca^{2+} channels*
TN……*true negative*
TP……*true positive*
VB……*ventrobasal*
VPA……*valproate*

V List of figures

1 Introduction

1.1 Epilepsy – a disorder of the central nervous system

Epilepsy is a chronic disorder of the brain and affects approximately 50 million people worldwide. It thus is one of the most common neurological diseases (World Health Organization, 2006). Spontaneous, transient, and periodic recurring seizures caused by aberrant changes in the neural activity, are a hallmark feature of epilepsy.

The causes of epilepsy are manifold, and the International League Against Epilepsy (ILAE) classified 2017 the etiologies into six main categories: structural, genetic, infectious, metabolic, immune, or unknown.

Moreover, epilepsies show a variety of clinical manifestations with many distinct seizure types. On that basis, the ILAE proposed a standardized classification of epileptic seizures (fig. 1.1). The classification of seizures can be essential to understand the causes underlying epileptic attacks and to develop treatment strategies (Scheffer et al., 2017). Seizures can be focal or generalized, determined by the origin of seizure onset. Though the origin of onset remains unknown in some cases.

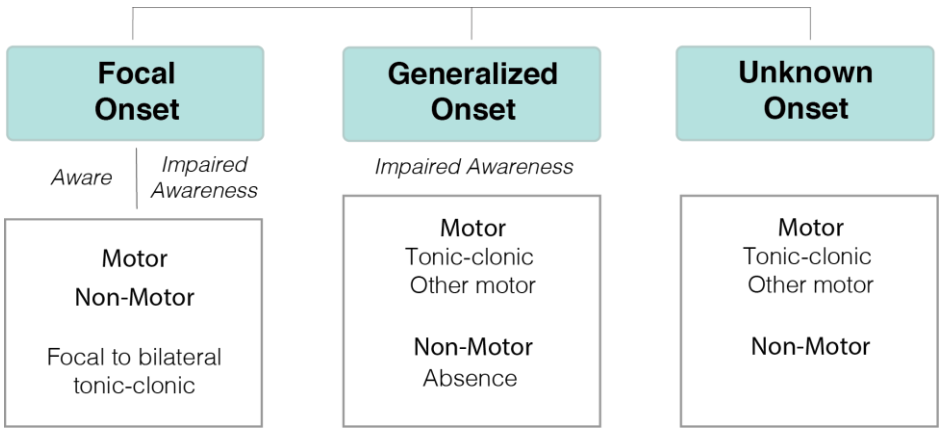

Figure 1.1: Types of epileptic seizures
The panel is adapted from the basic ILAE 2017 classification of seizure types (Scheffer et al., 2017). Seizures can be grouped into three main seizure types depending on their onset: focal, generalized, and unknown.

In generalized seizures the abnormal electrical activity instantly spreads over both hemispheres of the brain, whereas focal seizures originate in small groups of neurons and are restricted to one hemisphere. The symptoms in focal seizures depend on the affected brain areas and the seizures are not necessarily accompanied by an alteration of consciousness. In contrast to that a complete loss of awareness is a typical feature in generalized seizures. The main subtypes of generalized seizures are absence (petit mal) and tonic–clonic seizures (grand mal). Absence seizures do not show motor symptoms, but tonic-clonic seizures can be accompanied by spasms, shaking, stiffening, and the loss of muscle tone. Generalized seizures constitute nearly one-third of all epilepsies (for a review see Panayiotopoulos, 2005).

1.2 Absence Epilepsy and the thalamocortical circuit

Absence seizures are the prototype of generalized and non-convulsive seizures and are a typical feature of absence epilepsy. This type of epilepsy is one of the most common forms of childhood epilepsy, and approximately 7 per 100.000 children under the age of 15 are affected yearly (Olsson, 1988). Absence epilepsy is suggested to have a multifactorial genetic etiology. The precise identification of the genetic causation underlying the disease is not resolved yet. However, gene mutations associated with the γ-aminobutyric acid type A ($GABA_A$) receptor and mutations in the T-type calcium channel gene *CACNA1* have been found in patients with childhood absence epilepsy (Liang et al., 2006; Wallace et al., 2001).

The seizures start between three and eight years of age, and around 70% of the affected children show spontaneous remission around adolescence. Patients with absence epilepsy can suffer from up to 200 seizures per day. The typical absence seizures are characterized by sudden seizure onset and termination, accompanied by brief impairment of consciousness and behavioral arrest. Furthermore, absence seizures are associated with characteristic synchronized ~3 Hz spike-and-wave discharge (SWD), which can be detected in the electroencephalogram (EEG) (Crunelli and Leresche, 2002; Lockman, 1989; Manning et al., 2003).

A dysfunctional interplay between thalamic and cortical structures appears to promote the emergence and maintenance of absence seizures (Lüttjohann and van Luijtelaar, 2015; Steriade, 1990). The thalamus is a subcortical structure, that is critical for relaying sensory information from the periphery to specific areas of the cerebral cortex. Additionally, extensive reciprocal thalamocortical connections are crucial for the

generation of sleep-related but possibly also paroxysmal oscillations in the cortex (Beenhakker and Huguenard, 2009; McCormick and Bal, 1997). The principal thalamocortical circuit is formed by three sets of neurons: inhibitory neurons in the reticular thalamic nucleus (NRT), excitatory thalamocortical neurons (TC) in the dorsal thalamic nucleus, and excitatory pyramidal cortical cells (fig. 1.2) (Sherman and Guillery, 1996).

The NRT is an essential source for intra-thalamic inhibition. Its neurons contain the inhibitory neurotransmitter γ-aminobutyric acid (GABA) (for review see Halassa and Acsády, 2016). NRT neurons send inhibitory projections to TC neurons but receive glutamatergic excitatory input from both the thalamus and cortex (Jones, 1975; Pinault et al., 1997). The NRT is interconnected by inhibitory GABAergic synapses but also via electrical coupling through gap junctions and thus can precisely modulate the scale of thalamic inhibition (Landisman et al., 2002). The NRT, which provides both feed-forward and feed-back inhibition to TC neurons, is consequently an essential modulator for the thalamocortical information flow (fig. 1.2B).

TC neurons exhibit two distinct firing modes, known as tonic and burst firing (fig. 1.2C)(Ramcharan et al., 2000; Sherman, 2001). The switch between these firing modes depends on the activation state of low-threshold T-type Ca^{2+} channels (T-channels) and is underlying various vigilance and sleep stages (Crunelli et al., 2014). T-channels are prominently expressed in the thalamus and are encoded by genes from the Ca_v3 family (for review see Chen et al., 2014). Tonic firing occurs at the membrane resting potential during which T-channels are inactive. In this mode, TC neurons respond to external stimuli with unitary action potentials.

In contrast, burst firing requires a hyperpolarization of TC cells below approximately -65 mV, which de-inactivates the T-channels. Hyperpolarization-activated channels (e.g. HCN-channels) promote cationic currents known as the h-currents (I_h), which can depolarize the cells again (McCormick and Bal, 1997). A sufficient depolarization will than activate Ca^{2+} inward currents (I_t), leading to a low threshold spike, which triggers the burst of several, fast action potentials at a certain threshold (McCormick and Bal, 1997; Zhan et al., 2000). Thus, NRT mediated inhibition effectively activates TC neurons by promoting post-inhibitory rebound burst firing. As a consequence, the activity is transmitted back to NRT and the cortex, which causes a recurring excitatory cycle generating thalamocortical oscillations.

Several studies associate the presence of post-inhibitory rebound burst firing in TC neurons with the generation and/or maintenance of absence seizures (Huntsman, 1999; von Krosigk et al., 1993). This view is supported by the observation of increased SWD duration in a rat model of absence epilepsy, through microinjection of γ-vinyl-GABA, an irreversible inhibitor of GABA transaminase into the thalamic relay nucleus. In contrast, the local activation of GABA transmission in the NRT significantly suppressed seizure activity (Liu et al., 1991). Moreover, Sorokin et al. (2017) have used optogenetic methods, both *in vitro* and *in vivo*, to artificially switch between tonic and burst firing modes in TC neurons in an absence epilepsy model. Their findings indicate that synchronous burst firing of TC neurons is required for the emergence of absence seizures.

However, other studies contradict this view by showing largely paused TC burst activity during SWDs (Pinault et al., 1998; Steriade and Contreras, 1995). Based on *in vivo* unit recordings in freely moving rats McCafferty et al. (2018) recently demonstrated, that ictal burst firing of TC neurons is reduced, and instead, tonic firing is elicited during absence seizures. Furthermore, they state that the blockage of T-channels in TC neurons had no effect on seizures activity, while the same blockage in cortex and NRT suppresses SWDs.

The relative contribution and interactions of thalamocortical structures, underlying SWD generation, and maintenance remains controversially debated. However, over the last years, it has come to the fore, that absence seizures are initiated in the cortex, specifically in the primary somatosensory (S1) cortex (for review see Meeren et al., 2005). This “cortical focus theory” was inspired by the finding of Meeren et al. (2002), that SWDs always started in the cortex, leading the thalamus. The study was based on electrophysiological recordings in a rat model of absence epilepsy.

The hypothesis of an epileptic focus in the S1 cortex could be supported by pharmacological studies (cf. Chapter 1.4) (Meeren et al., 2002; Polack et al., 2009; Sitnikova and van Luijtelaar, 2004) and further analysis of the spatiotemporal properties of network oscillations during epileptic activity (Meeren et al., 2002; Polack et al., 2007).

Moreover, human studies also revealed a critical role of the cortex in the generation of SWDs (Holmes et al., 2004). Although the cortex is still the most probable site of seizure

emergence, the thalamus is proposed to be crucial for maintenance and termination of SWDs (Lüttjohann and van Luijtelaar, 2015).

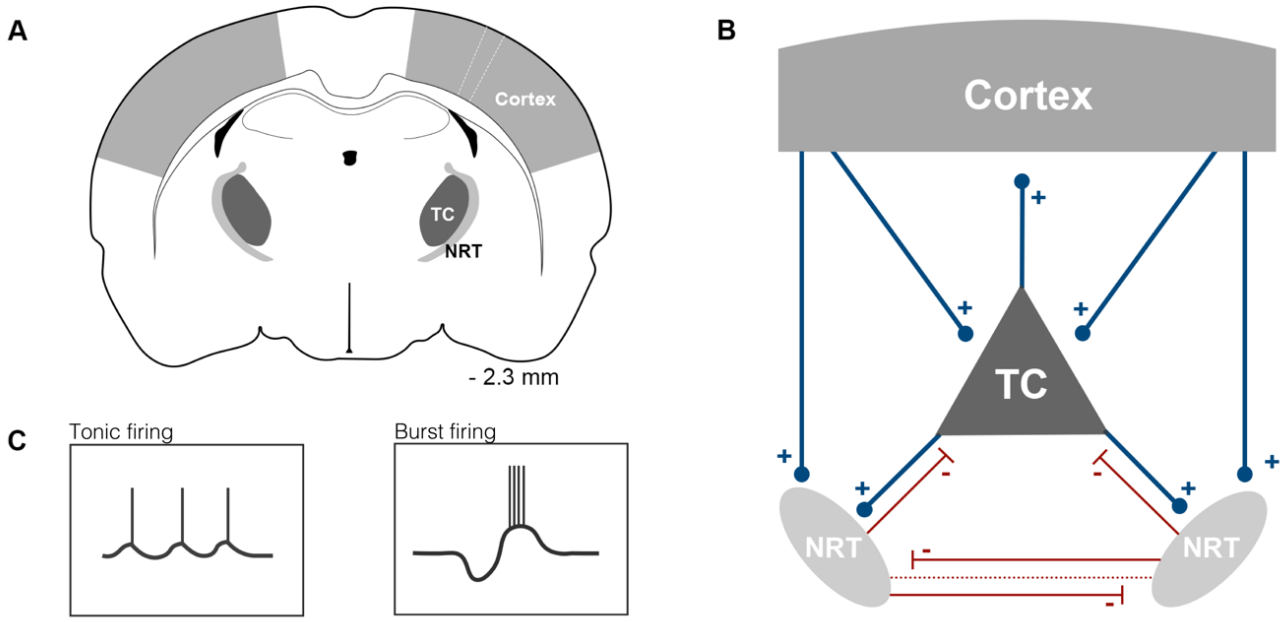

Figure 1.2: Cortico-thalamo-cortical interactions underlying SWDs
A) Schematic representation of a coronal brain section of a rat illustrating the brain areas relevant for the emergence and maintenance of SWDs. NRT, nucleus reticularis thalami; TC, thalamo-cortical neurons of the dorsal thalamus; Cortex, primary somatosensory cortex. Coordinates are adapted from the atlas of Paxinos and Watson (Paxinos and Watson, 2006) with bregma as a reference. B) Model of the cortico-thalamo-cortical network consisting of excitatory thalamocortical (TC) and inhibitory reticular thalamic nucleus (NRT) neurons in the thalamus and excitatory pyramidal cells in the cortex. Most probably, SWDs are generated in cortical areas. The thalamus is proposed to tip the system over towards a pro epileptic state and function as a resonator in SWD maintenance. C) Characteristic patterns of tonic and burst firing in TC neurons.

1.3 The Genetic Absence Epilepsy Rat from Strasbourg – an established model for absence epilepsy

Several of the key findings regarding the pathomechanisms of absence epilepsy were obtained in genetic rodent models. One of the most commonly used and best established models in experimental studies on this type of epilepsy is the Genetic Absence Epilepsy Rat from Strasbourg (GAERS) (for review see Depaulis et al., 2016 and Marescaux et al., 1992). The other well-established model in absence epilepsy research is the WAG/Rij rat, and both models show similar characteristics (for a review see Coenen and van Luijtelaar, 2003).

The GAERS strain was first described in 1982 by (Vergnes et al., 1982). The group observed that around thirty percent of their Wistar rats colony developed spontaneous seizures, which closely resemble human absence seizures. In line with findings of genetic data from human patients, a functional mutation of the *Cacna1h* gene encoding the $Ca_V3.2$ T-type Ca^{2+}-channel was identified in GAERS. This mutation results in faster recovery from T-channel inactivation and greater charge transference while high-frequency bursts (Powell et al., 2009).

During the seizures, the animals show subtle behavioral changes consisting mainly of behavioral arrest, which can be accompanied by rhythmic twitching of the vibrissae and jaw muscles. Besides that, the EEG of GAERS displays bilateral synchronous SWDs over the entire cortex, closely resembling the human SWDs characteristics. The seizure amplitudes vary between 300 – 1000 μV, and the seizure duration can last up to 60 seconds. However, it is interesting to note that the mean frequency of the SWDs in GAERS is in the range of 7 – 11 Hz, whereas classical SWD complexes in humans show frequencies around 3 Hz.

The occurrence of SWDs depends on the vigilance level of the rats. Accordingly, seizure activity predominantly occurs during passive wakefulness and somnolence, while SWDs are sporadic during active wakefulness, slow-wave, and paradoxical (rapid-eye-movement, REM) sleep (Drinkenburg et al., 1991; Van Luijtelaar and Coenen, 1988). The modulating impact of vigilance on the SWD-frequency has also been observed in humans (Kellaway et al., 1980). The relative age of manifestation and the dynamics of progression of the disease however differ between GAERS and humans. Whereas in humans absence seizures start at an early age (3 – 8 years of age) and usually disappear with puberty, absence seizures in GEARS progressively mature over a period of several months postnatally. Only after about four months all rats show SWDs. After six months

the maximum number of seizures is reached and will then persist over the lifetime of the rat.

A great advantage of the GAERS model is the nearly identical pharmaceutic profile with humans. The relatively easy monitoring and detection of epileptic brain activity combined with the predictive validity of GAERS makes it an excellent model to study novel therapeutic strategies in absence epilepsy.

1.4 Ethosuximide and valproate in the treatment of absence epilepsy.

Antiepileptic drugs (AEDs) are the mainstay of epilepsy treatment, whereas 25 – 30 % of the patients with epilepsy are pharmacoresistant (World Health Organization, 2006). Pharmacoresistance describes the condition, in which epileptic seizures cannot or can only be controlled partially by AEDs. A detailed definition of drug-resistant epilepsy was introduced in 2010 by the ILAE (Kwan et al., 2010). Non-pharmacological treatment options include resection surgeries, vagus-nerve stimulation, or a ketogenic diet. However, the non-pharmacological therapy is only feasible and successful in few selected cases (for a review see Kwan et al., 2011).

Over the last decades ethosuximide (ETX) and valproate (VPA) have been the drugs of choice in childhood absence epilepsy. The drugs topiramate, levetiracetam, and lamotrigine also show anti-absence efficacy in humans and GAERS (for a review see Manning et al., 2003). However, because of a lower efficacy, safety, and tolerability compared to ETX and VPA, they are clinically less relevant (Glauser et al., 2010). Moreover, other substances such as carbamazepine, vigabatrin, and gabapentin, which are highly effective drugs in the treatment of other forms of epilepsy, have an aggravating effect on seizures activity in both humans suffering from absence epilepsy but also GAERS. Commonly, drugs that facilitate the action of the inhibitory transmitter GABA show very good therapeutic efficiency in the treatment of various forms of epilepsy, as they increase chloride influx or potassium outflux and thus tend to hyperpolarize neurons. However, these drugs appear to exacerbate SWD appearance, which supports the view that absence epilepsy is perhaps related to a predominance of inhibitory activity (cf. Chapter 1.2).

Ethosuximide

Ethosuximide (2-ethyl-2-methylsuccinimide; ETX) was introduced in the 1950s and has since been considered first-line therapy in absence epilepsy (Zimmerman and Burgemeister, 1958). ETX is one out of three succinimides (ethosuximide, methsuximide and phensuximide) showing anticonvulsant activity, whereas ETX produces the greatest efficacy against absence seizures and is relatively well-tolerated (Browne, 1983). However, dose-dependent side effects related to the gastrointestinal tract, central nervous system, and hematopoiesis have been described (for a review see Gören and Onat, 2007). The apparent volume of distribution of ETX is about 0.7 L/kg in humans (Buchanan et al., 1969) and was found to be very similar in rodents (Bachmann et al., 1988). The volume of distribution is an estimate about how much of a drug distributes from the blood plasma into other body compartments. The larger the volume of distribution is, the more likely that the drug can distributes into the body tissues including the brain. Indeed, Patel et al. (1977) could show for ETX that it distributes homogenously throughout different brain areas in rats. Hepatic metabolism is the primary elimination route of ETX, and several metabolites with no significant activity have been reported (Millership et al., 1993). The elimination half-life of ETX in rodents ranges between 10 and 16 hours (Teschendorf and Kretzschmar, 1985) and in adult humans from 30 to 60 hours (Buchanan et al., 1969).

ETX has a narrow therapeutic profile, and the effect of the AED is selective for absence seizures. Until today the anti-absence mechanisms of ETX are not fully understood. In the classical view, ETX blocks I_t currents in TC neurons and therefore suppresses burst firing in these cells (Davies, 1995; White, 1999). This hypothesis is based on studies in brain slices of rats and guinea pigs, which showed a decrease of low-threshold calcium currents in thalamocortical neurons induced by therapeutically relevant ETX concentrations (0.2 – 0.75 mM) (Coulter et al., 1989; Macdonald, 1989). Later this could also be shown for NRT neurons (Huguenard and Prince, 1994). This explanation of the mode of action of ETX appeared to be sufficient, as the assumption that burst firing in TC neurons is crucial for the generation of pathological SWDs is widely accepted (cf. Chapter 1.2). However, other studies using the same recording method failed to detect the action of ETX on I_t currents. Instead, Leresche et al. (1998) claimed that suppressed burst activity rather results from a reduction of persistent Na^+ currents, and Ca^{2+}- activated K^+ currents in thalamic and cortical neurons.

In vivo studies revealed immediate and robust anti-absence action produced by ETX injection into the S1 cortex of GAERS. ETX injections in other cortical areas appeared to be less effective (Gülhan Aker et al., 2010; Manning et al., 2004). Indeed, microinfusions of ETX into the NRT and ventrobasal (VB) thalamus only partially decreased SWD after a time delay of approximately 30 minutes (Richards et al., 2003). The ventrobasal structure is strongly connected to the cortex via TC neurons (Sherman and Guillery, 1996). The outcome of these studies furthermore questions the thalamus as the exclusive site of action of ETX, though it supported the "cortical focus theory". A more recent study showed that ETX elevates synaptic inhibition in cortical areas by increasing spontaneous GABA release with no change in glutamate release. The authors thus concluded that cortical inhibition could contribute to the anti-absence effect of ETX (Greenhill et al., 2012).

A recent review by Brigo et al. (2019) aimed to determine the best choice of antiepileptic drugs in absence epilepsy by comparing clinical studies on the efficiency of valproate, ethosuximide, and lamotrigine. According to that, ETX represents the optimal initial monotherapy for patients suffering from absence seizures.

Valproate

Valproate (VPA) is a simple branched short-chain fatty acid, that was first synthesized by Burton in 1882. The drug's antiepileptic properties were discovered eighty years later (for a review see Löscher, 1999). VPA is also used in other neurological conditions such as migraine, neuropathic pain, or traumatic brain injuries (for a review see Romoli et al., 2019). The volume of distribution for VPA in rats is 0.66 L/kg (Löscher, 1999b), and the drug shows a rapid penetration into the brain (Lindberger et al., 2008). The elimination half-life of VPA in adult humans ranges from 9 to 18 hours (Löscher, 1978). Because of the relatively short elimination half-life of approximately two hours in rodents (Löscher, 1978), the anticonvulsant effects can be detected only for minutes or tens of minutes after application. Consequently, high doses of valproate are needed to evoke a more sustained suppression of seizures in animal models (Löscher, 2002). There are several routes of VPA metabolism in humans, and some metabolites of VPA exert anticonvulsant activity. However, the brain concentrations of these metabolites are too low to contribute to the drug's anticonvulsant effect significantly (Löscher, 1999b).
Although VPA is claimed to be a generally well-tolerated AED, several dose-related side effects have been described, such as weight gain, gastrointestinal, neurological, and metabolic disorders (for a review see Johannessen and Johannessen, 2003).

VPA is one of the drugs of choice for generalized absence seizures, but in contrast to ETX, VPA is highly effective in several seizures types such as absences, myoclonic, and generalized tonic-clonic seizures (Davis et al., 1994). As for ETX, the anti-absence mechanisms of action for VPA are not fully understood. However, a broad spectrum of antiepileptic properties has been proposed for VPA. Several studies demonstrated that VPA is enhancing the inhibitory activity of GABA by increasing its availability and facilitating GABA mediated responses (Chapman et al., 1982; Cunningham, 2003; Löscher, 1999b). Interestingly other drugs that potentiate the action of GABA appear to exacerbate the appearance of SWDs. However, enhanced GABAergic inhibition after valproate administration was found to be specific to particular brain areas such as the cerebral cortex (Frank Baldino and Geller, 1981), which would be in line with the therapeutic mechanisms proposed for ETX by Greenhill et al. (2012) (cf. Chapter 1.2).
A further antiepileptic mechanism of action of valproate appears to be an effect on ion channels. VPA has been shown to block Na^+-currents and repetitive firing in cortical neurons (McLean and Macdonald, 1986; Taverna et al., 1998). Moreover, Broicher et al., 2007 found that both VPA and ETX block I_T currents in isolated thalamic neurons. However, they reported that the effect of ETX is considerably more robust compared to VPA. Finally, if administered in high concentrations, VPA seems to increase the amplitude of the late potassium outward currents, which increases the threshold for epileptiform activity (Walden et al., 1993).

Serralta et al. (2006) revealed that acute intracerebroventricular (i.c.v.) injections of VPA (4.5mg/kg) suppressed seizures in a kindling epilepsy model. Though the treatment was accompanied by severe ataxia and, sedation. Furthermore, the duration of the effect did not exceed 15 minutes. Indeed, the study further showed that by continues i.c.v. infusion of VPA seizures could be controlled without producing obvious side effects.
In a neocortical rat epilepsy model, epileptiform activity was reduced through a cortical applied valproate releasing implant (Rassner et al., 2015). However, intracranial VPA application in absence epilepsy has to our knowledge not been described yet.

Finally, it has been shown that the combined treatment with ETX and VPA appeared to be infra-additive compared to the individual compounds in WAG/Rij rats (van Rijn et al., 2004), which could indicate that the two AEDs share some common cellular or molecular targets.

1.5 Neuropeptides in the treatment of absence epilepsy

Pathophysiological brain activity is initiated by an imbalance of excitatory and inhibitory activity in the brain. Neuropeptides are potent modulators of neuronal activity. They work through G-Protein-coupled receptors to modulate synaptic activity by adjusting neurotransmitter release or affecting ion channels, e.g., increasing potassium permeability or neurotransmitter receptors (Baraban and Tallent, 2004). Accordingly, neuropeptides are investigated as alternative anticonvulsant substances for the classical AEDs (for review see Kovac and Walker, 2013). Already one neuropeptide, the adrenocorticotropic hormone, is currently being used as a therapy for epilepsy (Mytinger and Joshi, 2012).

The term neuropeptide comprises a number of different endogenous peptidergic neuromodulators such as neuropeptide Y, somatostatin, galanin, angiotensin, and neurotensin, which are stored in large dense vesicles mainly in interneurons. Their release is calcium-dependent and is triggered by the repetitive firing of action potentials at high frequencies, which can also be associated with epileptiform discharges.

In several model organisms neuropeptides show anti-epileptic efficacy at extremely low doses. As endogenous substances, the neuromodulators are hardly affected by active elimination mechanisms in the CNS (Kovac and Walker, 2013). Thus, neuropeptides could be potential alternatives for AEDs considering the development of intracranial drug delivery applications.

Neuropeptide Y

One of the best-investigated neuropeptides in the context of epilepsy is the neuropeptide Y (NPY). NPY is a short peptide that is widely distributed in the CNS but can also be found in the peripheral nervous system and other tissues. NPY appears to have a modulating role in numerous physiological processes, including cortical excitability, circadian rhythms, stress responses, and food intake. Five G-protein coupled receptors (Y_1, Y_2, Y_4, Y_5, and Y_6) have been identified for NPY (for a review see Benarroch, 2009). The mechanisms underlying the NPY-mediated reduction of epileptiform discharges are not entirely understood and the involvement of the different NPY receptor subtypes is controversially debated. Though, patch-clamp recordings in rat brain slices revealed that exogenously applied NPY affects inhibitory as well as excitatory synaptic events in the cortex, most probably through acting on multiple receptors (Bacci et al., 2002). Moreover, NPY potentially inhibits excitatory synaptic transmission in the hippocampus of rodents by activating either Y_2 or Y_5 receptors. Both receptors have been associated with decreased glutamate release in this brain area (El Bahh et al., 2005; Ho et al., 2000).

These effects overall decrease the excitability in neuronal networks, which is suggested to be underlying the antiepileptic effect of NPY, described for several animal models of epilepsy (for a review see Clynen et al., 2014).

The anticonvulsant actions of NPY have been mainly studied in acquired limbic epilepsies (e.g., temporal lobe epilepsy) but were also demonstrated in generalized epilepsies (Kofler et al., 1997; Noè et al., 2008; Sørensen et al., 2009). Two studies reported an anti-absence effect of NPY in GAERS when administered directly into the brain or cerebrospinal fluid (van Raay et al., 2012; Stroud et al., 2005).
Stroud et al. (2005), described a significant reduction of SWDs after i.c.v. injection of very low doses of the neuropeptide (6 nmol) in GAERS; though, seizure suppression was only assessed for 90 min after treatment. Interestingly, an equal effect could be achieved by the i.c.v. application of a Y_2-selective agonists, whereas the selective activation of other receptor subtypes produced significantly weaker seizure suppression (Morris et al., 2007). Therefore, the authors argued that the anti-absence action of NPY is predominantly exerted via Y_2 receptor subtypes.
The focal administration of NPY into the secondary somatosensory (S2) cortex showed an anti-absence action in a dose-dependent manner. Interestingly the microinjection of NPY into the S1 cortex appeared to be less effective (van Raay et al., 2012). These findings could indicate differences in mechanisms of action compared to ETX because ETX shows the best anticonvulsant efficacy when applied to S1 cortex (Manning et al., 2004).

Somatostatin

Somatostatin (SST) is a small neuropeptide involved in the regulation of the endocrine system, affecting neurotransmission and cell proliferation. Besides the hypothalamus, SST can be found in various other brain areas, including the amygdala, hippocampus, striatum, cerebral cortex, olfactory regions, and the brainstem (Viollet et al., 2008). The neuropeptide acts on G-protein–coupled receptors SST_1, SST_2, SST_3, SST_4, and SST_5 (Patel et al., 1977).

In 1987, Sloviter showed in a rat model for temporal lobe epilepsy, the selective loss of SST containing neurons in the hilus of the dentate gyrus. These results indicated for the first time that SST could be involved in the pathology of epilepsy. Subsequent studies claimed robust antiepileptic properties of SST with the major site of action being in the hippocampus (for review see Tallent and Qiu, 2008). The antiepileptic effect could be

explained by inhibited presynaptic glutamate release via the activation of SST_2 receptors (Kozhemyakin et al., 2013).
Moreover, it has been demonstrated that i.c.v. treatment with SST is an effective method to decrease kindled seizures in rodents (Mazarati and Telegdy, 1992). Somatostatin and NPY showed similar antiepileptic activity in a model of self-sustaining status epilepticus. Both neuropeptides induced strong, but transient suppression of spikes and seizures (Mazarati and Wasterlain, 2002). The effect of SST on generalized absence seizures has to our knowledge not been described yet. Nevertheless, SST could be a potent anticonvulsant substance for novel therapeutics approaches.

1.6 Drug delivery for the treatment of neurological diseases

Only in 70 % of people diagnosed with epilepsy, the use of AED can sufficiently suppress seizure activity (World Health Organization, 2006). In other words, about 30 % of sufferers cannot be adequately treated by oral anti-epileptic therapy. One reason for the high ratio of pharmacoresistance could be the low availability of AEDs in the central nervous system (CNS) after systemic treatment (for a review see Sharma et al., 2015).
One great obstacle in systemic anti-epileptic pharmacotherapy is the blood-brain-barrier (BBB), limiting the uptake of active agents in the brain. The BBB is enclosing non-fenestrated blood vessels in the CNS and is mainly composed of endothelial cells connected by tight junctions, astrocytic endfeet, and pericytes (for review see Oby and Janigro, 2006). The BBB forms, on the one hand, a strong diffusion barrier between periphery and brain tissue and, on the other hand, also very efficiently removes drugs from the CNS by efflux transporters present in the BBB (Löscher and Potschka, 2005). The restricted BBB passage of active agents is underlying the need for excess peripheral drug concentrations, limiting their applicability through emerging peripheral side effects such as gastrointestinal, hepatic and pancreatic affection, teratogenicity, blood count abnormalities, and others. Moreover, systemic treatment of epilepsy and other brain diseases with potentially effective drugs is unfeasible due to BBB-impermeability of large or polar molecules (Pardridge, 2005).

One approach to by-pass the BBB is intrathecal (IT) administration of substances. IT administration describes the application of substances directly into cerebrospinal fluid (CSF) that is contained in the thecal sac of the brain (for review see Fowler et al., 2020). Transporting neuroactive components into the CNS via the CSF potentially holds several advantages over systemic treatment: IT delivery would widen the spectrum of potential

drugs by those that do not readily cross the BBB. Furthermore, this application method could lead to increased concentrations of conventional active substances in the brain while minimizing side effects caused by off-target drug exposure in other body compartments. Besides, drugs delivered into the CSF may be less affected by metabolization prolonging their half-life (Misra et al., 2003).

However, the application of agents into the CSF has also been critically discussed. It has for example been suggested that the drugs could be affected by rapid clearance because of the high turnover rate of the CSF. Though, the CSF turnover rate drastically varies between species. In humans the CSF volume is replaced 3 – 5 times a day, (Pardridge, 2016); whereas in rats the turnover rate is between 9 – 12 times a day (Chiu et al., 2012a). Furthermore, it has been argued that many molecules show very poor penetration into the parenchymal brain tissue after application into the CSF (Blasberg et al., 1975; Yan et al., 1994). Along these lines Pardridge (2016) argued that IT application rather works as a slow intravenous infusion by drug clearance into the bloodstream and subsequent distribution in the brain.

Drug transportation via the cerebrospinal fluid

In order to assess the potential of the IT administration routs, it is advantageous to understand the dynamics of the CSF flow. Though CSF flow is highly complex, and several aspects of the flow dynamics are not entirely understood (for review see Linninger et al., 2016).

In healthy humans the total CSF volume ranges from 250 ml to 400 ml and in rats between 200 µl – 400 µl (Chazen et al., 2017; Chiu et al., 2012b). The most considerable volume of the CSF resides intracranially in the ventricular system, cisterns, and subarachnoid space (SAS) (fig. 1.3). The ventricular system of rodents is turned by 90° compared to the human ventricular system apart from that the ventricular anatomy is very similar. The CSF flow throughout the CNS are maintained by unidirectional low active circulation (Di Chiro, 1966) and fast pulsatile movements, which are bidirectional and synchronized with the cardiac cycle (Reubelt et al., 2009). The steady circulation is driven by balanced CSF secretion and reabsorption, which is also essential for maintaining intracranial pressure. The CSF flows from the lateral ventricles (LVs) through the intraventricular foramen directly into the third ventricle. Passing the third and fourth ventricles, the CSF enters the cisterns surrounding the cerebellum and exits into the cranial and spinal SAS (fig. 1.3). The CSF movement is additionally supported by beating cilia of the ventricle's ependymal cells.

In the classic view, a significant portion of the CSF is secreted by the choroid plexus (CP) in the ventricles. However, according to a new hypothesis, the CSF is permanently produced and absorbed in the whole CSF system, as capillary walls in the surrounding CNS reabsorb and filtrate the fluid (for a review see Orešković and Klarica, 2010).
Still the CP epithelial cells, which are connected via tight junctions and enclosing blood vessels, are an essential component of the blood-CSF-barrier. In contrast to the BBB, the capillaries of the CP are fenestrated. Therefore, the exchange of fluids and molecules between CSF and blood is facilitated (for review see Spector et al., 2015). In humans, the arachnoid granulation functions as the CSF reabsorption route.
The CSF flow through the extracellular brain space is another possible route that is essential for substrate delivery into the brain. The mechanisms that drive the exchange between CSF and the brain's interstitial fluid (ISF) are either diffusion or bulk flow. The distance and velocity of diffusion depend significantly on the size and mass of the molecules. However, bulk flow occurs over more considerable distances, and all solutes in the CSF move at the same rate, regardless of size (for a review see Fowler et al., 2020). The ependymal cells lining the ventricular system, forming the CSF-brain barrier, do not possess tight junctions, and small solutes appear to move freely across ISF and CSF. Furthermore, in recent years, CSF has been shown to move into deep brain areas along perivascular spaces surrounding blood vessels. The CSF-ISF exchanges by convection from the brain-wide perivascular networks, also called the "glymphatic" system, could be a highly efficient route for drug delivery (Abbott et al., 2018).

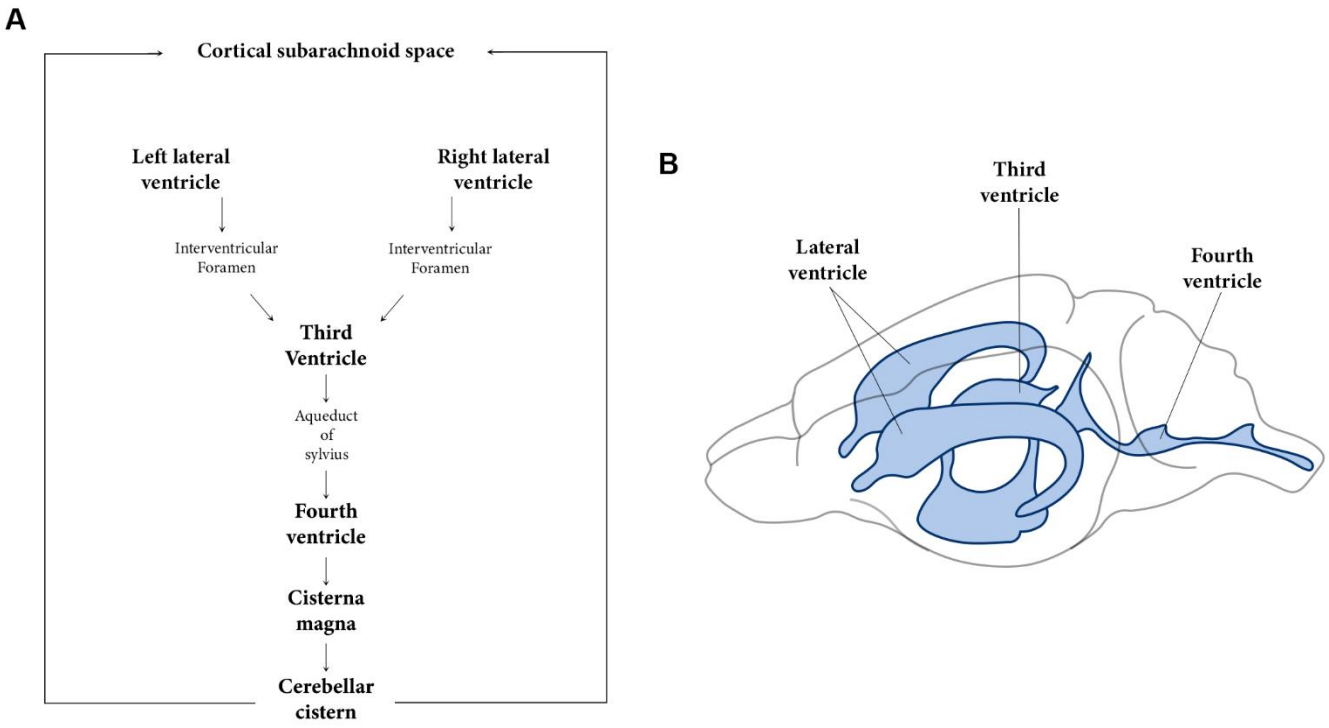

Figure 1.3: Cerebrospinal Fluid
A) Schematic diagram of cranial CSF circulation through ventricles, cisterns, and subarachnoid space. B) Anatomy of the ventricular system of a rodent brain.

1.7 Outline of the Study

Systemic drug application is the main approach of epilepsy treatment. However, the CNS is a particularly challenging target for drug delivery. Because the BBB is highly restricting the availability of drugs in the brain, only a minor fraction of systemically applied substances can reach its target (Pardridge, 2005). Consequently, to successfully suppress epileptic seizures, high drug concentrations in the systemic circulation are required. The systemic treatment with anti-epileptic drugs can thus be accompanied by severe side effects caused by off-target drug exposure. Furthermore, approximately 30% of patients with epilepsy are pharmaco-resistant (World Health Organization, 2006) and it appears that, decreased drug availability in the CNS caused by BBB mechanism can partly underly this drug resistance (Sharma et al., 2015). Accordingly, there is a great interest in developing new therapeutic strategies to improve CNS drug accessibility in order to suppress epileptic seizures.

Intrathecal (IT) administration of AEDs could be a possible route to bypass the BBB and increase the availability of neuroactive compounds in the CNS. This study's aim was an

in-depth evaluation of IT drug application in the genetic absence epilepsy rats from Strasbourg (GAERS) and to assess if this method is a reasonable approach to treat epilepsy.
The GAERS rats generate seizures, which can be monitored as characteristic SWDs in the EEG and the quantification of these seizures is a precise tool for assessing the efficacy of antiepileptic therapy (van Luijtelaar and van Oijen, 2020). Accordingly, to analyze seizure occurrence in GAERS and elucidate if pharmacological treatment effectively suppresses SWDs, EEG recordings combined with automated seizure detection have to be performed. Based on the quantification of detected seizures, we[1] can then test and compare systemic and localized drug applications in epilepsy.

On the one hand, we will investigate the efficacy of two standard anti-absence drugs, VPA and ETX, for different application routes (i.v., i.p. and i.c.v.), on the other hand, the efficacy of alternative antiepileptic substances such as the neuropeptides SST and NPY, which do not cross the BBB, will be explored after i.c.v. application in these animals. Neuropeptides are endogenous neuromodulators and thus, they have the advantage over classical AEDs that they show antiepileptic activity at extremely low doses and are less affected by the elimination mechanisms of the CNS (for a review see Clynen et al., 2014). In order to identify intracranial therapeutic concentrations of anticonvulsant substances, dose-response experiments will be implemented and analyzed for all substances.
The distribution of drugs into the brain parenchyma after applying them into the CSF is highly complex, and the underlying mechanisms are controversially discussed (Fowler et al., 2020). To gain a closer insight into the fate of drugs after i.c.v. administration, we will monitor ETX distribution throughout several body compartments after utilizing different application methods. Furthermore, the injections of dyes can visualize the propagation of molecules into the brain and elucidate target areas that can be reached by i.c.v. applied drugs.

Finally, we want to investigate the cortical surface as a potential site for localized drug application in absence epilepsy, as this brain region would be surgically more accessible, less invasive, and less restricted by size compared to the ventricular system

[1] In accordance with usual scientific writing style the pronoun ‘we’ is used throughout the thesis when describing my own ideas or findings.

2 Materials & Methods

2.1 Animals

All experiments were performed following the German law on animal protection and approved by the Animal Care and Ethics Committee of Christian-Albrechts-Universität zu Kiel (CAU). In total n=139 Wistar rats of the Genetic Absence Epilepsy Rats from Strasbourg (GAERS) strain were used for this study. All animals used in this study were male rats between 6 and 9 months of age. The rats were bred and housed in the Victor-Hensen-Haus, CAU (local animal facility) under standard laboratory conditions with free access to food and water, 12h light/dark cycle (light on at 6 am), and a temperature-controlled environment. The animals were housed in groups of 3 – 4 animals until surgery. Rats with an implanted head-stations or drug application implants were single housed. For experimental sessions, the animals were moved to the Physiological Institute, CAU Kiel, where they stayed for a maximum of five consecutive days before being returned to the Victor-Hensen-Haus.

2.2 Neural implants

EEG-head-station

To detect the brain signals in GAERS, custom made neural interfaces, referred to as head-stations, were used (fig. 2.1A). Stainless-steel screws were used as epidural electrodes, and the neural signal acquisition involved four recoding electrode and one ground electrode. The recording screws had a major diameter of (1.2 mm) and were 3 mm long. Via an insulated stainless-steel wire (Ø 0.075 mm), the electrodes were connected to gold-plated sockets (model E363/0, Plastics One, USA). For each recording channel, one of the sockets was inserted into a 6-channel plastic pedestal (model MS363, Plastics One, USA). The central opening of the pedestal stayed empty, as only 5-channels were used for the electrophysiological recordings. The pedestal functioned during the recordings as an electronic interface to a 6-channel, meshed EEG cable (model 363-363, Plastics One, USA). Finally, in order to stabilize the head-station, a thin layer of dental cement (Paladur®) was put above the sockets.

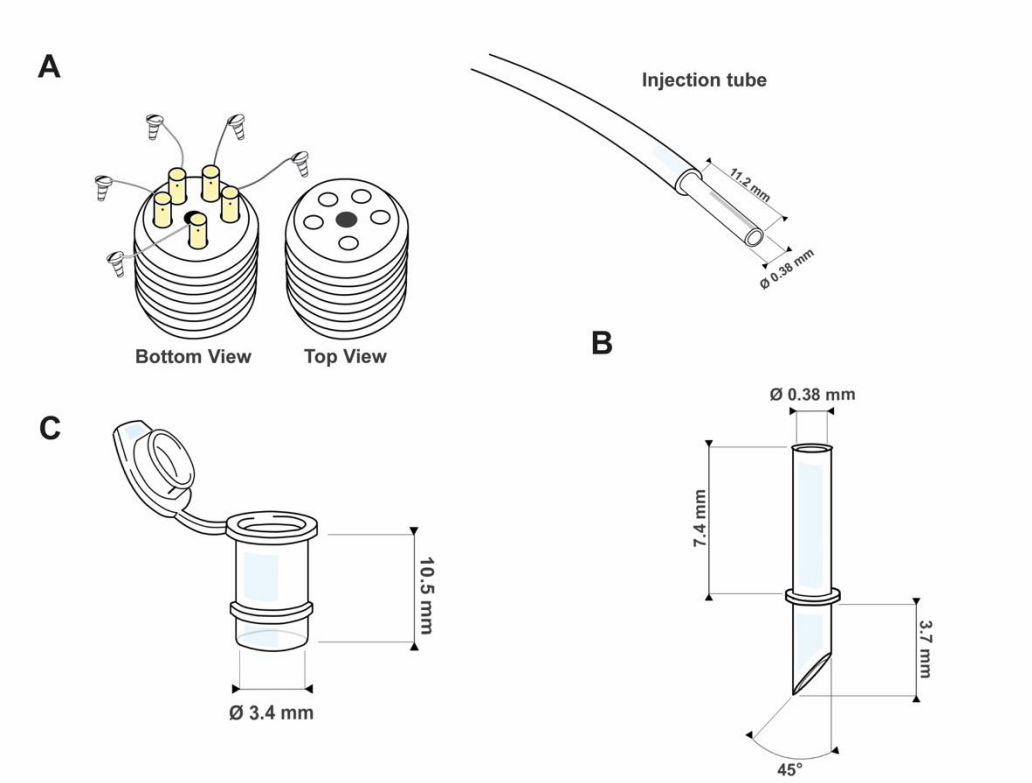

Figure 2.1: Schematic illustrations of custom-made neural implants used in this study
A) Head-station for brain signal recordings. The top view shows the cable connector, which is consisting of the 6-channel pedestal. The bottom view illustrates the stainless-steel screws (recording electrodes) connected to gold-plated sockets and inserted to the pedestal. B) Guide-Cannula for chronic implantation into the lateral ventricle (bottom) plus the corresponding injection tube (top). C) Epidural-Cup for cortical drug application.

Guide cannula for chronic implantation into the lateral ventricle

To explore the effectiveness of intracerebroventricular (i.c.v.) pharmacotherapy, antiepileptic substances were administered into the lateral ventricle of GAERS by chronically implanted guide cannulas. The custom-made cannulas (fig. 2.1B bottom panel) consisted of biocompatible polyethylene tubes. For the application of dissolved substances, tubes with an inner diameter of 0.38 mm and an outer diameter of 1.09 mm (ProLiquid, Germany), were used for cannula building. The final guide cannulas consisted of a short (3 mm) and long (7.4 mm) part, which were separated by a ring-shaped bulge at the outer surface of the tube. The shorter end of the cannula had a pointy tip, to facilitate the brain implantation and to reduce tissue damage during tissue penetration. The long and blunt end of the cannula was utilized to guide an injection needle for drug application (fig. 2.1B, top panel). Each guide cannula had a matching

dummy made from a stainless-steel injection needle. Before surgery, the cannulas plus the cannula dummy were kept in 70% ethanol for sterilization.

Epidural Cup

In order to investigate cortical ETX application, epidural cups were implemented based on the method of Ludvig et al., 2009. The epidural cup (fig. 2.1C) was constructed from 200 µl capped reaction tubes (Kisker Biotech GmbH & Co, Germany). The bottom part of the tube was cut to create an opening with a diameter of about 4 mm. The final height of the cup was 10.5 mm. The edges of the opening were sanded down and a thin layer of biocompatible silicone adhesive (Kwik-Cast Sealant, World Precision Instruments, USA) was applied. Hence, sharp edges were removed, and the dura mater was prevented from being damaged during surgery. Finally, a ring-shaped protrusion was created by heating at the outer walls of the cup. Consequently, the cup had a better grip on the dental cement, which was applied during the surgery to stabilize the neural implant.

2.3 Surgical procedures

Placement of the head-station

Before starting the surgical procedure, the rats were intraperitoneally (i.p.) injected with chloral hydrate (400 mg/kg, Sigma-Aldrich, Germany) to stably anesthetize the rats over one to two hours (Field et al., 1993). If necessary, the anesthesia was prolonged by a subsequent chloral hydrate injection with 20 – 30% of the start concentration. To counteract the depressing effect of chloral hydrate on the cardiovascular systems, the rats received atropine sulfate (0.2 mg/kg, B. Braun, Germany) subcutaneously (s.c.). For analgesia carprofen (5 mg/kg, Rimadyl) was administered s.c., pre- and postoperatively. Furthermore, prilocainhydrochlorid (Xylonest) was applied locally on the skin and the skull's periosteum. After full analgesia and anesthesia, which was confirmed by testing for the toe pinch reflex, rats were placed on a heating map and adequately fixed in a stereotactic frame. During surgery, the eyes of the animals were covered with protective ointment, to prevent them from drying out.

A vertical incision was made in the sagittal plane between the ears and the skull was exposed. The periosteum was removed from the bone, so that lambda and bregma suture-crossings, were clearly visible. Based on these landmarks, the stereotaxic coordinates for the five EEG electrodes were determined and marked. At these positions, small holes were drilled into the skull, and ideally, the dura mater was not damaged during the procedure. The stainless-steel screw electrodes of the head station were fixed

epidurally. Two recording electrodes were placed bilaterally over the frontal cortex (anteroposterior (AP), +3.9; mediolateral (ML), ±2.0) and two electrodes over the parietal cortex (AP -6.4, ML ±4.0) (fig. 2.2A). Additionally, one ground electrode was implanted above the cerebellum. Finally, the head-station was fixed to the rat's skull with dental cement (Paladur®). As soon as the dental cement was fully cured, the skin was closed around the head station using stitches. After surgery, the animals were placed into a new cage and monitored until fully awake and behaving normally.

Cannula Implantation

For animals that received i.c.v. treatment (n=79), a guide cannula was implanted unilaterally into the right lateral ventricle. General methods of anesthesia and analgesia were as described above. For the cannula implantation, a hole was drilled unilaterally at the position AP -0.5 and ML -1.2 (fig. 2.2A). The exposed dura was carefully pierced with a needle and any bleedings that occurred were immediately stopped. The guide cannula was then slowly lowered into the brain with the help of the stereotactic manipulator. The required depth of 3.5 mm was reached when the protrusion of the cannula (fig. 2.2B) reached the skull surface. After the cannula was fixed to the skull by dental cement and it was detached from the stereotactic manipulator. Finally, the cannula was closed by the dummy to prevent possible CSF leakage and the entry of dirt into the brain. Animals that underwent i.c.v. treatment combined with EEG recording received six craniotomies. In the case of cannula implantation without the need for brain recordings, three additional anchor screws were implanted in close approximation to the cannula craniotomy.
After at least three days of recovery and 1 to 2 days before starting the EEG recordings, the correct placement of the cannula was tested by i.c.v. injection of 100 ng Angiotensin II (AGII, Sigma-Aldricht, Germany) dissolved in 5 µl Ringer solution (McKinley et al., 2003). Only the animals showing drinking behavior over 20 min after AG II injection were included in the study. Furthermore, a 10 % methylene blue solution was injected via the cannula into the brain after the animals were sacrificed. By visual inspection of dye distribution in the dissected brain, the correct placement of the cannula was confirmed. If the dye was not distributed in the ventricular system, the rats were excluded from analysis. However, this final test could not be performed in all rats as some of the animals were used for concentration or histological studies.

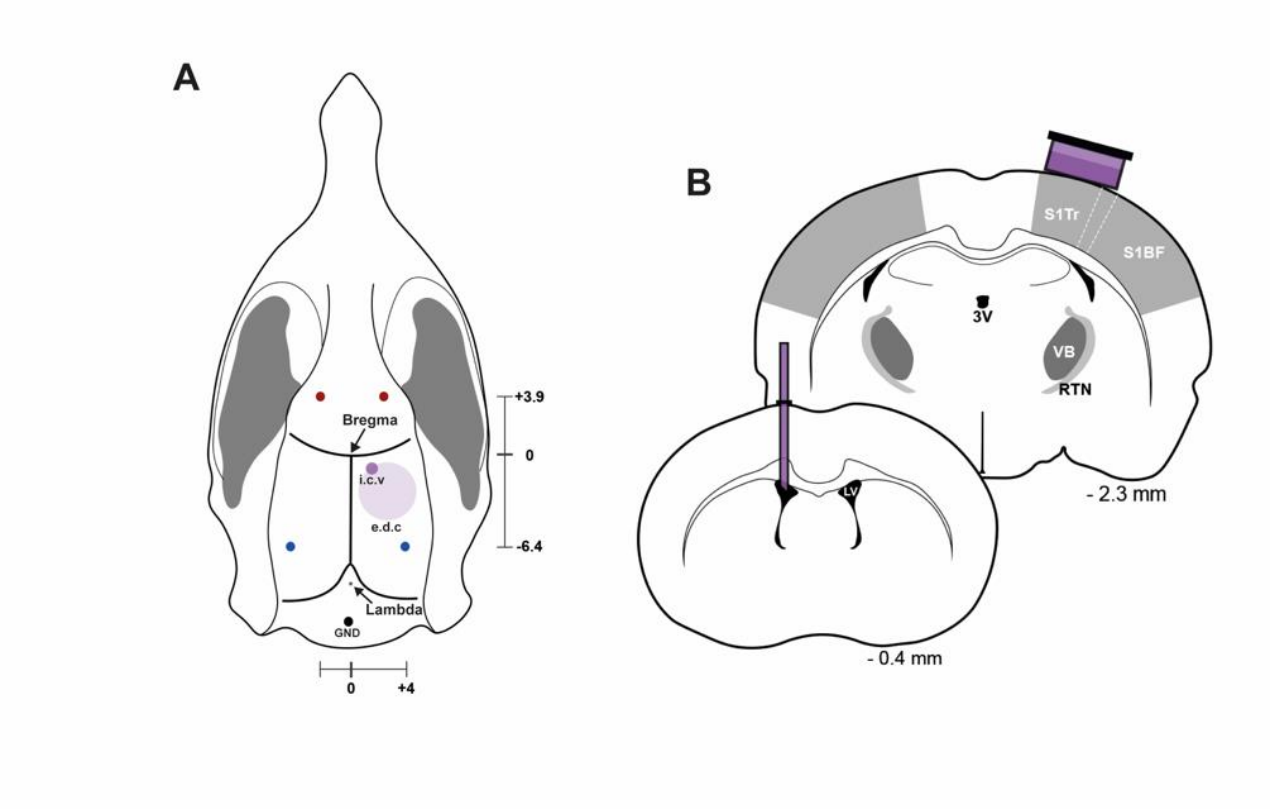

Figure 2.2: Placement of EEG screws and neural implants
A) The craniotomy for the epidural cup (e.d.c) is shown in light purple, whereas the intracerebroventricular (i.c.v) cannula placement is displayed in dark purple. The recording sites are indicated as dots above the frontal cortex (red) and the parietal cortex (blue). An additional ground electrode (black) was implanted above the cerebellum. B) Schematic representation of coronal sections that are relevant for localized pharmacological treatment. The rostral coronal section (-0.4mm) shows the implantation site for the guide cannula (purple). The more caudal coronal section (-2.3 mm posterior to bregma) shows the implantation site of the epidural cup (purple). Furthermore, the shaded areas represent brain regions that play a critical role in the emergence of absence seizures: RTN, nucleus reticularis thalami; VB, ventrobasal thalamus; S1Tr, primary somatosensory cortex, trunk region; S1BF, primary somatosensory cortex, barrel field. The coordinates are derived from the atlas of Paxinos and Watson (Paxinos and Watson, 2006) with bregma as reference.

Epidural Cup Implantation

In n=3 animals, in addition to the electrodes, an epidural cup was implanted unilaterally above the primary somatosensory (S1) cortex (fig. 2.2A and B). To implant the cup a craniotomy with a diameter of 4.2mm was needed. Therefore, enough bone around the center point (AP -2.0, ML -2.0) was slowly ablated with a drill. In order to prevent brain swelling due to overheating of the tissue, ice-cold saline was repeatedly applied to the skull. Once the bone was thin enough, the remaining layer could be removed carefully utilizing fine forceps. It was essential that the dura mater was not injured during the complete procedure. The epidural cup was gently positioned on the dura and held in place using an alligator clamp. The gap between the cup and the bone was sealed with a

low toxicity silicone adhesive (Kwik-Cast Sealant, World Precision Instruments, USA). After the epidural cup was fixed to the skull by dental cement, it was filled with saline, to protect and moisten the brain. Finally, the cup was carefully closed with its cap to prevent the entry of dirt.

2.4 Recording of brain signals and seizure detection

For video- and EEG monitoring, the animals were transferred to Phenotyper cages (Noldus Information Technology, Netherlands). The cages had plexiglas walls and a floor area of 45 cm x 45 cm. The top unit of the Phenotyper cages contains an infrared-sensitive camera and a light system, which enables the experimenter to control the light conditions externally. Two Phenotyper cages were placed in one isolation boxes, of which two were used. Within these boxes, a constant day/night cycle was guaranteed, and the animals were not disturbed by external noise. The temperature in the boxes was continuously monitored, and regular air circulation was ensured. During the EEG recordings, the animals were connected to a recording cable. Therefore, a cable conduit was implemented into the top unit of the cages. To permit free horizontal mobility in the cages, the cables were tethered to an electrical swivel (Bilaney, Germany). The swivel was fixed to a counterbalanced arm in order to facilitate the vertical head movements of the rats. The EEG signals were recorded using a Neuralynx data acquisition system (Neuralynx, Bozeman, MT, USA). The weak electrical signal (microvolts) from the brain was pre-amplified via an eight channel headstage (HS-8-CNR-MDR50, Neuralynx, USA). Afterwards, the signals were digitized at 16 kHz and online band-pass filtered between 0.1 and 100 Hz by the Cheetah 6.2.0 recording software. Before starting the brain recording the channel producing the best signal to noise ratio in the other electrodes was chosen visually as reference electrode.

Data Processing and Seizure Classification

Due to the generalized occurrence of absence seizures over the entire cortex, only one channel was needed for offline seizure detection. Therefore, the channel with the cleanest signal was identified visually using Neuroexplorer analysis software. Further signal processing was implemented in MATLAB.

In a first preprocessing step, a low-pass filter (40 Hz) and a high-pass filter (5 Hz) was applied to the signal, as the best seizure detection results were archived in this frequency range. Especially artifacts due to head movements of the animals could be diminished by the 5 Hz high-pass filter. For seizure detection, the data was split into time intervals of

one second. As SWD complexes in GAERS show high amplitudes and a prominent oscillating activity between 7 – 11 Hz in the EEG (Marescaux et al., 1992), the autocovariance function is a useful tool to detect epileptic activity (Rodgers et al., 2015).

$$r_{xx}[L] = \frac{1}{N-L}\sum_{n=1}^{N-L}(x_{n+L} - \bar{x})(x_n - \bar{x}).$$

Accordingly, for seizure classification the autocovariance, $r_{xx}[L]$, was evaluated with a lag (L) of ± 250ms and computed for the one-second data segments (x). The information contained in the autocovariance were used as features underlying a classification model to categorize the segments into "ictal" and "interictal" periods. In order to choose the best detection model and train it, a pre-classified dataset was implemented. To this end, all segments of a one-hour baseline recording (3600 seconds) were categorized by the experimenter based on visual inspection of the EEG traces and the related autocovariance graphs (fig. 2.3). For classifying a segment as "ictal," it was a requirement that in at least two consecutive data segments, spike and wave activity was identified. Finally, the segments were labeled with either a "1" for ictal or a "0" for interictal activity. The pre-labeled dataset was used to automatically train a selection of different classification models in the Matlab R2019b classification learner app. The cross-validation method showed a predictive accuracy above 98 % for the k-nearest neighbors algorithm. Therefore, the classifier for seizure detection used in this study is based on this model.

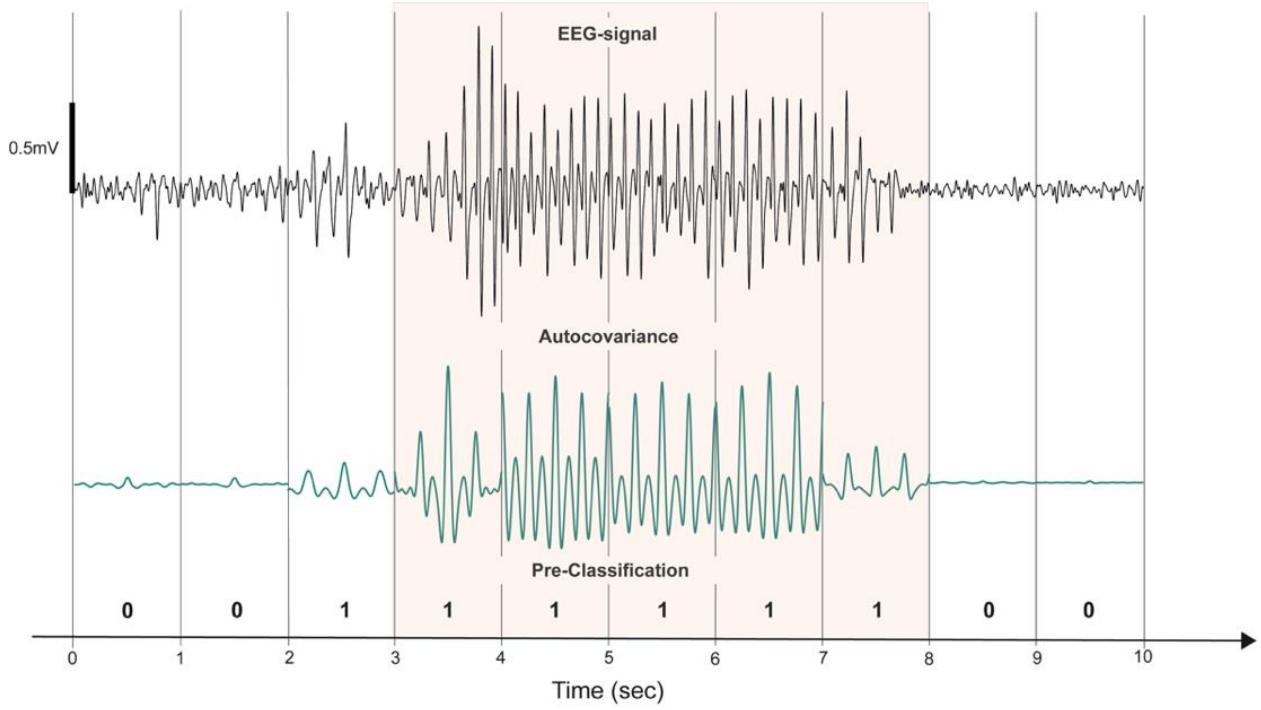

Figure 2.3: Seizure detection using autocovariance
The EEG signal (black trace) form a GAERS rat shows a recording from one channel over 10 seconds containing one SWD complex. The green trace shows the corresponding autocovariance plots. A five-second burst of spontaneous SWD was detected by the implemented classifier (red highlighted), whereas during the pre-classification by the experimenter, six-seconds of epileptic activity were detected (bottom numbers: ictal = 1, interictal = 2). Hence for this 10 second data segment, the classifier shows an accuracy of 90 %.

The performance of the classifier was tested via a test dataset containing 600 consecutive segments from each animal recorded in this study (n=60). The test dataset was classified by the described model and the experimenter. The respective results were compared, and a confusion matrix was created by including all true positive (TP), false positive (FP), true negative (TN) and false negative (FN) classifications. These values were used to compute the overall accuracy, recall, and precision of automated seizure detection:

$$Accuracy = \frac{TP + TN}{TP + FP + TN + FN}$$

$$Precision\ (ictal) = \frac{TP}{(TP+FP)} \qquad Recall\ (ictal) = \frac{TP}{(TP+FN)}$$

$$Precision\ (interictal) = \frac{TN}{(TN+FP)} \qquad Recall\ (interictal) = \frac{TP}{(TN+FN)}$$

In order to have a better metric to evaluate an imbalanced dataset the F-Score, which considers recall and the precision was additionally computed.

$$F - Score(ictal) = 2 \times \frac{Precision \times Recall}{Precision + Recall}$$

All animals with an accuracy below 97 % were excluded from the analysis.

2.5 Drug application and analysis of therapeutic efficacy

Table 1: Pharmacotherapeutics used in this study

Pharmacotherapeutics	Provider	Application method				Reference
		i.p.	i.v.	i.c.v.	e.p.c.	
Ethosuximide (ETX)	Sigma-Aldrich Biochemie GmbH, Hamburg, Germany	+	+	+	+	(Marescaux et al., 1992)
Valproic acid sodium salt (VPA)	Sigma-Aldrich Biochemie GmbH, Hamburg, Germany	+	-	+	-	(Marescaux et al., 1992)
Neuropetide Y (NPY)	Sigma-Aldrich Biochemie GmbH, Hamburg, Germany	-	-	+	-	(Stroud et al.,2005; Morris et al., 2007)
Somatostatin (SST)	Sigma-Aldrich Biochemie GmbH, Hamburg, Germany	-	-	+	-	(Mazarati and Telegdy, 1992)
Chloral Hydrate	Carl Roth GmbH + Co. KG	+	-	-	-	(Field et al., 1993)

Baseline recording

For habituation, the animals were placed into the experimental cages and connected to the recording cables at least five hours before starting the experiment. During all experiments, the animals had access to food and water ad libitum. For the baseline recordings, the rats were continuously video- and EEG recorded for 12 (from 6 pm – 6 am next day, n=60) or 24 hours (from 6 pm – 6 pm next day, n=5) without any disturbance. All animals shown in this experimental study underwent one baseline recording.

Systemic treatment of seizures

Within this study, the systemic anti-epileptic effect of three substances (tab. 1) was tested. To this end, the rats were i.p. injected with these pharmaceuticals. All substances were dissolved in saline before administration. Animals that only received systemic treatment were solely implanted with a head-station for EEG recordings.

For systemic drug testing, rats underwent two treatment sessions on two consecutive days. Immediately after each treatment, around 6 pm, the video monitoring and EEG recordings started for either 12h or 24h. The first experimental day served as a control session, and the animals were solely treated with i.p. ringer solution in the exact same way as in the experimental session. On the second day, the experimental session, the GAERS were i.p. injected with the substance of interest. For each substance, one dose

was tested (tab. 2). Some animals (n=6) in this study, were systemically treated with VPA as well as ETX, however in between i.p. injection with the respective drug, there was a wash-out-phase of at least one week.

Intracerebroventricular treatment of seizures

The efficiency of localized drug therapy was investigated on the basis of intracerebroventricular (i.c.v.) treatment in GAERS using four potential antiepileptic substances (tab. 1). The animals that received i.c.v. treatment were implanted with a head-station and an i.c.v. cannula (fig. 2.2). The correct placement of the cannula was confirmed before starting the experiments by AGII injection (cf. Chapter 2.3). The substances of interest were dissolved in saline before administration. In order to test substances and the application method, rats underwent two treatment sessions on two consecutive days. Immediately after each treatment, around 6 pm, the video monitoring and EEG recordings started for 12 hours. The first experimental day served as a control session, and animals were treated only with ringer solution i.c.v. On the second day, the experimental session, the GAERS were i.c.v. injected with the substance of interest. For the i.c.v. administration, a constant volume of 20 µl (ETX, VPA) or 2 µl (NPY, SST) was injected. The injection needle connected to a polyethylene tube, plus Hamilton syringe was carefully inserted into the guide cannula, and the fluid was slowly injected (fig. 2.1). During the injection, the animals were handled by the experimenter. After removing the injection cannula, the guide cannula was closed again with the dummy. For all substances, several concentrations were tested (tab. 2). The animals were treated repeatedly with different substances and doses. The wash-out-interval between tests was at least one week.

Epidural treatment of seizures with ETX

In order to investigate the potential of epidural drug applications, ETX was directly applied to the S1 cortical surface in three animals. Animals that received epidural treatment were implanted with a head-station and an epidural cup (fig. 2.1). For the investigation of this application method, rats underwent two treatment sessions on two consecutive days. Immediately after each treatment, around 6 pm, the video monitoring and EEG recordings started for 12 h. The first experimental day served as a control session. To this end the epidural cup was filled with 20 µl ringer solution. On the second day, the cup was filled with ETX dissolved in 20 µl ringer solution.

During the treatment, the animals were handled by one experimenter while another person was carefully pipetting the solution into the center of the cup as close to the brain surface as possible. All animals were treated with two drug doses (tab. 2). In between the experimental trials, a wash-out-phase for ETX of at least one week was observed.

Table 2* : *Study design for substance application combined with EEG recordings

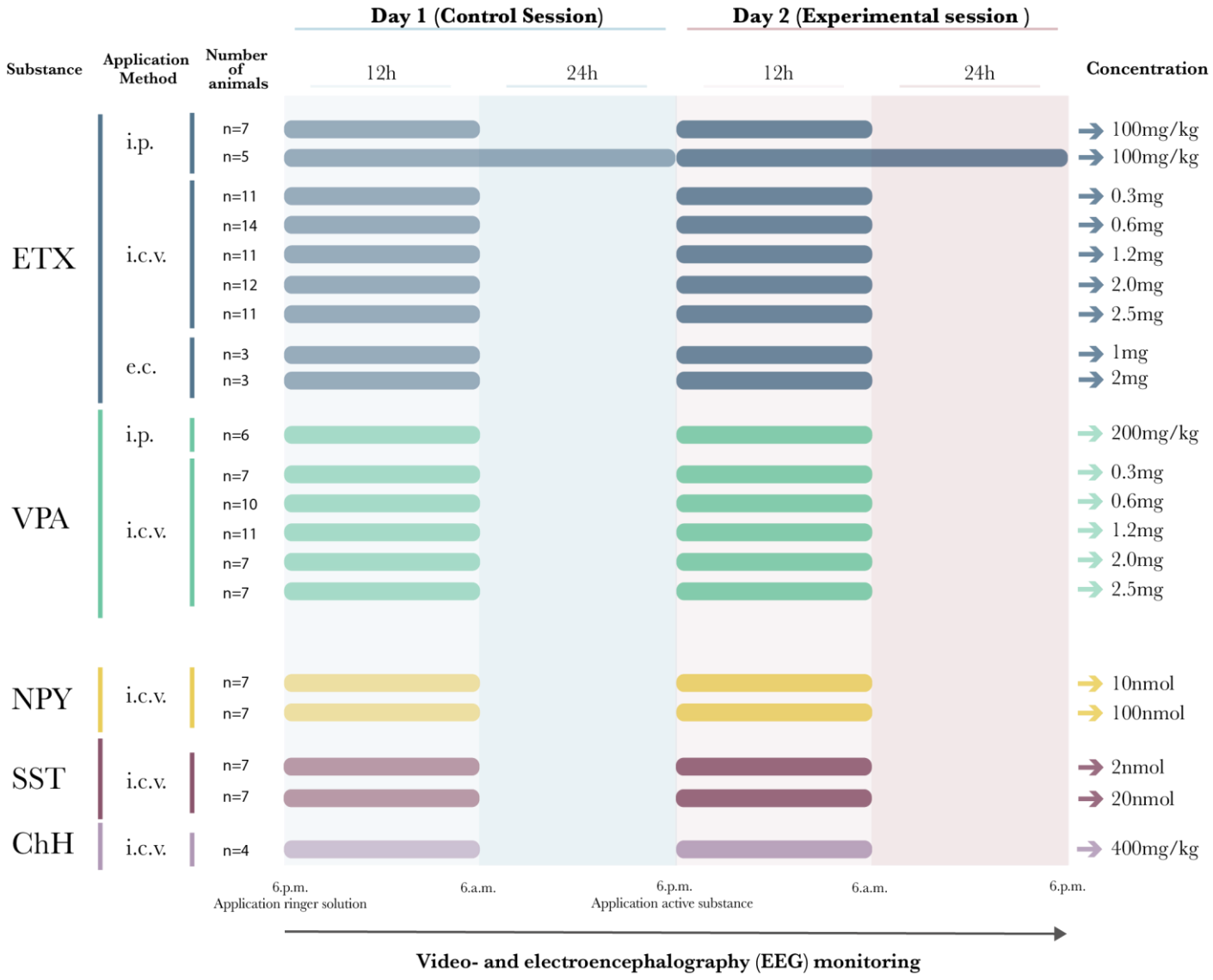

Within animal comparison of different ETX administration routes

In a final experiment, the effectiveness of three different administration routes was compared directly, in one cohort of eight animals. The different application methods used in this experiment were intraperitoneal (i.p.) injections, intravenous (i.v.) injections into the tail vein and intracerebroventricular (i.c.v.) injection. The different treatments were performed in three experimental trials in three consecutive weeks. The animals received in each case an ETX dose of 2mg per animal. The GAERS used in this experiment were implanted with a head-station and an i.c.v. cannula.

Each experimental trial consisted of two treatment sessions on two consecutive days. Immediately after each treatment, around 6 pm, the video monitoring and EEG recordings started for 12 hours. The first day was a control session, where animals were treated with ringer solutions via the same application route as in the subsequent experimental session. However, in order to prevent clotting of the vein during the i.v. trial, a sham control (no ringer injection) was performed. On the second day GAERS, were treated with ETX. For i.c.v. treatment, a constant volume of 20 µl was injected whereas during i.v. and i.p. treatment an injection volume of 0.1 ml was used (tab. 3).

Table 3: Study design for within animal comparison of different ETX administration routes combined with EEG recordings .

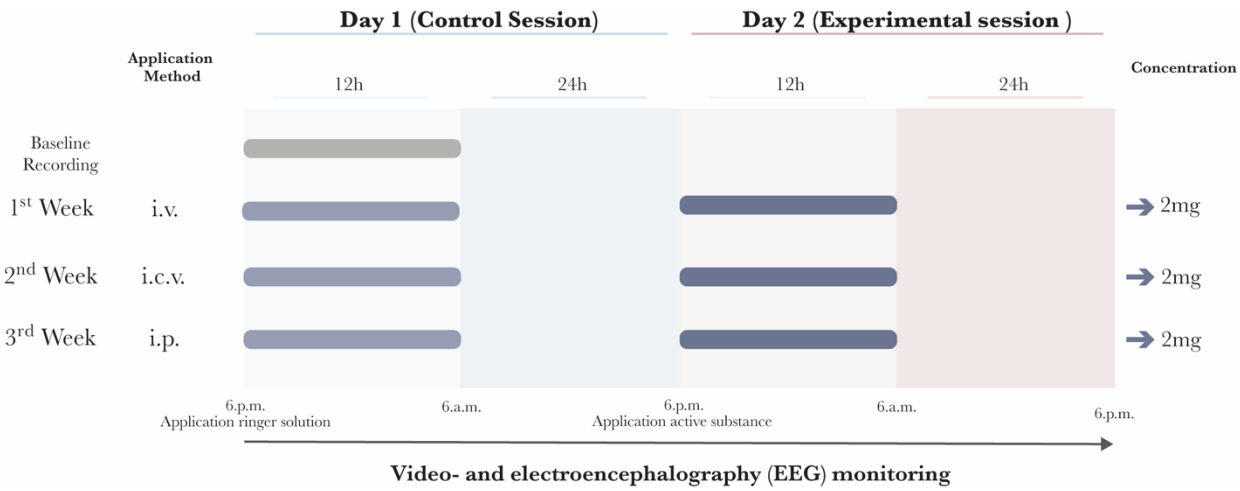

2.6 Analysis of ETX distribution throughout different body compartments after i.c.v. and systemic administration

The ETX concentration was quantified in the blood plasma, brain tissue, and the CSF after application in order to understand the distribution dynamics of this drug. The ETX concentration measurement was performed for three groups of animals which received different types of treatment:

In the first group, including five non-operated animals, the samples were collected one hour after i.p. treatment with the therapeutic concentration of ETX (100 mg/kg). In a second group, the drug distribution was determined after i.c.v. therapy. The animals that received ETX via i.c.v. injection underwent cannula implantation one week before sample collection. One day before ETX treatment, the animals were i.c.v. injected with AGII to confirm correct cannula placement. For the sample collection, all animals (n=12) were i.c.v. treated with an ETX dose of 2 mg per animal. In order to further analyze a time-dependent drug distribution, the samples were collected 15 minutes (n=4), one hour (n=4), and four hours (n=4) after ETX injection. In the final group, including 12 non operated rats, the samples were collected after i.v. injection of 2 mg per animal ETX. The samples were collected 15 minutes (n=4), one hour (n=4), and four hours (n=4) after ETX injection. To have reference samples for the HPLC analysis in each group, one animal received only a vehicle injection, and one additional animal received no treatment at all.

CSF Collection

The CSF was collected from the cisterna magna employing a cisternal puncture technique (Li et al., 2016). During CSF sampling, the animal was deeply anesthetized with chloral hydrate (400 mg/kg). After confirming anesthesia, the rat was placed in a stereotactic frame and the head was fixed in a flexed position, with the nose pointing downward. The puncture site of the cisterna magna is located between the occipital protuberance and the atlas, which was felt as a depressive spot at the back of the head. Next, a 25G infusion needle attached to a polyethylene tubing was carefully inserted centrally into the atlanto-occipital membrane until a “give” was felt. After gentle aspiration, CSF started flowing, and around 20 – 100 µl CSF was collected. The color of the CSF was closely observed to avoid blood contamination. The CSF was immediately put on ice and until further analysis stored at -80°C.

Blood Plasma collection

Following the CSF collection, a cardiac puncture technique was used to acquire blood plasma samples (Sharp and Villano, 2012). After the rat received a lethal dose of chloral hydrate, it was placed on its back. A 21G cannula attached to a syringe was inserted underneath the rips at a 30° angle slightly left of the sternum. As soon as the needle entered the heart, 1ml of blood was collected in heparinized tubes (Microvette® 500, Sarstedt). The heparinized blood samples were centrifuged at 2.000 x g for 15min. After centrifugation, the supernatant, respectively, the plasma was carefully collected in an Eppendorf® tube. The plasma was until further analysis stored at -80°C.

Brain tissue collection

Immediately after the plasma and CSF samples were collected, the brain of the animal was surgically removed. In order to wash away the extraneous blood, the brain was rinsed in ice-cold PBS and thereafter placed dorsoventrally onto an ice-cold brain matrix (model RBMS-300C, World Precision Instruments, USA). In order to dissect specific brain regions, a coronal brain slice between -1 mm to -3 mm in relation to bregma was collected. The brain slice was put on an ice-cold metal block and further dissected. Based on the visual identification of anatomical landmarks, brain regions of interest were isolated. The brain areas of particular interest were the thalamus and the somatosensory cortex from both hemispheres. The coordinates were based on the matrix-guided trimming protocol of Defazio et al. (2015).

The brain samples were collected in Eppendorf® tubes and weighted. For each sample, twice the volume of cold ultrapure water was added to the tube, and the collected brain tissue was homogenized by grinding (B.Braun, Germany). Next, the homogenized samples were centrifuged at 16.000 x g for 15min. After centrifugation, the supernatant was carefully collected and stored at -80°C for further analysis.

The following formula was used to calculate the final ETX concentration (C_F) in the brain tissue:

$$C_F(\mu g/g) = \frac{(C_D * V_D)}{W}$$

where C_D is the measured drug concentration (µg/mL), V_D the volume of added ultrapure water (mL) and W the weight of the brain sample (g).

HPLC analysis

In cooperation with Prof. Dr. Regina Scherließ and Hanna Göttsche at the Institute of Pharmacy, CAU Kiel, the ETX concentration in the different specimens (blood plasma, CSF, and brain samples) was quantified by high-performance liquid chromatography (HPLC, Waters Corporation, Milford, USA) following UV detection. The mobile phase for the HPLC procedure was composed of 90 % ddH2O (the pH was adjusted to 2.2 by H_3PO_4) and 10 % acetonitrile and had a constant flow rate of 1.0 ml/min. In order to separate the analyte, a LiChro- CART® 125-4 LiChrospher® 100 RP-18 (5 µm) column combined with a pre-column (Merck KGaA, Darmstadt, Germany) was used. The column temperature was set to 50°C. A volume of 10 µl was injected into the apparatus, and the detection wavelength was set to 205 nm (detector PDA 2998). The calibration curve for ETX was linear over the concentration range of 0.055–156.0 µg/ml.

Fast green diffusion test

After i.c.v. administration, the pharmacotherapeutics must penetrate through the brain's extracellular space and reach specific target areas to show antiepileptic efficacy. In absence epilepsy, the S1 cortex and the thalamus are of particular interest (Meeren et al., 2005). In order to visualize substance penetration into the brain tissue, the dye fast green (FG; Merck) was i.c.v. injected in three rats. Prior to the i.c.v. administration of 2 % FG (dissolved in ringer solution), the animals were deeply anesthetized with chloral hydrate (400 mg/kg). If necessary, the anesthesia was prolonged by a subsequent chloral hydrate injection with 30 % of the start concentration. A constant injection volume of 20 µl FG was used. In order to further analyze a time-dependent drug distribution, animals were killed either 5 min (n=1), one hour (n=1), or four hours (n=1) after FG injection. After the respective time was elapsed, the rats were euthanized with a lethal dose of chloral hydrate. The animals were immediately decapitated, and the brains were surgically removed from the skull. In an ethanol/dry ice bath, the brains were shock-frozen and embedded in OCT. Until sectioning, the brains were stored at -80°C. Brains were cut into 80 µm thick coronal sections on a Leica CM 3050S cryostat (RRID:SCR_016844). To see the dye distribution more clearly digital photographs were taken directly from the embedded brain in the block.

2.7 Neurotoxicity tests

Behavior

To determine if the intracerebroventricular injections of ETX causes adverse effects in GAERS several behavioral tests were performed. For the Irwin test (Honack and Löscher, 1995) animals were placed in an open field (OF) and observed for ten minutes consecutively. Attention was paid to abnormal behavior such as hyperlocomotion, sedation, ataxia, head swaying, circling, stereotypic sniffing, hypermetric gait, wet dog shakes and, flat body posture. The observations on behavioral abnormalities were scored as described in table 4.

Furthermore, the responses to external stimuli were tested utilizing the hyperexcitability test (HET) (Rice et al., 1998). The HET consists of four different test sessions. The first session was an "approach-response test", consisting of a pen slowly moving towards the rat's nose. In a direct follow up session, respectively the "touch-response test" the rat was carefully touched with the same pen at the rump. During the "finger-snap test" a clicking noise was generated a few centimeters above the animal's head. Finally, the rat was picked up by grasping it around the rump which is called the "pick-up test". For all tests the animal's reactions were observed closely and scored as describe in table 4.

The motor coordination was analyzed using the RotaRod test (Dunham and Miya, 1957; Tollner et al., 2011). To pass this test, animals had to balance on a rotating rod (Ø 7.5; 8 rpm) without falling off for at least 2 min in one of three trials.

Experimental Setup

Two days before starting the behavioral experiments, animals were habituated with the different test procedures. The animals were tested once without any treatment, one day after i.c.v. application of ringer solution, and one day after i.c.v. treatment with ETX (0.3 mg, 0.6 mg, 1.2 mg, 2.0mg, 2.5 mg; n=5). Hence the animals were undergoing all tests (OF-, HET- und Rotarod-Test) within a period of five consecutive days. Furthermore, the bodyweight of the animals was taken at each day of behavioral testing. The tests were always performed at 5 pm i.e., one hour before starting the next treatment.

Table 4: ***Selected Tests to Assess Behavioral Impairment caused by i.c.v. applied ETX***

Test	Parameters	Score
Open Field-Test (OF) (Honack and Löscher, 1995)	Hyperlocomotion / Sedation Ataxia Head Swaying Circling Stereotypic Sniffing Hypermetric Gait Wet Dog Shakes Flat Body Posture	0 - absent 1 - equivocal 2 - present 3 - intense
Hyperexcitability Test (HET) (Rice et al., 1998)	1. Approach-Response Test	1 - no reaction 2 - the rat is sniffing at the object 3 - the rat moves away from the object 4 - the rat is freezing 5 - the rat jumps away from the object 6 - the rat attacks the object
	2. Touch-Response Test	1 - no reaction 2 - the rat is moving toward the object 3 - the rat moves away from the object 4 - the rat is freezing 5 - the rat is moving toward the touch 6 - the rat is moving away from the touch 7 - the rat jumps away with or without vocalization
	3. Finger-Snap Test	1 - no reaction 2 - the rat jumps slightly (normal reaction) 3 - the rat jumps dramatically
	4. Pick-Up Test	1 - very easy 2 - easy with vocalization 3 - more difficult, the rat rears and faces the hand 4 - the rat is freezing 5 - difficult, the rat is avoiding the hand 6 - very difficult, the rat behaves defensively, and may attack the hand
Rotarod-Test (Dunham and Miya, 1957)	2 min on a rotating rod	Test passed at the 1st, 2nd or 3rd trial

2.8 Data analysis and statistics

In order to evaluate the epileptic activity in GAERS, three parameters were analyzed after seizure detection: the cumulative time in SWDs, the number of epileptic incidences, and the mean duration of the individual seizures. To assess time depended changes of epileptic activity after treatment, line graphs were plotted to display quantitative values of the distinct parameter within one-hour bins over the entire time of recording. To quantify the change of epileptic activity after drug application in a direct within-animal comparison, the percentage of control was computed for each animal individually.

$$\text{percentage of control } = \frac{Epileptic\ activity\ after\ drug\ injection}{Epileptic\ activity\ after\ vehicle\ injection} * 100$$

However, as percentage of control and the control value (epileptic activity after vehicle injection) are mathematically coupled, the statistical analysis between these two values could be misleading (Tu, 2016). Therefore, all the statistical tests reported in this thesis were performed on the averaged group data per hour computed over a time window of interest (12 h, 5 h, or 2 h) compared to the control group.

The data was statistically analyzed using the GraphPad Prism 8 Software (Graph-Pad Software, San Diego, CA, USA). The D'Agostino-Pearson test was used to determine if the data were normally distributed. For all data, a parametric test could be used. Drug effects were assessed by repeated-measures analysis of a one-way analysis of variances (ANOVA) or a two-way ANOVA, followed by post-hoc testing for individual differences with the Tukey's test. The data were presented as mean ± stand error of the mean (SEM). Statistically significant differences are highlighted by asterisks depending on the p-value: (*)$P \leq 0.05$, (**) $P \leq 0.01$,(***) $P \leq 0.001$, (****) $P \leq 0.0001$.

3 Results

In 25 – 30 % of people diagnosed with epilepsy, seizures cannot be effectively suppressed with standard pharmacotherapy (World Health Organization, 2006). A general problem of systemic drug therapies of brain diseases is the limited permeability of the blood-brain-barrier (BBB), which is restricting the accessibility of the central nervous system (CNS) for many drugs. It thus remains challenging to reach therapeutic drug concentrations at the desired site of action. Accordingly, there is great interest in developing new therapeutic strategies to improve CNS drug accessibility and control brain diseases like epilepsy. In this study, the potential of localized pharmacotherapy was investigated. To this end, the effect of intracerebral drug application was explored in the Genetic Absence Epilepsy Rats from Strasbourg (GAERS).

3.1 EEG-based analysis of seizure activity in GAERS

GAERS represent one of the best-established models for generalized epilepsy and the pathological neuronal activity underlying the epileptic seizures have been described in detail by Marescaux et al. (1992). The quantification of this epileptic activity is a particularly precise tool for assessing the efficacy of antiepileptic therapy. Therefore, it was essential to establish high-quality EEG recordings in our laboratory and compare patterns of pathological activity with those reported in the literature, to implement efficient seizure detection in GAERS.

Analysis of EEG signals revealed clean phase-locked oscillations consisting of a spike followed by a slow wave, with spike amplitudes ranging between 0.2 and 1.2 mV (fig. 3.1), resembling those previously described for this model in the literature (Danober et al., 1998). The distinct morphology of the spike-and-wave discharges (SWDs) was consistent over all epileptic events. However, there was variability in the duration of seizures episodes: some events comprised only a few spikes, whereas others lasted for several minutes (fig. 3.1A). Both seizure onset and termination were abrupt, and during interictal phases, the animals showed regular brain activity. The spectrogram of SWDs displayed nearly horizontal energy ridges indicating a harmonic structure of the signal (fig. 3.1B).

The fundamental frequency, which describes the first harmonic, was detected around ~7 Hz in the power spectrum and the spectrogram (fig. 3.1B and D). These findings agree with the key observation that SWDs are a quasi-periodic signal (Hese et al., 2003).

The autocovariance is strongly related to the spectral analysis and is thus a useful tool to assess rhythmic activity, such as SWDs, in EEG data (fig. 3.1C)(Rodgers et al., 2015). The autocovariance plot shows two repeating peaks varying in amplitude and phase (fig. 3.1C). The flatter curve corresponds to the wave complex; the higher peak corresponds to the spike complex. Both peaks appear approximately every 0.14 s, which again reflects the fundamental 7 Hz SWD-frequency and its harmonics. Thus, the autocovariance reflects amplitude, frequency, and the morphology of SWD complexes.

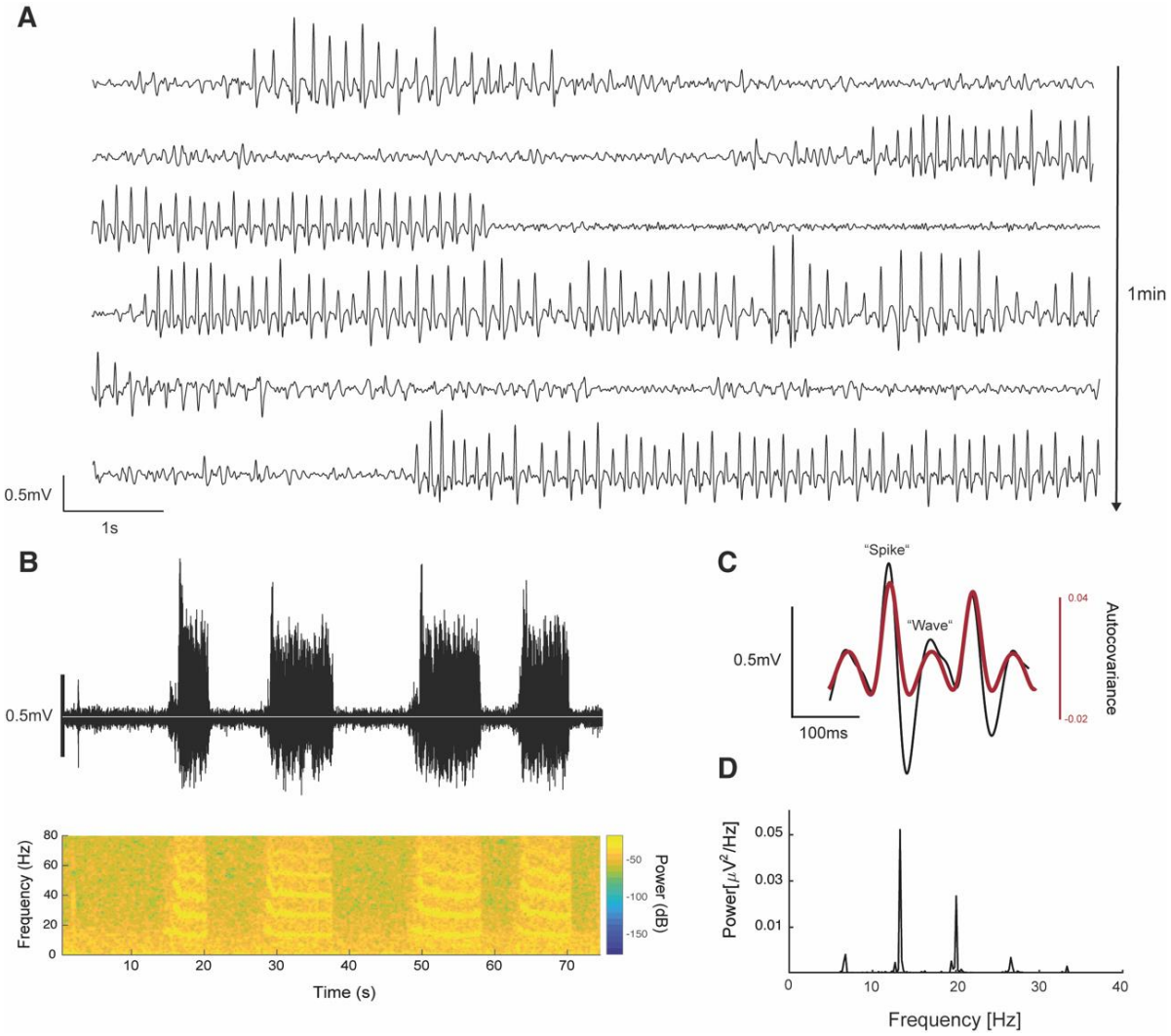

Figure 3.1: EEG recordings and analysis of epileptic activity in GAERS
A) Example EEG recording showing several SWD epochs. The characteristic morphology of the SWDs remains constant over, within, and between individual epochs. However, the duration of SWD epochs shows variability. B) The upper trace shows a 75 s EEG fragment containing four SWD epochs. Below the EEG, the corresponding spectrogram is displayed. The spectrogram highlights the intense rhythmic activity and harmonic patterns of the SWDs. C) The black trace shows two SWD complexes with the corresponding scaled and superimposed autocovariance function (red trace). The typical "spike" and "wave" complexes in the EEG recording, which are characteristic for absence seizures, are highlighted. D) The power spectrum of a five-second SWD epoch, displaying the fundamental frequency of ~7 Hz and its harmonics.

3.2 Automated detection of SWDs in the cortical EEG of GAERS

The automated detection of SWDs would allow fast and consistent quantification of seizures in GAERS. The EEG recordings showed prominent features of SWDs based on amplitude, frequency, and waveform morphology (fig. 3.1), representing ideal conditions for implementing an automated seizure classification system. Therefore, a classifier was trained in MATLAB on a dataset of 3600 seconds of EEG recordings with the computed autocovariance that was used as feature vector. The thereby implemented classifier was then applied to a test dataset in order to assess its performance. The test dataset consisted of a 36000-second-long EEG recording from GAERS (fused 10-minute datasets from each animal recorded within this study). This dataset had been pre-classified into "ictal" and "interictal" events by visual inspection. Visual inspection revealed that the animals spend approximately 10 % of the recorded time in seizures since 32662 seconds were classified as "interictal" and only 3338 seconds as "ictal" (fig. 3.2B). Furthermore, this counting showed that the dataset was imbalanced, which is essential to note when assessing the classifier's performance (Sun et al., 2009). An imbalanced dataset is characterized as having many more instances of one class (in our case, "interictal" events) compared to the other class ("ictal" events).

The confusion matrix visualizes the performance of automated seizure detection by presenting all false positive (orange), false negative (red), true positive (blue) and true negative (white) classifications (fig. 3.2). An exemplary performance analysis, tested on one animal, is shown in figure 3.2A. Highlighted detection errors in the EEG plot demonstrated that most false classifications occur either at the beginning or the end of a seizure.

The final evaluation of automated seizure detection over the complete test dataset, with the corresponding confusion matrix and accuracy, is shown in figure 3.2B. The confusion matrix reflected a relatively low and even number of false positive and false negative detections. The classifier showed an overall accuracy above 99 %; however, as the dataset was imbalanced, the accuracy measure could be a misleading metric to evaluate the performance of classification (Sun et al., 2009). Accordingly, we also analyzed the F-Score. The F-Score considers both the recall and the precision of "ictal" events and is consequently a more realistic measure of the SWD detection performance. Recall denotes the proportion of actual ictal or interictal events that were retrieved correctly, while precision denotes the proportion of retrieved ictal or interictal events that were identified correctly. The F-Score for ictal events was above 95 %, which was considered adequate for the purpose of this study.

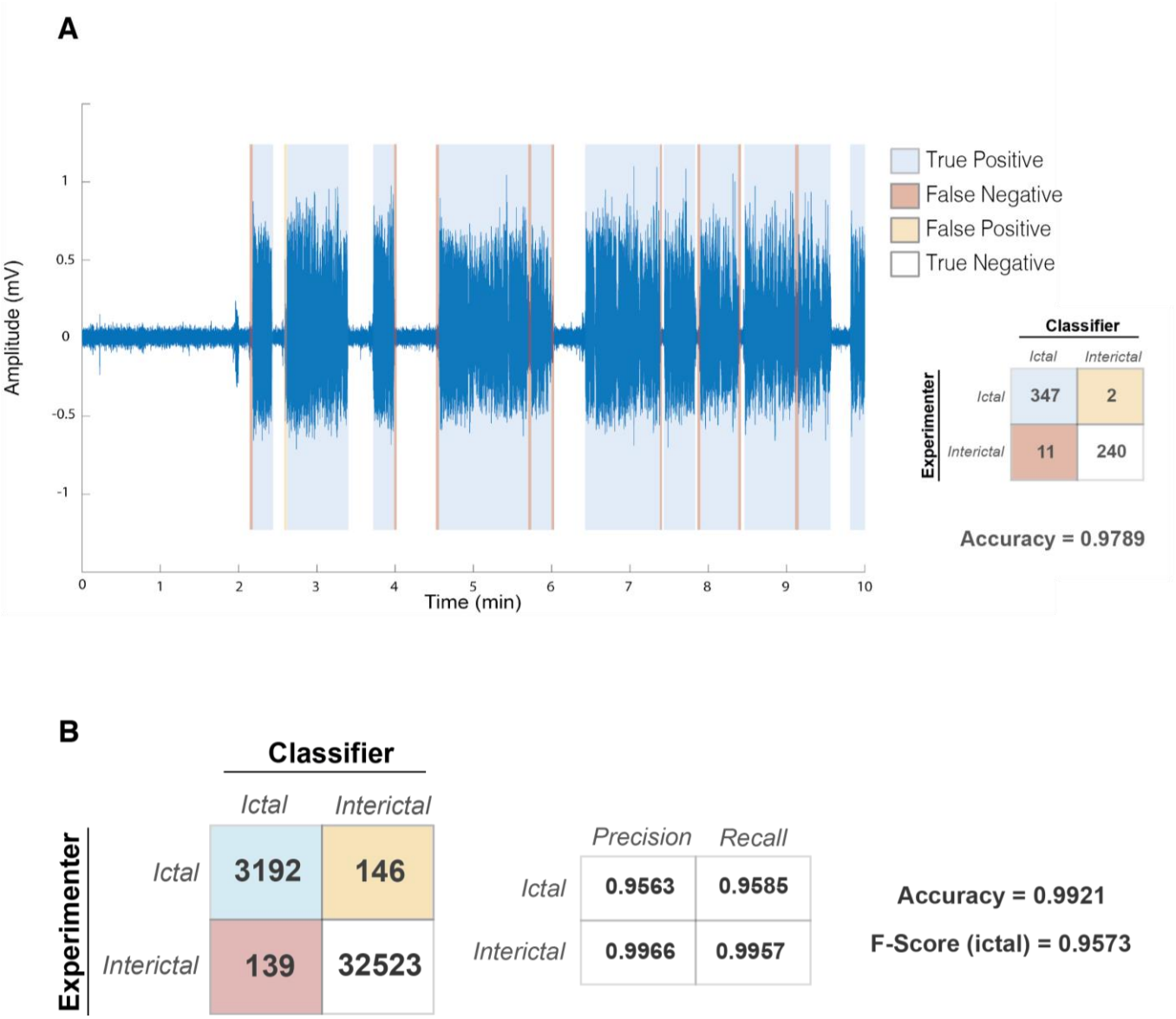

Figure 3.2: Performance of automated seizure detection in GAERS
A) The left panel shows a 10 minutes long EEG recording (dark blue line) from one GAERS rat. Each second in the recording was classified either as "ictal" or "interictal" by both the experimenter and the automated seizure detection. The blue marked time windows represent correctly identified "ictal" events by the implemented classifier (true positive classification). Brain activity with no colored background indicates correctly classified "interictal" events (true negative classification). The EEG marked orange represents time sections that were incorrectly classified as "ictal" (false positive classification). The red time windows show incorrectly classified "interictal" events by automated detection (false negative classification). Interestingly false predictions appear always at the end or beginning of a seizure. The right panel shows the corresponding confusion matrix and the computed accuracy of the implemented classifier. B) The final performance of automated seizure detection, used in this study, is visualized via a confusion matrix (left panel). In order to better evaluate the performance of the classifier, precision and recall were also computed for "ictal" and "interictal" periods (middle panel). The accuracy measurement takes all values from the confusion matrix into account, whereas the F-score for ictal events considers recall and precision (right panel).

3.3 The circadian dynamics of spike and wave discharge

It has been shown that the vigilance level of GAERS strongly influences the occurrence of epileptic activity (Lannes et al., 1988). Therefore, it is essential to decouple the circadian dynamics underlying seizure occurrence from antiepileptic drug efficacy testing during the experimental phase. To examine the circadian dynamics of seizure activity in GAERS under drug-free conditions, all baseline recordings performed in this study were combined. The cumulative time in SWDs (fig. 3.3A), the number of SWDs (fig. 3.3B; green), and the mean duration of SWDs (fig. 3.3B; pink) were analyzed over 12 or 24h in one-hour bins.

As expected, we found that the cumulative time animals spend in seizures showed dynamics that closely followed the circadian rhythm (Van Luijtelaar and Coenen, 1988). Elevated and stable seizure activity during the first seven hours of the dark phase was followed by a noticeable increase of SWD activity between 1 pm and 4 pm, which was again followed by a steep drop in seizure activity towards the end of the dark phase (fig. 3.3A). In general, seizure activity was slightly decreased during the light phase; however, the cumulative time in seizures increased again towards the end of the day. It is of interest to note that 46 of the individual recordings were performed during the 12 hours of the dark phase (6 pm – 6 am), whereas only an additional 15 animals were recorded over 24h (6 pm – 6 pm). This explains a higher variability in seizure occurrence during the light phase (fig. 3.3).

The cumulative seizure duration is a composite of the incidences and the mean duration of SWDs (fig. 3.3B). The number of SWDs stayed almost stable over the complete 24h with 29.35 ± 0.72 (mean ± SEM) of SWD incidences per hour. Only at the end of the dark period, during deep slow-wave sleep (Van Luijtelaar and Coenen, 1984), the number of seizures dropped noticeably to 22.3 ± 1.65 (mean ± SEM) seizures per hour. The variation of the mean duration of SWDs over time more closely followed the described dynamics of total time spend in seizures. Particularly notable is the peak after 10 hours in the dark period, showing an individual seizure length of 15.15 ± 0.50s (mean ± SEM) followed by a drop of more than six seconds between 5 am and 6 am.

Baseline recordings showed that the epileptic activity is highly dependent on the sleep-wake states of the animals. Hence drug efficacy was always tested at the same time of day to control circadian effects. In the first few hours of the dark period, we observed a high incidence of SWDs and stable seizure activity; consequently, we chose to test for antiepileptic drug effects during this time period.

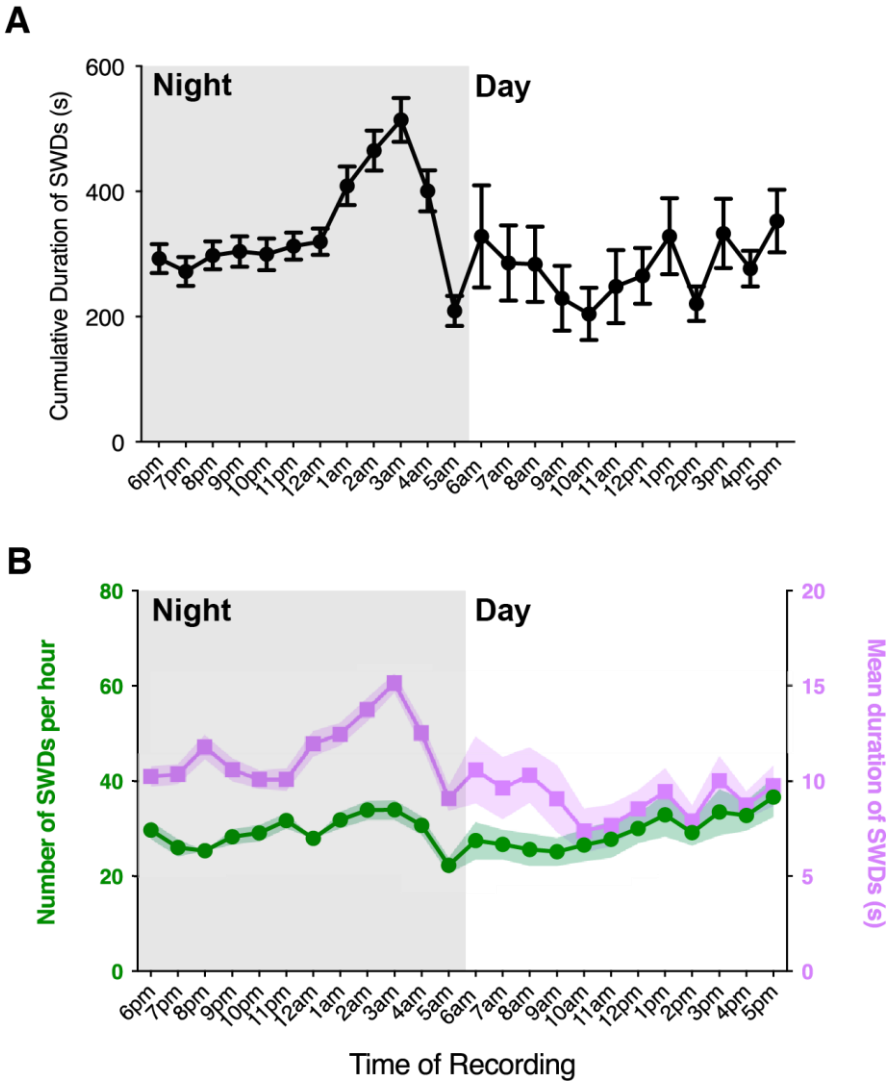

Figure 3.3: SWD activity follows a circadian rhythm
A) The black line shows the temporal dynamics of the cumulative duration GAERS spent in seizures over 24h under drug-free conditions in one-hour bins. All baseline recordings performed in this study were included (graphs show mean ± SEM, Night: n=61, Day: n=15). Note the peak of cumulative time in SWDs between 3 pm and 4 pm, followed by a steep drop at the end of the dark phase. B) The number of SWDs is shown in green; the mean duration of SWDs is shown in pink (solid lines and symbols indicate the mean, shaded areas indicate ± SEM).

3.4 Systemic treatment of GAERS with VPA and ETX

The GAERS model has a nearly identical therapeutic profile as human absence epilepsy, and classical AEDs such as VPA and ETX show systemically good anti-absence efficacy at the therapeutic dose (Marescaux et al., 1992). To analyze and compare the antiepileptic activity of VPA and ETX in more detail, the therapeutic response was evaluated over a time course of 12 or 24h after systemic (i.p.) drug application. We analyzed the cumulative time of SWDs, the number of epileptic incidences, and the mean duration of seizures. By analyzing these different parameters, we gain insights into the mechanisms and brain regions controlling SWDs and can thus possibly retrace how and where seizure suppressing drugs exert their action. Whereas the number of SWDs is mainly determined by the excitability of the cortex, the mean duration is affected by different endogenous mechanisms involved in aborting ongoing SWDs in the thalamus (Lüttjohann and van Luijtelaar, 2015).

ETX

The intraperitoneal injection of 100 mg/kg ETX (n=7) (Marescaux et al., 1992) caused an immediate reduction of epileptic activity (fig. 3.4; pink trace). The reduction of SWDs was nearly complete during the first five hours after drug application. During the next four hours, the seizure activity very slowly increased. After 10 hours, the cumulative time of SWDs peaked, followed by a sharp drop of epileptic activity towards the end of the dark period. This peak's timing paralleled the endogenous rhythm of seizure occurrence in GAERS (cf. fig. 3.3) and was also observed in controls (n=13; fig. 3.4A). Consequently, for the recording time of 12 hours, the cumulative time in seizures after treatment was significantly lower ($p=0.0003$) than in the controls. All statistical tests reported in this manuscript were performed on the absolute values (average per hour) of the three parameters within a specific time window (here 12 hours) (fig. 3.4; middle panels).

To better quantify the reduction of epileptic activity after drug application and to consider inter-individual differences of GAERS, the percentage of control was computed for each animal individually (fig. 3.4; right panels). On average, the systemic treatment, with the therapeutic dose of ETX (100 mg/kg), reduced the cumulative time in seizures by 86.47 ± 2.8 % (mean ± SEM) compared to vehicle injection over the complete 12h of recording.

The temporal dynamics are strikingly similar for cumulative time in seizures and the number of SWDs (fig. 3.4A and B), which could indicate that the decreased number of seizures can, to a large extent, explain the antiepileptic effect of ETX. Over the first nine

hours only a few seizures are evident followed by a peak in seizure number after 10 hours and a subsequent drop of seizures towards the end of the dark phase (fig. 3.4B; left panel). Furthermore, over the complete 12 hours the number of SWDs is decreased by approximately 86.81 ± 2.0 % (mean ± SEM) after ETX treatment compared to vehicle injection, which coincides with the percentage of change shown for cumulative time in seizures (fig. 3.4A and B; right panel). Accordingly, the number of seizure incidences after treatment was significantly lower ($p = <0,0001$) than in the controls (fig. 3.4B; middle panel).
Systemically applied ETX effects the mean duration of SWDs differently compared to the number of epileptic incidents (fig. 3.4C). After drug application, during the first five hours, the mean duration of SWDs is reduced compared to vehicle injection. However, it is important to note that, on average less than one seizure occurs per hour during this period of time. Therefore, the mean duration was computed over a small number of epileptic incidences and can be considered inconclusive. Six hours after ETX treatment, the mean duration of SWDs has completely recovered, and no differences between the control and the experimental group are visible (fig. 3.4C; left panel). Consequently, for the recording time of 12h, no significant difference could be identified for the mean duration of SWDs between ETX and vehicle injection ($p = 0.44$) (fig. 3.4C; middle panel).

To evaluate if the therapeutic efficacy of ETX exceeds the described 12 hours, five additional animals were i.p. injected with the therapeutic concentration of the AED (100 mg/kg) and recorded for 24 hours (fig. 3.5). The cumulative duration of SWDs shown in figure 3.5 indicates that the seizure reducing effect did not persist beyond the first 12 hours after ETX application.

VPA

The systemic treatment with the therapeutic concentration of 200 mg/kg VPA (n=6) (Marescaux et al., 1992) resulted in an immediate and nearly complete reduction of seizure activity in GAERS (fig. 3.4; green trace). However, already three hours after VPA treatment, a steep increase of the cumulative duration of SWDs is visible. Consequently, when compared to the control experiment, no difference in cumulative SWD duration was obvious ($p = 0.64$). Similarly, mean seizure duration and the number of seizures dropped at the beginning of the recording and quickly recovered after about two hours (fig. 3.4B and C). As the antiepileptic efficacy of VPA only lasted two hours after treatment, none of these parameters showed a statistically significant change compared to the control experiments over the 12h recording period.

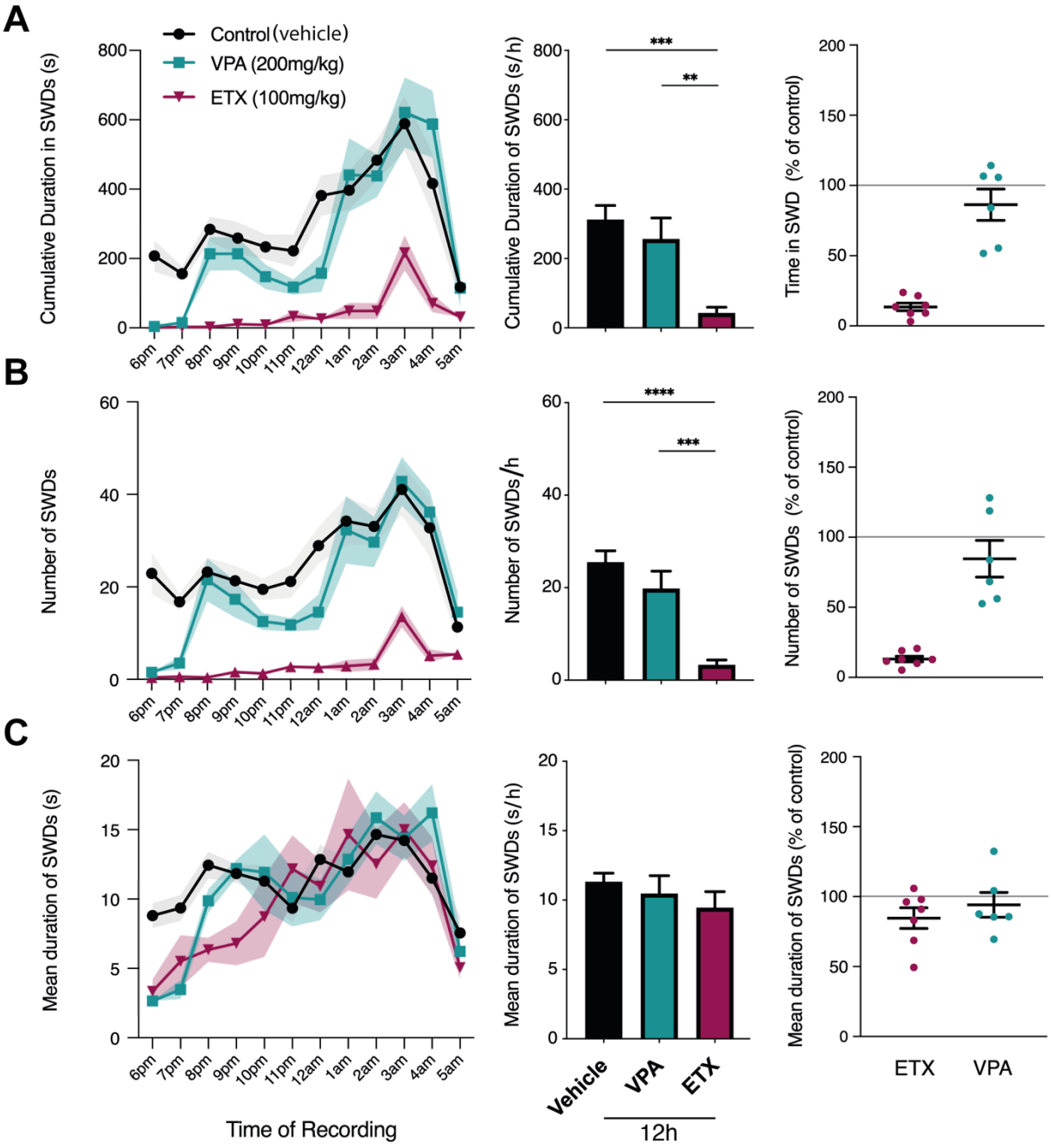

Figure 3.4: Epileptic activity in GAERS during the first 12 hours following systemic treatment with VPA or ETX

The analysis of epileptic activity is divided into A) the cumulative duration in SWDs, B) the number of SWDs, C) the mean duration of SWDs. The left panels show the time course of the respective parameter over 12h (one-hour bins) after systemic treatment with the therapeutic dose of either VPA (green; n=6) or ETX (pink; n=7) (solid lines and symbols indicate the mean, shaded areas indicate ± SEM). The bar plots in the middle panels display the average/hour (± SEM) of the distinct parameter computed over the complete 12 hours of recording. The right panels show the analysis of the percentage of control within animals, with dots representing individual animals. The statistical analysis was performed by one-way ANOVA with Tukey's post-hoc test. (**) $P \leq 0.01$,(***) $P \leq 0.001$, (****) $P \leq 0.0001$.

Comparison of systemic treatments with ETX and VPA showed longer antiepileptic efficacy for ETX, in accordance with the pharmacokinetics (e.g., half-life and clearance) of the respective drugs (cf. Chapter 1.4 and Löscher, 2007). Considering the entire 12 h after drug application, the systemic treatment with ETX was significantly more efficient in reducing cumulative time in SWDs ($p = 0.004$) and the number of seizures ($p = 0.0003$) than VPA.

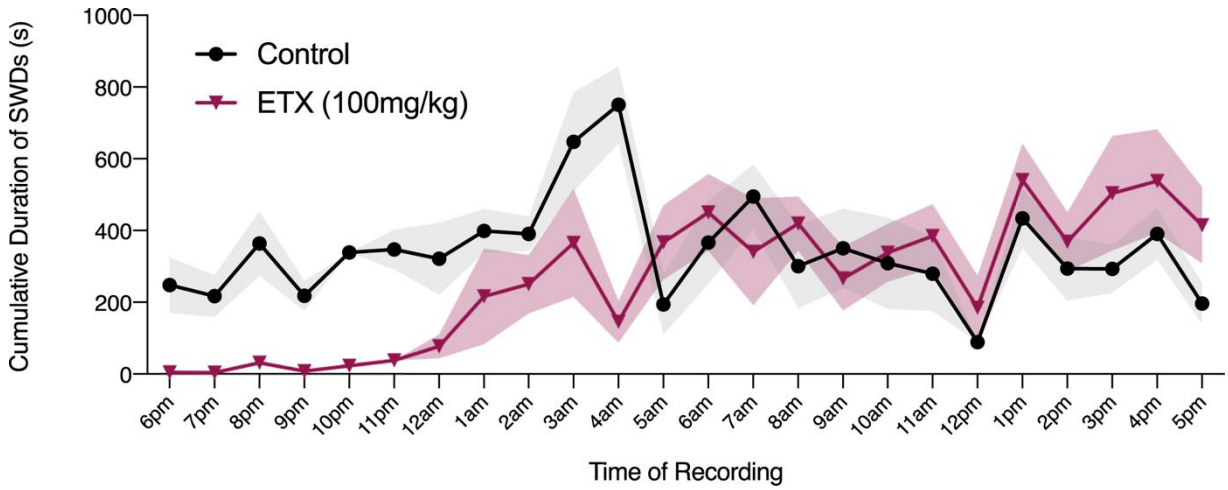

Figure 3.5: Epileptic activity in GAERS after systemic treatment with ETX over 24 hours
The time graph shows the cumulative duration of SWDs over 24h in one-hour bins after systemic treatment with the therapeutic dose of ETX (pink; n=5). The control recordings (black; n=5) show the cumulative duration in SWDs after vehicle injection (solid lines and symbols indicate the mean, shaded areas indicate ± SEM). Over the first 11h, GAERS show the expected reduction in SWDs, but the seizure reducing effect did not persist beyond 12h.

3.5 Intrathecal treatment of GAERS with VPA and ETX

Two key areas involved in initiation and propagation of absence seizures are the somatosensory cortex and the dorsal thalamus (for a review see Meeren et al., 2005), which both lay in proximity to the ventricular system. Thus, we reasoned that i.c.v. injections of antiepileptic drugs might represent an efficient route of drug application, bypassing the blood-brain-barrier (BBB) (cf. fig. 2.2). Therefore, we implanted guide cannulas into the right lateral ventricle and gauged the effectiveness of ETX (fig. 3.6) and VPA (fig. 3.7) for intracranial applications. To find therapeutic concentrations, a dose-response experiment was performed using doses between 0.3 and 2.5 mg for both drugs.

Unilateral i.c.v. application of ETX

Modulated onto the time course, we observed a dose-dependent reduction of SWDs between 1.2 mg and 2.5 mg but not for 0.3 mg or 0.6 mg ETX. The onset of the anticonvulsant effect showed a time delay of 1 to 3 hours and lasted between 4 – 5 hours with some variability (fig. 3.6A; left panel).
To take into account the limited duration of the anticonvulsant activity, we evaluated in more detail the therapeutic effect of the different ETX doses for the five consecutive hours showing the most robust decrease in epileptic activity. The five-hour time-window was chosen based on the visual inspection of SWD dynamics over time (fig. 3.6; left panels) and on our finding of the pharmacokinetics of ETX after systemic treatment (fig. 3.4; pink trace). The most effective time window – termed “best five hours” from now on – was determined via a sliding window separately for each animal, as we observed intraindividual variability. On average, the best five hours started after 1.9 hours.

The statistical analysis and the within animal percentage of control for all parameters were based on these best five hours after ETX treatment. The dose of 0.3 mg ETX showed no appreciable effect, whereas 0.6 mg ETX already reduced seizure activity by 24.24 ± 8.42 % (mean ± SEM)(fig. 3.6A; right panel), although this was statistically not significant different from vehicle injection (fig. 3.6A;middle panel). The dose of 2.0 mg ETX showed the most potent anticonvulsant effect with a reduction to 58.25 ± 6.0 % (mean ± SEM) in cumulative time in SWD. Based on the absolute values this was significantly different from the controls ($p = <0.0001$). Within the best five-hour time window, the treatment with the 2.5 mg dose induced a slightly weaker anti-absence efficiency as the treatment

with 2.0 mg ETX (-41.24 ± 8.38 % (mean ± SEM)). However, the absolute values showed still significant different between vehicle und 2.5 mg ETX injection.

Indeed, even over the complete 12 hours, the time in seizures after i.c.v. treatment with 2.0 mg ETX was significantly lower (data not shown; p=0.02) than in the controls. Because of a sharp increase in seizures after midnight, the highest dose of 2.5 mg ETX was noticeable less effective than 2 mg ETX (fig. 3.6A; left panel) over the entire recording time. Compared to vehicle injection, the seizure duration even slightly increased by 20.37 ± 25.78 % (mean ± SEM; data not shown), although this was not statistically significant (data not shown, p=0.92). Interestingly, the observations of an inverted U-shaped relation between ETX dose and seizure suppression has previously been reported for direct injections of ETX into the thalamus (Richards et al., 2003).

Only the ETX doses which induced statistically significant seizure reduction in the rats – 1.2 mg, 2.0 mg, and 2.5 mg – were included in the graphs of figure 3.6B and C. Over the best five hours, the treatment with the most promising dose of 2.0 mg ETX evoked a significant decrease in both the number of SWDs (p=0.0005) and the mean duration of SWDs (p=< 0.0001)(fig. 3.6B and C; middle panels). Interestingly, the AED induced a higher percentage of change for the mean duration of SWDs (-36.5 ± 5.13 % (mean ± SEM)) compared to the percentage of change of seizure incidences (-28.1 ± 9.59 % (mean ± SEM) (fig. 3.6B and C; right panels). A similar outcome was observed for the i.c.v. treatment with 2.5 mg. However, the application of 1.2 mg resulted in a significant reduction in the number of seizures (p=< 0.0001) but not for the mean seizure duration of SWDs (p=0.6).

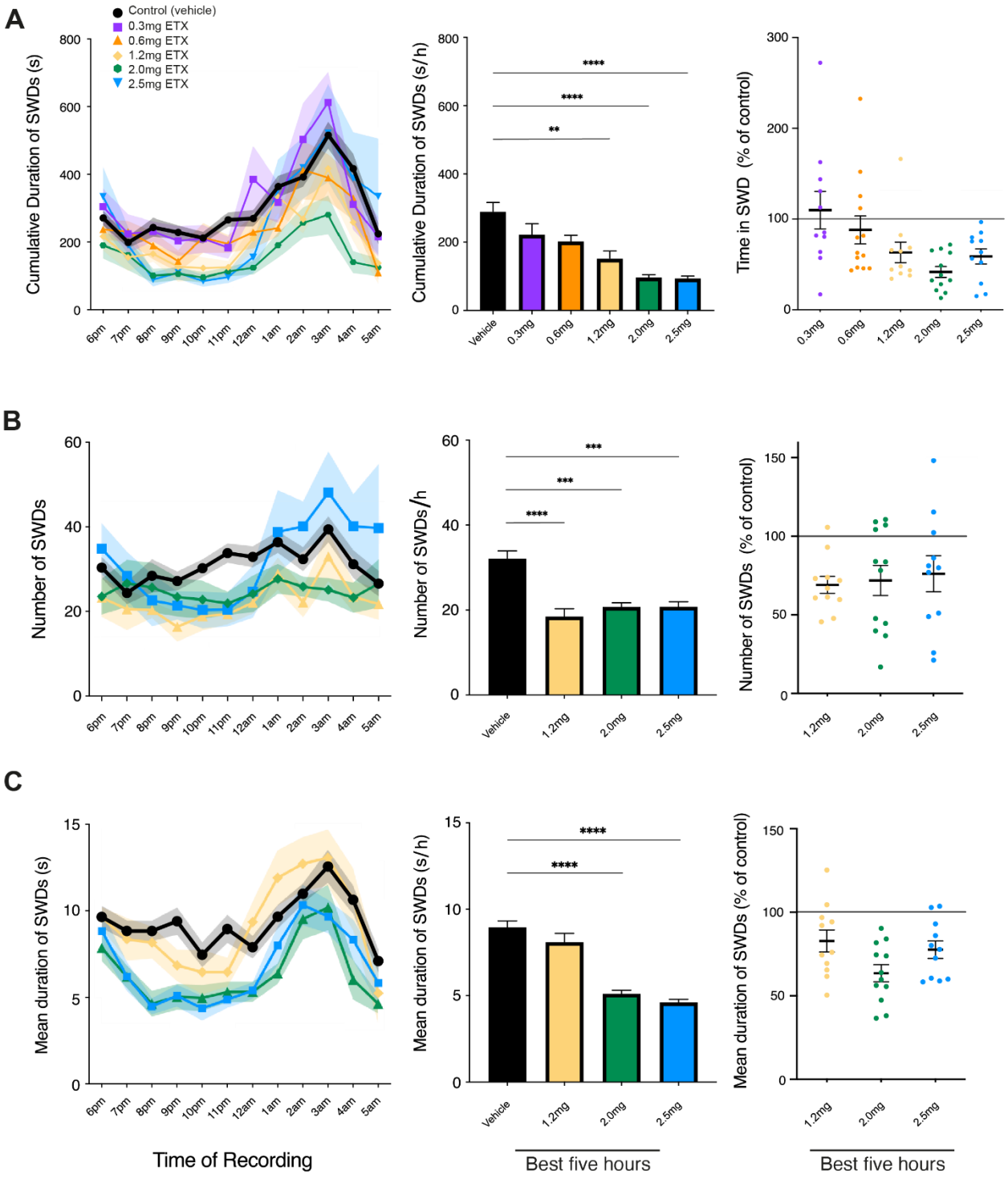

Figure 3.6: Epileptic activity in GAERS after i.c.v. treatment with different doses of ETX
The analysis of epileptic activity is split into A) the cumulative duration in SWDs, B) the number of SWDs, C) the mean duration of SWDs. Different colors denote different doses of ETX (black = control; purple = 0.3mg; orange = 0.6mg; yellow = 1.2mg; green = 2.0mg; blue = 2.5mg).The left panels show the time course of the respective parameter over 12h (one-hour bins) after i.c.v. treatment with different doses of ETX (solid lines and symbols indicate the mean, shaded areas indicate ± SEM). The bar plots in the middle panels display the average/hour (± SEM) for the distinct parameter, considering the best five hours of recording. The right panels show the within animal analysis of the percentage of control for the best five hours. The dots represent individual animals. The statistical analysis was performed by one-way ANOVA with Tukey's post-hoc test. (*)P ≤ 0.05, (**) P ≤ 0.01,(***) P ≤ 0.001, (****) P ≤ 0.0001.

Unilateral i.c.v. application of VPA

The i.c.v. treatment with VPA, regardless of the dose, did not induce complete seizure suppression; however, a dose-dependent antiepileptic effect could be identified.
Interestingly, the results imply that the relatively low dose of 0.6 mg is the most promising local concentration (fig. 3.7A; left panel). The i.c.v. application of 0.6 mg induced the greatest drop in cumulative SWD duration. Also, the usage of 2.0 mg VPA locally induced suppression of SWD numbers in GAERS. The anticonvulsant effect appeared with a time delay of approximately two hours and lasted between two and three hours (fig. 3.7A; left panel). The treatment with other VPA concentrations did not result in an apparent decrease in seizure occurrence. Interestingly our analysis revealed, that on average, the animals injected with 0.3 mg VPA intraventricularly spend more time in seizures after treatment than the controls (fig. 3.7A; left panel). Independent of treatment, the time courses of epileptic activity followed the expected circadian rhythm (cf. fig. 3.3) with an initial period of stability followed by a peak between 2 am, and 4 am and a subsequent decline. Taking the entire 12-hour recordings into account, none of the doses showed a significant change in seizure activity compared to the control experiments ($p \geq 0.78$).

To take into account the limited duration of the anticonvulsant activity, we evaluated in more detail the therapeutic effect of the different VPA doses for the two consecutive hours showing the most robust decrease in epileptic activity. The two-hour time-window was chosen based on the visual inspection of SWD dynamics over time (fig. 3.7; left panels) and on our finding of the pharmacokinetics of VPA after systemic treatment (fig. 3.4; green trace). The most effective time window – termed “best two hours” from now on – was determined via a sliding window separately for each animal, as we observed intraindividual variability. The best two hours started on average 1.8 hours after treatment. Note that the i.c.v. injection of 0.3 mg VPA induced an increase of epileptic activity in GAERS. Thus, we chose for this dose a defined time window between 7 pm – 9 pm for the statistical analysis of SWD incidences and mean duration of seizures.

The 0.6 mg VPA was the only dose that statistically significantly affected the cumulative duration of SWDs compared to vehicle injection over the best two hours ($p=0.024$) (fig. 3.7A; middle panel). The i.c.v. treatment with 0.6 mg VPA reduces the time in seizures by 75.71 ± 4.66 % (mean ± SEM) compared to vehicle injection (fig. 3.7A; right panel). The i.c.v. application of 2.0 mg in GAERS reduced the cumulative time of SWDs by

about 63.5 ± 8.31 % (mean ± SEM), although this was statistically insignificant based on the absolute values.

For the purpose of clarity, only the doses which evoked noticeable changes in epileptic activity (0.3 mg, 0.6 mg, 2.0 mg) are shown in the graphs displaying the number of SWDs and the mean duration of SWDs in figure 3.7B and C. The treatment with the most effective dose of 0.6 mg VPA induced a significant decrease in the number of SWDs ($p=0.0009$) as well as in the mean duration of SWDs ($p=0.001$) compared to vehicle injection. Also, the local treatment with 2.0 mg VPA significantly reduced the number of SWDs ($p=0.0018$); however, the mean duration of SWDs was not significantly affected ($p=0.07$). The application of 0.3 mg VPA significantly promoted the emergence of SWDs ($p=0.007$) without an apparent impact on the mean duration of seizures (fig. 3.7B and C; middle panels).

When expressed as percentage of control in a within animal comparison, we found a reduction to 40.62 ± 7.93 % (mean ± SEM) in seizure incidences and to 63.97 ± 11.59 % (mean ± SEM) in mean SWD duration after treatment with 0.6mg VPA. In conclusion, the number of seizures was more effected by locally applied VPA of the most effective dose than the mean duration of SWDs (fig. 3.7B and C; right panels).

In summary, this analysis indicates that intra-ventricular injection of low dose of VPA or ETX produced a dose-dependent anticonvulsant effect. For VPA, we found the most potent anticonvulsant effects with 0.6 mg/animal, whereby increased doses did not increase the therapeutic effect. The dose of 0.3 mg VPA appeared to promote epileptic activity, indicating that the therapeutic window for intracerebroventricular anti-absence therapy with VPA is rather narrow. The local treatment with ETX showed strong anticonvulsant effectiveness for doses above 0.6 mg. The therapeutic effects of ETX lasted considerably longer than those of VPA. For ETX, we found a U-shaped relation between dose and seizure suppression with the strongest anticonvulsant effects at 2 mg/animal ETX with unilateral i.c.v. injections. We thus focused on this drug and dose for subsequent experiments.
We also found that i.c.v. treatment with the most effective VPA dose had a slightly higher effect on the number of SWDs than on the mean duration of SWDs. In contrast, the treatment with the most effective ETX dose showed the opposite result. These findings may indicate different sites of action after the local application of the two AEDs.

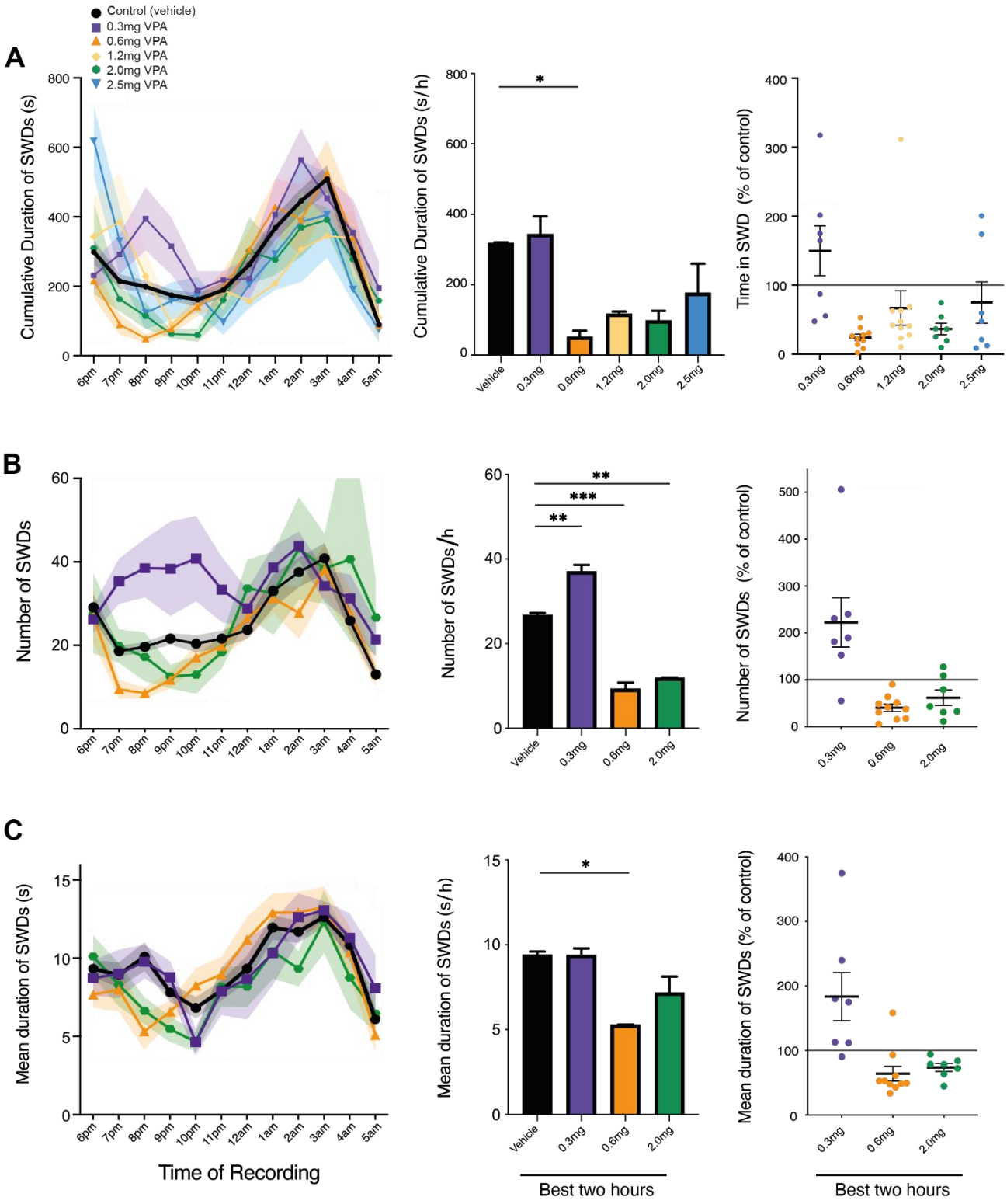

Figure 3.7: Epileptic activity in GAERS after i.c.v. treatment with different doses of VPA
The analysis of epileptic activity is divided into A) the cumulative duration in SWDs, B) the number of SWDs, C) the mean duration of SWDs. Different colors denote different doses of VPA (black = control; purple = 0.3 mg; orange = 0.6 mg; yellow = 1.2 mg; green = 2.0 mg; blue = 2.5 mg). Left panels show the time course of the respective parameter over 12h (one-hour bins) after i.c.v. treatment (solid lines and symbols indicate the mean, shaded areas indicate ± SEM). The bar plots in the middle panels display the average/hour (± SEM) for each parameter considering the best two hours of recording. The right panels show the within animal analysis as percentage of control for the best two hours. The dots represent individual animals. The statistical analysis was performed by one-way ANOVA with Tukey's post-hoc test. (**) $P \leq 0.01$,(***) $P \leq 0.001$, (****) $P \leq 0.0001$.

3.6 Intracranial versus systemic treatment with ETX

The previous results did show a strong anticonvulsant effect of i.c.v. treatment with low doses of ETX. However, it is uncertain if via the i.c.v. route quantitatively significant drug concentrations reach deep parenchymal tissue. It has been suggested that i.c.v. applied substances rapidly exchange between CSF and blood. Hence the observed therapeutic effects could rather result from a slow intravenous infusion via the CSF than from a direct penetration of brain tissue from the CSF (Pardridge, 2016). If this was true, the intravenous (i.v.) injection of low doses ETX should result in similar anti-absence efficacy compared to i.c.v. treatment. In order to address this question, we treated an additional eight animals with the doses of 2 mg/animal ETX sequentially via i.c.v., i.p. or i.v. administration routes and directly compared the antiepileptic efficacy.

In compliance with the previous results, the i.c.v. application of ETX induced a strong seizure reduction by more than 66.69 ± 3.31 % (mean ± SEM) over the best five hours compared to vehicle injection. In strong contrast, administration of 2 mg ETX either via i.v. or i.p. injection did not produce any attenuation of SWDs considering percentage of control (i.v. = 104.89 ± 9.95 %, i.p. = 94.44 ± 19.40 % (mean ± SEM); fig. 3.8A; right panel). Statistical analysis using the average time GAERS spend in seizures after vehicle injection (n=24) showed a small but significant decrease in cumulative seizure duration for the i.v. treatment with 2.0 mg ETX (p=0.035) but not for the i.p. injection (p=0.18) (fig. 3.8A; middle panel). The comparison between different administration routes confirmed a significantly better anticonvulsant effect over the best five hours for i.c.v. application of ETX versus i.p. or i.v. application (i.c.v. vs. i.v.: p=0.0244; i.c.v. vs. i.p.: p=0.0046, fig. 3.8A; middle panel).
Furthermore, if seizure suppression was quantified for the entire recording time of 12 hours, we found that i.p. or i.v. administration had no significant effect on SWD, but i.c.v. administration caused a significant reduction in seizure duration (data not shown, p=0.007). These results indicated that the therapeutic efficacy of ETX strongly depended on the administration route and revealed that i.c.v. application is by far more efficient than systemic routes of drug application in low doses.

Finally, we directly compared the efficiency and dynamics of seizure suppression after ETX treatment by either i.c.v. application of 2 mg/animal ETX (all tested animals n=20) or systemic treatment with 100 mg/kg ETX (n=7) (fig. 3.8 B).

Whereas seizure suppression started immediately after i.p injection, it was delayed approximately 2 hours after i.c.v. injection. Besides, the duration of the anticonvulsive effect was extended after i.p. high-dose application compared to i.c.v. low-dose application. The cumulative time in SWDs was decreased by approximately 85% after i.p. and by 58% after i.c.v. injection for the best 5 hours, which suggested that high-dose i.p. application is about 25% more efficient than low-dose i.c.v. application (fig. 3.8B; right panel). In summary, these data indicated that unilateral i.c.v. application of low doses of ETX showed a delay in onset, shorter duration, and slightly lower amplitudes of therapeutic efficacy when compared to standard high dose systemic therapy.

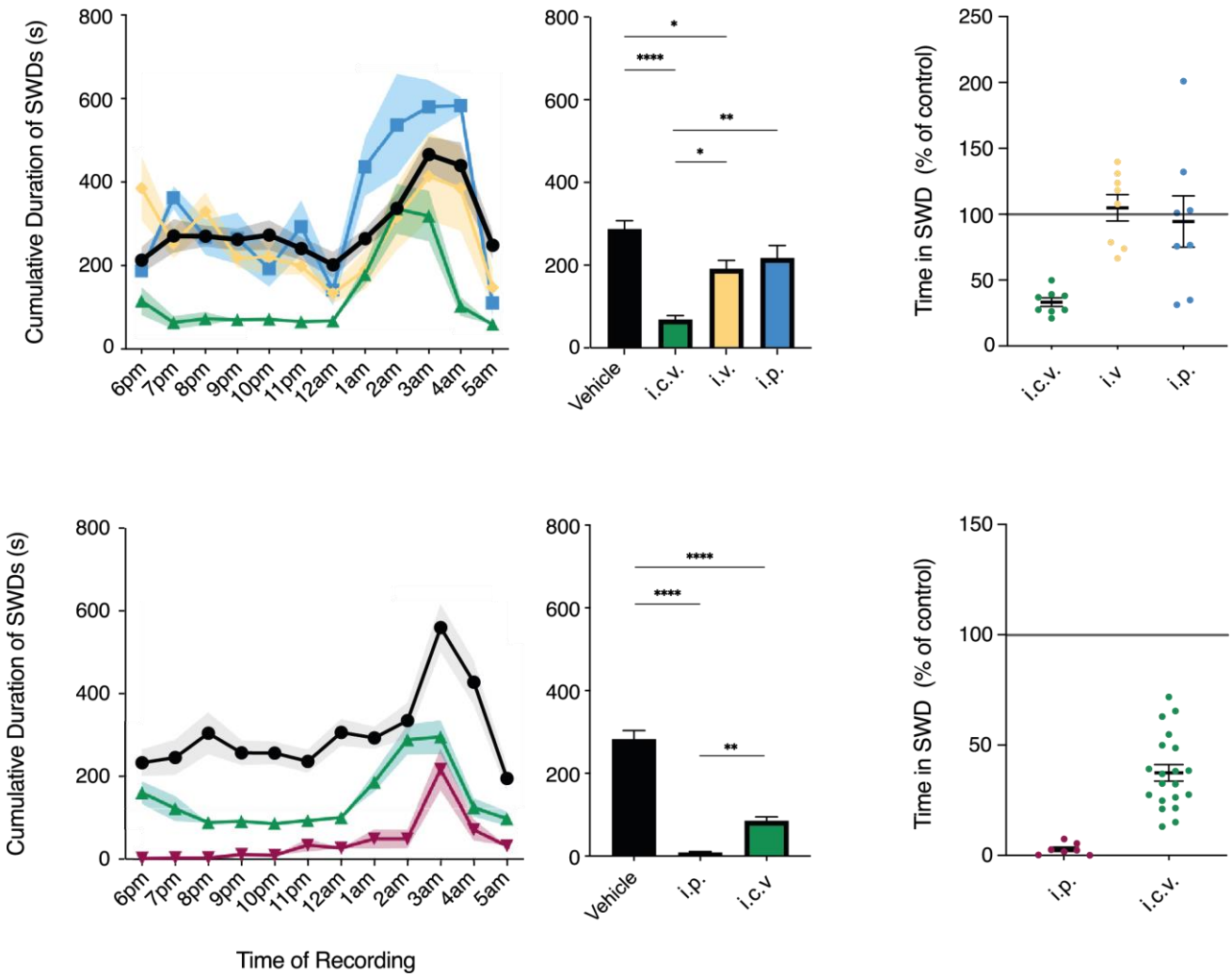

Figure 3.8: Epileptic activity in GAERS after ETX treatment using different application routes

The right panels show the time course of the cumulative duration in SWDs over 12h (one-hour bins) after treatment (solid lines and symbols indicate the mean, shaded areas indicate ± SEM). The bar plot in the middle represents the average ± SEM time GAERS spend in seizures within one hour, considering the most effective five hours after drug administration. The right panels show the within animal analysis of the percentage of control for the most effective 5 hours. The dots represent individual animals. Different colors denote different application methods (black = control; blue = i.p. (2 mg/animal); yellow = i.v. (2 mg/animal); green = i.c.v. (2 mg/animal); pink = i.p. (100 mg/kg)). A) Compares i.c.v. application with systemic treatment (i.v. or i.p.) utilizing the same drug dose (2 mg/animal; n=8). B) Compares i.c.v. application of 2 mg/animal ETX (n=20) with the standard therapeutic dose (100mg/kg) of intraperitoneal applied ETX (n=7). The statistical analysis was performed by one-way ANOVA with Tukey's post-hoc test. (*)P ≤ 0.05, (**) P ≤ 0.01,(***) P ≤ 0.001, (****) P ≤ 0.0001.

3.7 ETX distribution throughout different body compartments after i.c.v. and systemic administration

The intracranial application of ETX significantly reduced the occurrence of SWDs in GAERS at a dose of 2.0 mg/animal, as shown in the previous results (fig. 3.6). Furthermore, we could show that at these low doses, the i.c.v. application of ETX is more efficient compared with systemic drug application (fig. 3.8). Increased intracranial drug concentrations, after localized drug injection, could explain these results.

In order to compare how the application routes – i.c.v. or i.v. – affect ETX distribution in the brain, the drug concentrations were analyzed in blood plasma, CSF, and brain tissue after the respective treatment. For systemic ETX application, it has been reported that the AED rapidly and evenly distributes (distribution volume of 0.7 l/kg) throughout the body, including brain tissue and CSF (Gören and Onat, 2007). We were particularly interested in the ETX concentration within brain areas involved in absence epilepsy, i.e. thalamus and somatosensory cortex (Meeren et al., 2005). To further investigate whether the distinct time course of seizure suppression (fig. 3.6A; left panel) is related to the distribution properties of ETX, samples were taken at three different time points after drug injection (15 min, 1 hour, and 4 hours). Finally, we analyzed if drug concentrations differed between brain hemispheres, as ETX was applied unilaterally.

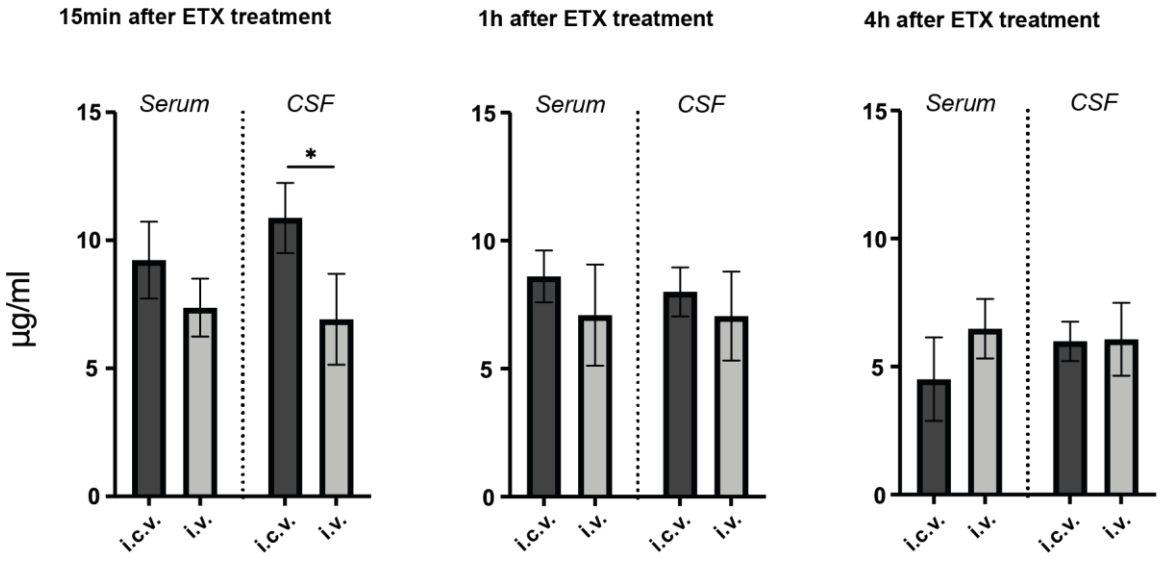

Figure 3.9: ETX distribution in CSF and plasma after i.v. or i.c.v. treatment
The ETX concentration (µg/ml) in CSF and plasma after i.c.v. (2mg/animal; dark grey) or i.v. (2mg/animal; light grey) drug administration at different time points (mean ± SEM). The statistical analysis was performed by one-way ANOVA with Tukey's post-hoc test. (*)P ≤ 0.05.

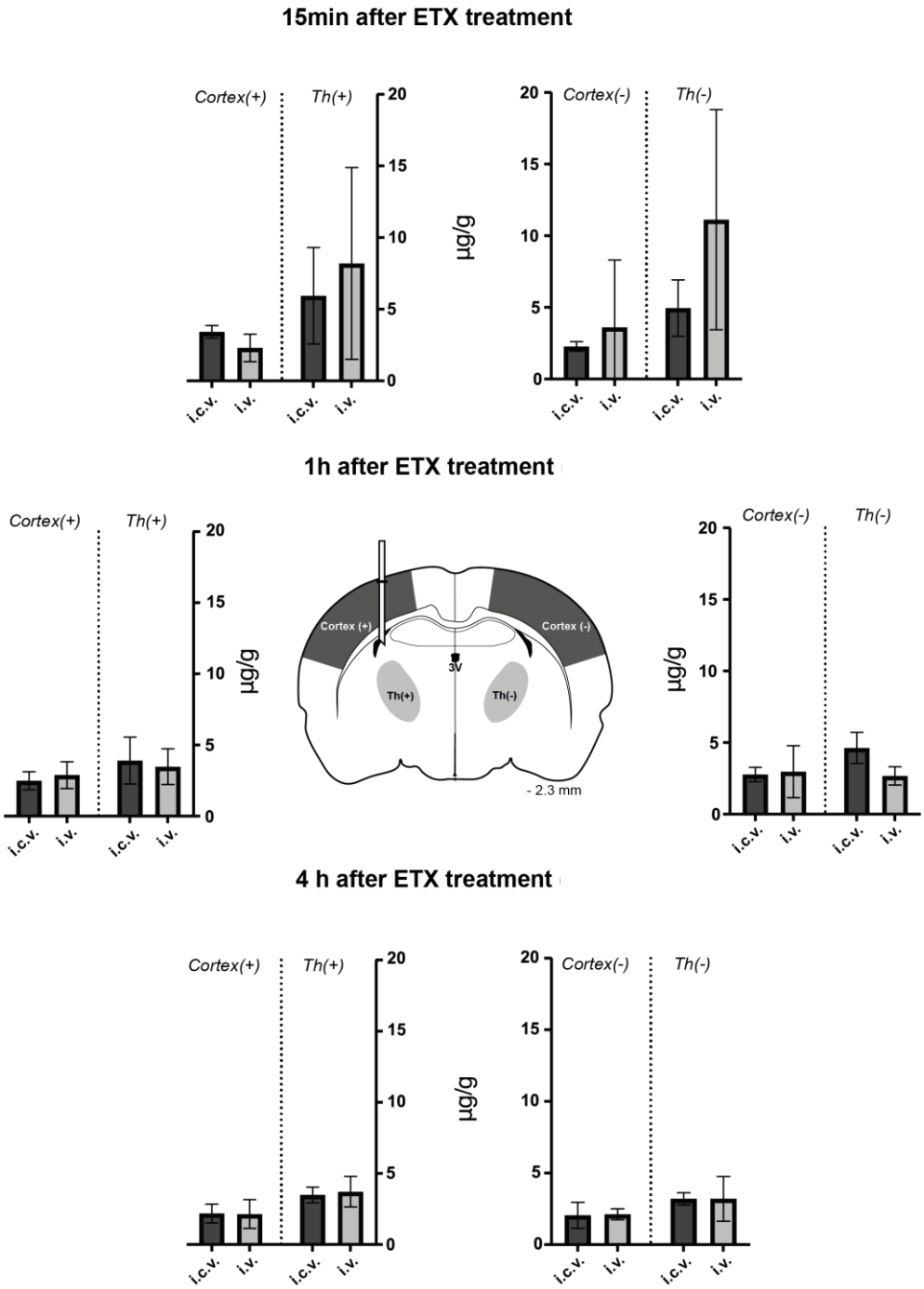

Figure 3.10: ETX distribution in brain parenchyma after i.v. or i.c.v. treatment
ETX concentration (µg/g) in the cortex and thalamus (Th) after i.c.v. (2mg/animal; dark grey), or i.v. (2mg/animal; light grey) drug administration at different timepoints (mean ± SEM). The (+) denotes the hemisphere with canula implantation and the (–) without cannula implantation. The middle panel shows a schematic representation of a coronal section, which highlights the dissected areas and the injection site. The statistical analysis was performed by one-way ANOVA with Tukey's post-hoc test.

A slight but steady decrease of the ETX concentration, independent of the application method, can be observed in the CSF and plasma over time (fig. 3.9). Although the concentration change over time was not statistically significant but in line with the proposed half-life of ETX in rats (Löscher, 2007). The ETX was already after 15 minutes, evenly distributed throughout the CSF and plasma, and the measured drug concentrations were hardly affected by the application method. Only the i.c.v. application of ETX resulted, after 15 minutes, in significantly higher drug concentration in the CSF compared to the corresponding i.v. injections (fig. 3.9; left panel). Though it is important to note that CSF samples contaminated with blood were excluded from the analysis, and we thus only included two out of four samples collected 15 minutes after i.c.v. treatment in the analysis. In all other tests the four samples could be used. The samples from the control experiments (vehicle injections) showed no traces of ETX in plasma or CSF (cf. supplementary data; tab. S.2).

The analysis of drug distribution in the brain tissue showed 15 minutes after treatment, higher ETX concentrations in the thalamic compared to cortical areas (i.c.v. and i.v.) in both hemispheres, although this was statistically insignificant (fig. 3.10). One hour after drug application, ETX was evenly distributed throughout the brain areas. Interestingly, i.c.v. application of ETX did not result in higher local drug concentration compared to intravenous drug injections. However, the samples collected after vehicle injection (control samples) also showed ETX concentration in the thalamus and cortex (cf. supplementary data; tab. S.2). Therefore, a careful interpretation of the measured ETX concentration in the brain tissue is necessary.

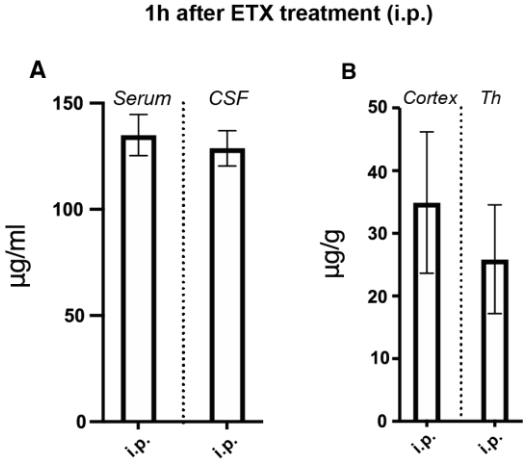

Figure 3.11: ETX distribution throughout different body compartments after standard systemic high dose treatment
A) ETX concentration (µg/ml) in CSF and plasma one hour after i.p. (100 mg/kg) drug administration. B) ETX concentration (µg/g) in the cortex and thalamus one hour after i.p. (100 mg/kg) drug administration (mean ± SEM). The statistical analysis was performed by one-way ANOVA with Tukey's post-hoc test.

Samples after standard systemic high dose treatment with 100 mg/kg ETX (i.p.) were taken one hour after treatment. The CSF and plasma reached ETX-levels approximately 18-fold higher compared to i.c.v. treatment with 2 mg ETX (fig 3.11 and fig. 3.9). Furthermore, in the thalamus and cortex, considerably higher AED concentrations could be found. These results show that ETX rapidly distributes between compartments independent of the application route, which is in accordance with its linear distribution kinetics (Patsalos, 2005). However, because of the deficient control experiment, the final interpretation of ETX levels in brain parenchyma is impossible (cf. Chapter 4.5).

3.8 Substance entry into brain parenchyma after i.c.v. injection

To approach the question why i.c.v. treatment was so much more effective in seizure suppression than systemic treatment with the same dose of ETX despite similar concentrations in plasma and CSF we made i.c.v. dye injections with fast green (FG) to visualize substance penetration into brain tissue after unilateral i.c.v. injection (fig. 3.12). Directly after FG administration, the substance appears well distributed throughout the ventricular system with little transfer into the brain parenchyma (fig. 3.12A). However, one hour after dye administration, FG clearly stained the tissue surrounding the ventricles, including the potential target sites of ETX in absence epilepsy, such as thalamic areas around the third ventricle and somatosensory cortical areas (fig. 3.12B). At four hours post FG injection, we found extensive staining of relevant areas also at larger distance to the ventricular system (fig. 3.12C).

Interestingly, obvious staining one and four hours after dye injection remained largely restricted to the ipsilateral side of injection. Accordingly, although FG differs from ETX in molecular size and polarity, which in turn will influence tissue distribution, these data could indicate that ETX after i.c.v. injection reaches its target areas by direct penetration into brain tissue from the CSF rather than indirect recirculation via the blood.

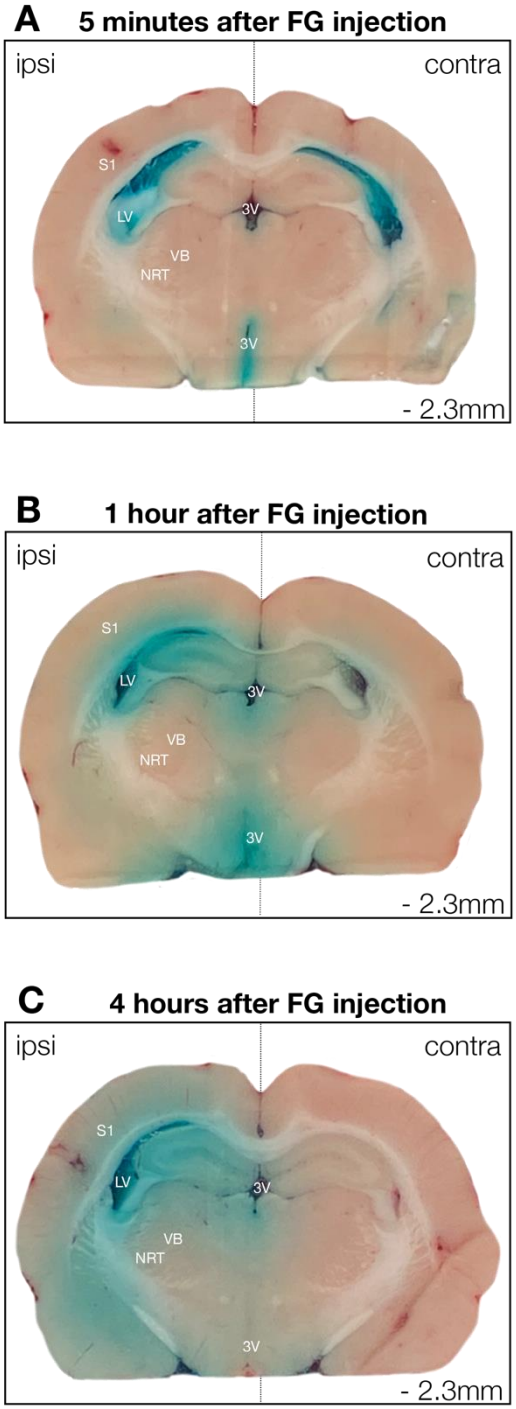

Figure 3.12: Dye tissue distribution after i.c.v. fast green administration
Ventricles and structures, which are known to be involved in the generation of absence seizures are labeled. NRT, reticular thalamic nucleus; VB, ventrobasal thalamus; S1, primary somatosensory cortex; LV, lateral ventricle; 3V, third ventricle. Images show dye distribution A) five minutes B) one hour and C) four hours after dye injection.

3.9 Adverse effects after i.c.v. application of ETX

To evaluate whether localized drug application could indeed be an alternative and effective treatment approach in absence epilepsy, we had to also test for neurotoxic effects after intracerebroventricular ETX administration. All intracranial applied ETX concentrations (0.3 mg, 0.6 mg, 1.2 mg, 2.0 mg, 2.5 mg) were tested each in five animals. The Open Field-Test (OF) was used to detect behavioral abnormalities and locomotor deficits in the animals (Honack and Löscher, 1995). Sedation and ataxia, as well as stereotyped behaviors including circling, head swinging, or stereotypical sniffing in the OF, are possible indicators for adverse effects of localized drug application. However, the animals tested in the OF, after i.c.v. treatment with ETX scored zero for all parameters regardless of drug concentration.

To further determine if i.c.v. treatment affects the rat's responses to external stimuli, a hyperexcitability test (HET) was performed with the animals. During the HET, the experimenter was interacting with the rats and scoring their behavior (cf. Chapter 2.7; tab 4). Indeed, the scores of the ETX injected animals did not differ from the vehicle controls (fig. 3.13B).

Motor coordination of i.c.v. treated animals was assessed by the rotarod test (Dunham and Miya, 1957). Thus, the animals had to balance on a rod that rotated at a specific speed (cf. Chapter 2.7). To pass this test, the rats had to stay on the rod without falling off for at least 2 min in one of three trials. All tested animals passed the rotarod test before and after i.c.v. treatment with ETX, regardless of concentration.

A significant reduction in body weight of the GAERS could only be observed after treatment with the highest concentration of 2.5 mg compared to vehicle injection ($p=0.02$) and to no treatment ($p=0.04$) (fig. 3.13A).

The behavioral results indicated that i.c.v. treatment does not cause adverse effects in GAERS, especially 2.0 mg ETX, the most promising dose, was well tolerated by all animals.

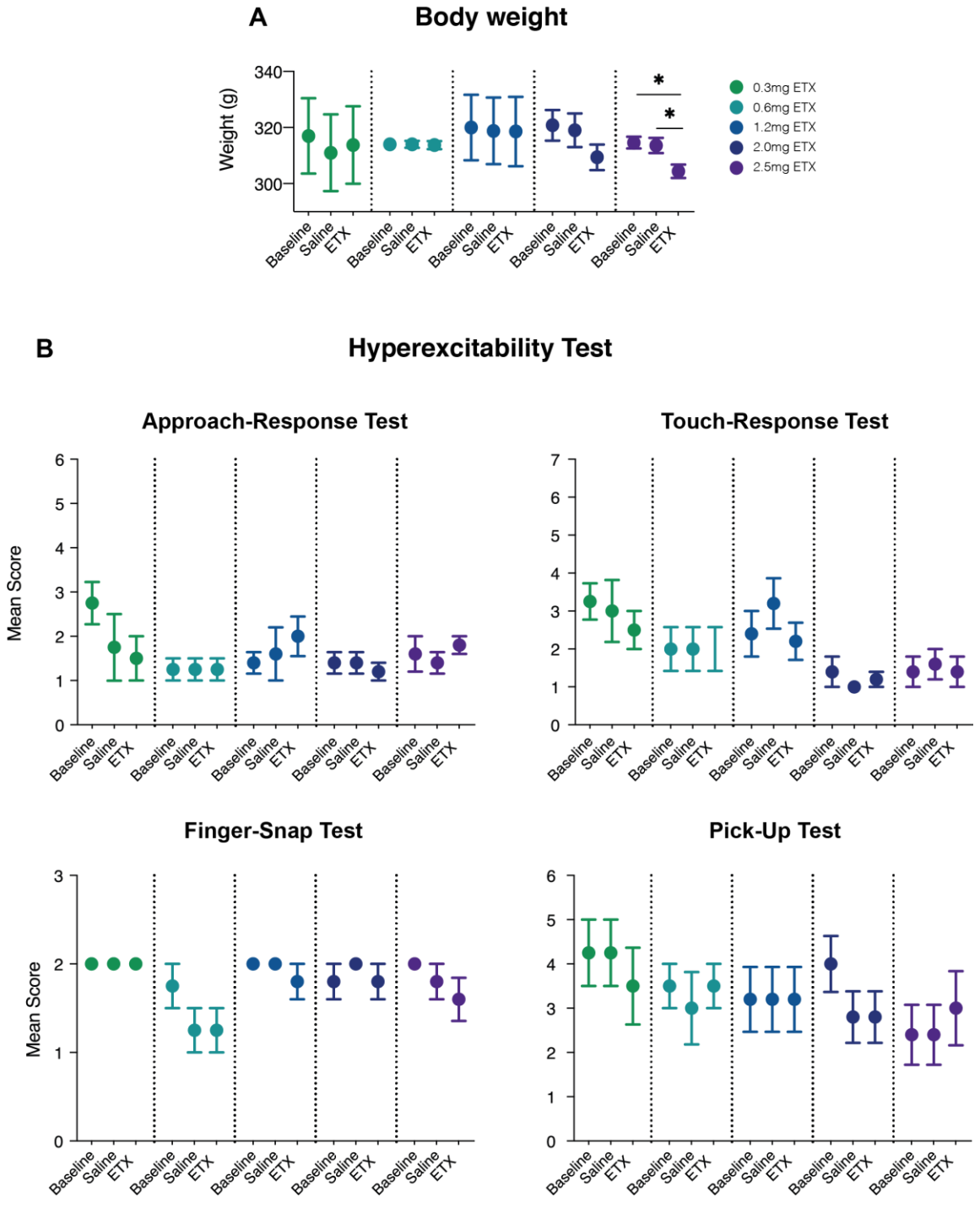

Figure 3.13: Adverse effects in response to unilateral i.c.v. administration of ETX
All behavioral tests were performed with non-treated animals (baseline), vehicle-injected animals (saline), and ETX injected animals (ETX). For ETX treatment, different doses were tested. The colors of the dots and error bars denote the used doses of ETX (green = 0.3 mg; turquoise = 0.6 mg; blue = 1.2 mg; dark purple = 2.0 mg; purple = 2.5 mg). A) Shows the body weight of the animals after the different treatments (mean ± SEM). B) The HET consist of four subsequent behavioral tests: the approach-response test, the touch-response test, the finger-snap test, and the pick-up test. The dots present the mean ± SEM score given by the experimenter. The statistical analysis was performed by one-way ANOVA with Tukey's post-hoc test. (*)P ≤ 0.05.

3.10 Unilateral cortical ETX application via an Epidural cup

The "cortical focus theory" implies that absence seizures are initiated in the somatosensory (S1) cortex of rodents (Meeren et al., 2005) and pharmacological studies showed, that the injection of ETX into the S1 cortex of GAERS immediately and nearly complete suppresses SWDs (Manning et al., 2004). Therefore, we investigated an alternative application route for AEDs in closer proximity to the S1 cortex. To this end, we removed parts of the skull and installed an epidural cup directly on the cortical surface (cf. Chapter 2.2; fig. 2.2). The dura mater was left intact during the procedure, as it has been shown that transmeningeal substance delivery is possible (Ludvig et al., 2008). The surgery was little invasive, and the cortical surface provided enough space for a potential drug depot. The epidural application method was tested in three animals with two different concentrations of ETX (1 mg and 2 mg). However, for both concentrations, no therapeutic effect in GAERS could be observed at any time point (fig. 3.14).

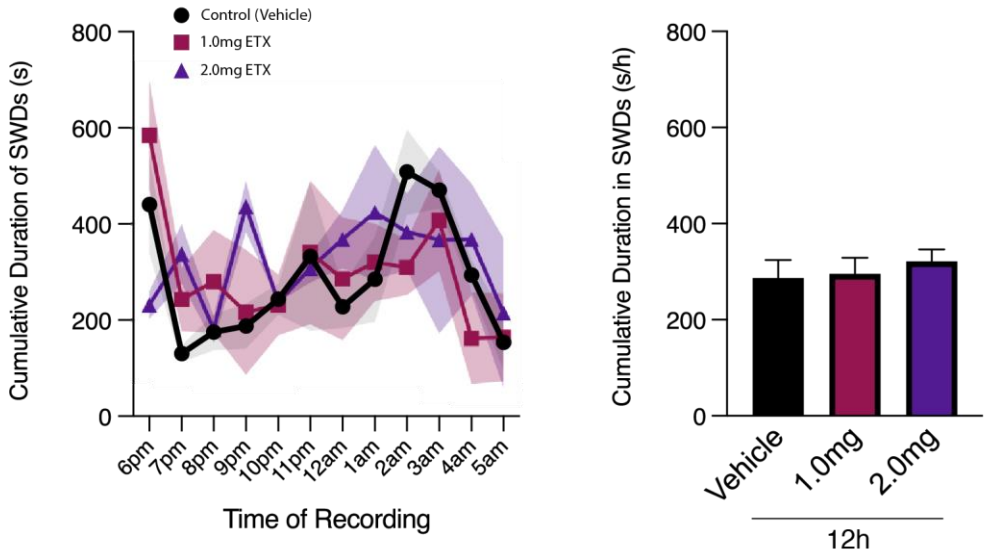

Figure 3.14: Epileptic activity in GAERS after epidural ETX application
The left panel shows the time course of the cumulative duration of SWDs over 12h (one-hour bins) after epidural ETX application with the doses 1.0 mg (pink) and 2.0 mg/animal (purple; n=3). The reference (black; n=3) displays epileptic activity after vehicle application (solid lines and symbols indicate the mean, shaded areas indicate ± SEM). The bar plot represents the average±SEM time GAERS spend in seizures per hour, considering the complete time of recording. Statistical analysis reveals no significant difference between the vehicle and drug application. The statistical analysis was performed by one-way ANOVA with Tukey's post-hoc test.

3.11 Unilateral i.c.v. application of the neuropeptides Neuropeptide Y and Somatostatin

Neuropeptides are key modulators of neural activity and have been discussed as potential alternatives to classic antiepileptic drugs for several years (for a review see Kovac and Walker, 2013). In particular, neuropeptides are potent even at low doses. However, they show poor blood-brain barrier penetration, which hinders their systemic application but makes them attractive candidates for localized pharmacotherapy in epilepsy.

One of the best-explored neuropeptides in the context of epilepsy is the Neuropeptide Y (NPY). It has already been shown that NPY, when injected intracerebroventricularly, effectively suppresses SWDs in GAERS over 90 minutes at a dose of 6 nmol (Stroud et al., 2005). In order to verify in more detail, the therapeutic potential of NPY, we included this neuropeptide in our study. Furthermore, the efficacy of another neuropeptide, Somatostatin (SST), for localized therapy in absence epilepsy was tested. We chose SST because, in status epilepticus, this neuropeptide showed similar anticonvulsant efficacy as NPY at a dose of 1nmol (Mazarati and Wasterlain, 2002). However, SST has to our knowledge not yet been tested in a model for absence epilepsy.

The i.c.v. injection of NPY did not produce any attenuation of SWDs over the complete 12 hours neither for 10 nmol ($p=0.7$) or for 100 nmol ($p=0.9$) compared to vehicle injection (fig. 3.15A; left panel). To directly compare our results to those reported in the literature, we analyzed in more detail the first 90 minutes after treatment (Morris et al., 2007; Stroud et al., 2005) (fig. 3.15B; left panel). Therefore, the percentage of time spent in seizures was plotted in 15-minute time bins. However, even the higher time resolution did not reveal any clear anticonvulsant effects of NPY.

Also, the i.c.v. application of 2 nmol ($p=0.9$) or 20 nmol ($p=0.1$) of the neuropeptide SST did not influence seizure activity in GAERS over the complete 12 hours (fig. 3.15A; right panel). Three hours after i.c.v. treatment with 20nmol SST, an increase in cumulative seizure duration of SWDs can be observed. However, this increase was not statistically significant ($p=0.45$) compared to controls at this time point. Furthermore, the closer evaluation of the first 90 minutes after treatment did not reveal any antiepileptic activity of SST (fig. 3.15A; right panel). In summary, the i.c.v. application in GAERS of the neuropeptides NPY or SST did not show any anti-absence effects in our hands. This approach for localized drug therapy was thus not further pursued in this study.

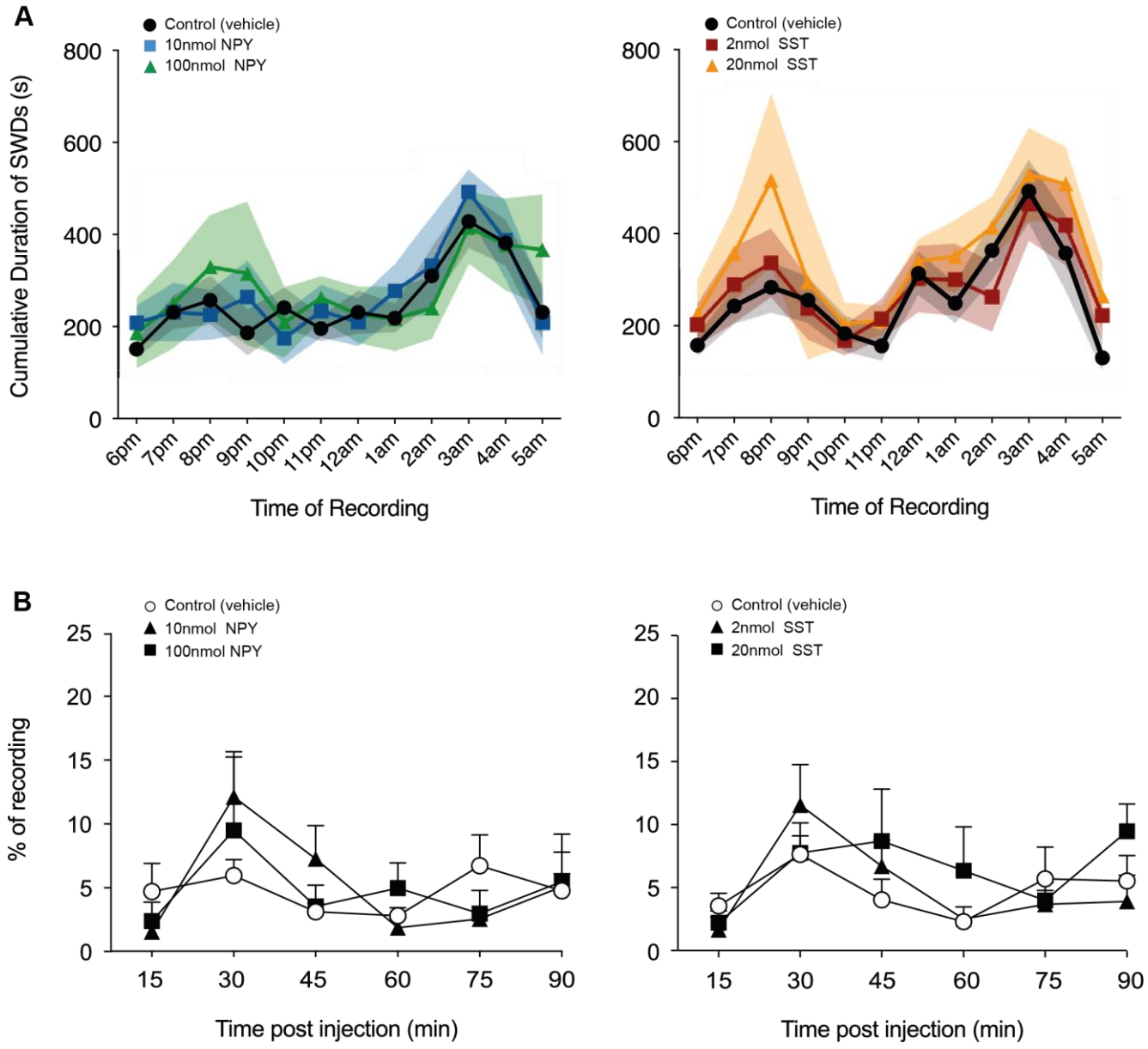

Figure 3.15: Epileptic activity in GAERS after i.c.v. treatment with different doses of NPY and SST

A) The left panel shows the time course of the cumulative duration of SWDs over 12h in one-hour bins after i.c.v. treatment with the NPY doses 10 nmol (blue; n=7) and 100 nmol/animal (green; n=7). The right panel shows time in seizures over 12h after i.c.v. treatment with the SST doses 2nmol (red; n=7) and 20nmol/animal (yellow; n=7). Black traces in both panels show the time spent in epileptic activity after vehicle injection (n=14) (solid lines and symbols indicate the mean, shaded areas indicate ± SEM). B) The left penal shows the time course of percentage time in SWDs over 90 minutes in 15 minutes bins after i.c.v. treatment with the NPY doses 10 nmol (σ) and 100 nmol/animal (ν). The right panel shows the time course of percentage time in SWDs over 90 minutes in 15 minutes bins after i.c.v. treatment with the SST doses 2nmol (σ) and 20nmol/animal (ν). Statistical analysis revealed no significant differences between the vehicle and neuropeptide application. The statistical analysis was performed by one-way and two-way ANOVA with Tukey's post-hoc test.

3.12 Brain activity and SWDs during chloral hydrate anesthesia

It is imperative to quantify seizure occurrence directly after drug application while testing antiepileptic efficacy of a substance, in order to understand the time course of the pharmacological effect. Thus, the implantation of a drug-releasing material requires that the animals are under anesthesia. Therefore, we were interested in evaluating if seizures arise under chloral hydrate anesthesia (400 mg/kg) and/or how long after anesthesia seizure detection becomes possible again. Typically, general anesthesia evokes a characteristic EEG pattern, so-called burst suppression (Swank and Watson, 1949; Urrego et al., 2014). The background EEG during anesthesia, which is referred to as "suppression period," is dominated by flat amplitudes with a dominating frequency between 0.5-4.0 Hz. The EEG trace is consistently interrupted by quasiperiodic, high amplitude "bursts". Undergoing chloral hydrate anesthesia, all three recorded animals showed these characteristic burst suppression patterns starting approximately 10 minutes after chloral hydrate application. In figure 3.16A, typical burst suppression patterns in a 60 second EEG recording of one animal under chloral hydrate anesthesia are shown. During the bursts, the spectrogram shows a high power in all frequency ranges up to approximately 40 Hz (fig. 3.16B). The start and termination of the bursts were abrupt, and the amplitudes varied between 0.1 – 0.3 mV. Compared to SWDs, the bursts were brief and did not show a characteristic oscillatory morphology (fig. 3.16A & fig. 3.1A). Therefore, false positive "ictal" classification by automated detection did not appear.

The anesthetic period, showing burst suppression patterns, lasted approximately 40 minutes. Afterward, the animal's EEG recordings displayed brain activity typical for deep-slow wave sleep (Bjorvatn et al., 1998). Hence the neural oscillations were dominated by delta waves, i.e. high amplitudes and frequencies between 1 – 5 Hz (data not shown). Five hours after chloral hydrate injection, the first seizures could be recognized by automated detection (fig. 3.16A). The cumulative time in seizures reached baseline values six hours after the injection of the anesthetic. As a reference, the average time GAERS spend in seizures from the baseline sessions of all recorded animals (n=61) was included in the graph shown in figure 3.16A.

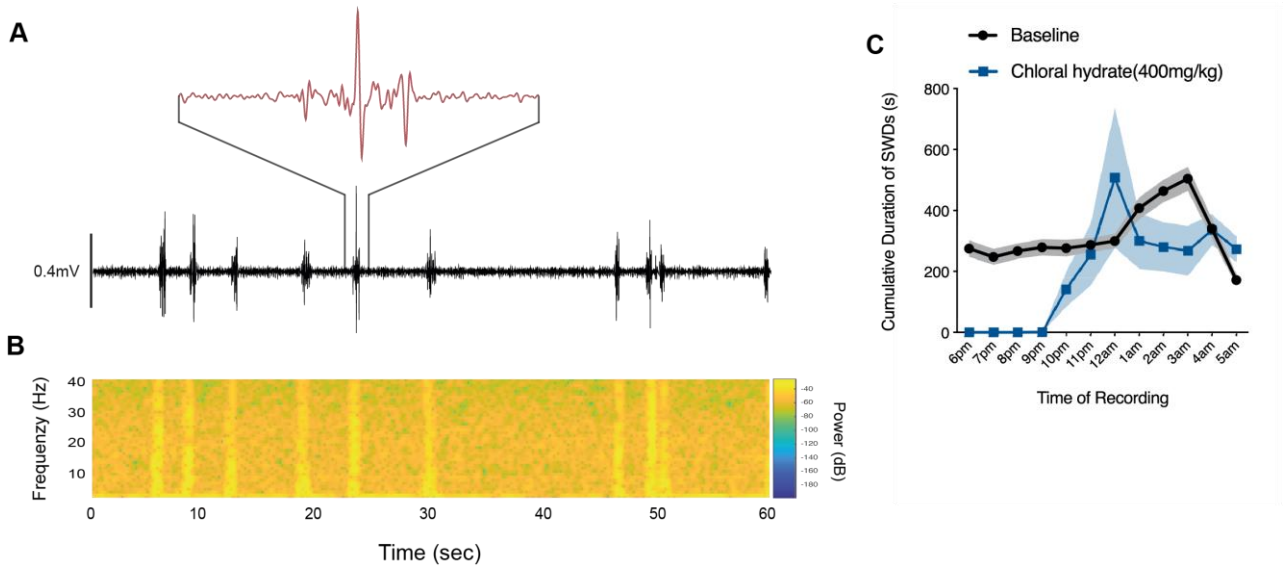

Figure 3.16: Chloral hydrate anesthesia affects brain activity and SWDs
A) The 60 second EEG recording shows typical burst suppression in a GAERS rat under chloral hydrate anesthesia. The enlarged EEG complex displays a characteristic burst with high amplitudes. B) The power spectrogram corresponding to the EEG recording reveals low frequencies during the suppression phase and during the bursts, high power in all frequencies up to 40 Hz. C) The blue trace in the time graph (one-hour bins) shows the cumulative duration GAERS spent in seizures over 12h after chloral hydrate injection (n=3). The black trace is included as a reference and contains the average seizure duration over 12h from the baseline sessions (n=61) (solid lines and symbols indicate the mean, shaded areas indicate ± SEM). The first five hours after the anesthetic injection, no seizures could be detected; however, after six hours the animals under chloralhydrate anesthesia showed similar epileptic activity as the baseline group.

4 Discussion

Absence epilepsy is one of the most common types of childhood epilepsy and is characterized by sudden and recurring non-convulsive seizures accompanied by the loss of consciousness and behavioral arrest. The seizures result from aberrant neural activity, which can be observed as characteristic patterns in the electroencephalogram (EEG) dominated by spike-and-wave discharge (SWD) (Crunelli and Leresche, 2002). The thalamocortical networks appear to play a critical role in the emergence and maintenance of SWDs (Lüttjohann and van Luijtelaar, 2015; Steriade, 1990) and the respective brain areas are suggested to be the targets of pharmacological treatment (Manning et al., 2003).

The systemic application of antiepileptic drugs (AEDs) is the current mainstay to treat epilepsy. Although the drug transport into the CNS via the blood is highly restricted by the blood-brain barrier (BBB) and thus high drug concentrations in the systemic circulation are required to suppress seizures (cf. Chapter 1.6). The direct drug application into the thecal sac, that surrounds the CNS and contains cerebrospinal fluid (CSF), may be a potential alternative approach to treat epilepsy. Intrathecal (IT) drug application would minimize side effects caused by off-target drug exposure in the periphery and increase neuroactive components in the CNS (Fowler et al., 2020). This study aimed to test if IT treatment can robustly control seizures in the genetic absence model GAERS and to compare the anticonvulsant efficiency of different application approaches.

4.1 Automated detection of spike and wave discharge in GAERS

The quantification of epileptic activity and seizure suppression is a particularly precise tool in the assessment of the efficacy of antiepileptic therapy. The SWDs, of GAERS, show characteristic and repeating patterns in the EEG (fig. 3.1). On this basis we were able to successfully implement automated seizure detection algorithms using the computed autocovariance of one-second data segments as feature vectors (Rodgers et al., 2015). With this method, seizure detection achieved an F-score of 96 % (fig. 3.2), which is comparable to other seizure detection applications (van Luijtelaar et al., 2016).

Detection errors of our classifier often appeared at the end or the beginning of a seizure, more precisely, within those time windows, in which the switch between brain states (ictal ⇆ interictal) occurred (fig. 3.2A). It is possible that an increase in the time resolution of seizure detection would reduce this type of error. Hence, the application of

a sliding window with a smaller step-size instead of computing the autocovariance for a fixed time window of one second would be favorable.

Further possible detection errors occur because of local field potential (LFP) components, that resemble SWDs (e.g. sleep spindles and artifacts caused by head movements or grooming). During preprocessing of the data movement artifacts have been reduced by high pass filtering the data at 5 Hz, and most sleep spindles were correctly classified as non-ictal by seizure detection, as we set the condition that SWDs had to last longer than one second. Nevertheless, a more advanced processing procedure of the recorded data could be advantageous to increase seizure detection specificity. Whereas seizure detection performance was adequate for the aims of this study, future applications such as e.g. a "closed-loop" device that converts online seizure detection into immediate, controlled drug release would benefit from enhanced detection performance.

4.2 The dynamics of spike and wave discharge

The 24-hour and 12-hour recordings of untreated GAERS revealed endogenous undulations of seizure activity with a peak accumulated time in SWDs between 2 am and 4 am (fig. 3.3). This observation agrees with earlier studies, that showed that epileptic activity depends on the vigilance level in this model organism. SWDs increase during passive wakefulness and light stages of non-rapid eye movement sleep (NREM), but occur more sporadically during active arousal, slow-wave and paradoxical sleep (Drinkenburg et al., 1991; Van Luijtelaar and Coenen, 1988). This tendency of SWD occurrence is shared between humans and rats (Kellaway et al., 1980). These findings indicated that epileptic activity in parts temporally coincidences with the occurrence of the majority of sleep spindles (Dijk et al., 1993), which supported the hypothesis that sleep spindles and SWDs may result from identical thalamocortical interactions and that sleep-related circuits get co-opted to generate epileptiform activity (Beenhakker and Huguenard, 2009).

However, sleep spindles are generated in the intra-thalamic circuit, whereas cortico-thalamic inputs seem to be required to initiate SWDs (Meeren et al., 2002). Thus, in recent years it has been critically discussed, whether SWDs indeed result from aberrant oscillations of natural sleep (Leresche et al., 2012).

Nonetheless, consensus exists that the neuronal networks in the thalamocortical loop play distinct functional roles in the generation, maintenance and seizure termination. The cortical focus theory assumes that SWDs are initiated in the S1 cortex

(Meeren et al., 2005). The thalamus has been proposed to tilt the system towards a pro epileptic state and to function as a resonator in SWD maintenance. Finally, the termination of seizure activity is probably initiated by cortico-thalamic as well as intra-thalamic processes (Lüttjohann and van Luijtelaar, 2015). Based on these dynamics it can be concluded that the mechanisms involved in initiation, maintenance and termination are reflected in some of the SWD features: the number of SWDs per time is mainly determined by the excitability of the cortex, whereas the mean duration depends on mechanisms involved in aborting ongoing SWDs in the thalamus (Lüttjohann et al., 2014). On average the untreated animals spent about 300s/h in seizures. The total time in seizures is composed of approximately 30 seizures per hour with a mean duration of 10 seconds (fig. 3.3).

4.3 Suppression of SWDs by systemic application of the therapeutic doses of VPA or ETX

Systemic drug delivery is the conventional method to treat disorders of the CNS, although the BBB prevents the movement of active agents between the peripheral system and the CNS to a significant degree. Only a minute fraction of small molecules and hardly any large-molecules can access the brain (Pardridge, 2005). However, it is a major advantage of systemic drug application that every neuron is in close proximity to a brain capillary (Schlageter et al., 1999). Therefore, diffusion distances to the site of action are very short for substances that cross the BBB after systemic application. To assess IT drug application as an alternative to systemic application we set out to compare these two routes regarding therapeutic efficacy and dynamics. Accordingly, we initially evaluated the anti-epileptic activity of systemically applied VPA and ETX as reported in the literature to generate reference values to assess subsequent IT drug application efficiency.

The high predictive validity of GAERS, make them an excellent model to evaluate the anti-absence action of novel pharmaceutical strategies (van Luijtelaar and van Oijen, 2020). The predictive validity refers to assessing medication effects in humans based on the animal models response to drug application. The most commonly used drugs in childhood absence epilepsy are ethosuximide (ETX), and sodium valproate (VPA)(Manning et al., 2003). The effectiveness of these AEDs has also been demonstrated at a therapeutic concentration in GAERS (Marescaux et al., 1992).

In accordance with previous findings, the administration of a standard systemic 100 mg/kg ETX dose produced an immediate and strong suppression of SWDs over approximately 11 hours. Seizure suppression was nearly complete over the first five hours, after which the epileptic activity gradually increased again (fig. 3.4; pink trace). Interestingly, in the first few hours after ETX treatment the number and duration of SWDs were both affected, which has also been described by van Luijtelaar et al., 2013. Approximately five hours after drug application seizure duration recovered and the decreased number of SWD incidences was sufficient to explain the anti-absence effect of ETX. A possible explanation is that the drug-induced anti-absence mechanisms initially affect both cortex and thalamus but that these actions persist longer within cortical brain areas. However, these observations could also be compromised by analytical problems, as too few seizures have been recorded in the first five hours (approximately 1 or 2 seizures per hours). Consequently, the seizure duration would hardly be affected by the systemic treatment of ETX, which could indicate that the anti-absence effect over the entire therapeutic time window is mainly caused by drug effects in the cortex (Greenhill et al., 2012; van Luijtelaar and van Oijen, 2020).

The anticonvulsant action of systemic VPA was also instantaneous, but considerably shorter compared to ETX. The anti-absence efficacy was apparent only over the first two hours after i.p. injection of the therapeutic dose of 200 mg/kg VPA. The short duration of seizure suppression for VPA could be explained by active, carrier-mediated transport at the BBB (Frey and Löscher, 1978), which supports the fast entrance of VPA into the CNS but also results in rapid extrusion from the brain. Moreover, the half-life of VPA (2 – 3 hours) is considerably shorter compared to ETX (10 – 16 hours) (Löscher, 2007). Within the therapeutic time window of approximately two hours both seizure duration and SWD incidence were significantly decreased.

4.4 Exploration of alternative application routes – intracerebroventricular application of VPA and ETX

Our approach to bypass the BBB in order to increase the drug concentrations intracranially was the IT administration of substances. Drug application into the CSF was achieved by injection into the right lateral ventricle (intracerebroventricular - i.c.v.). We examined, whether i.c.v. drug delivery could principally be an option for the treatment of epileptic disorders. To this end, we have systematically investigated the therapeutic effects of i.c.v. injections of ETX and VPA.

The unilateral i.c.v. application of ETX and VPA showed a dose-dependent reduction of epileptic activity (fig. 3.6 & fig. 3.7). For ETX, similar results were reported earlier for WAG/Rij rats, which represent another established absence epilepsy model (van Luijtelaar et al., 2000). This study reported sufficient SWDs suppression by injecting 0.3 mg ETX. In GAERS, however, higher drug doses seem to be required as a significant decrease of SWD activity could only be seen for doses higher than 0.6 mg.
Interestingly, the dose dependence of seizure suppression followed an inverted U shape for ETX, and SWD activity started to increase again with drug doses exceeding 2.0 mg (fig. 3.6). Similar observations have been made previously with injections of ETX into the thalamus (Richards et al., 2003). Our results suggest a therapeutic range between 1.2 – 2.0 mg for i.c.v. applied ETX. In contrast, administration of the low dose (2 mg/animal) did not produce any anticonvulsive effects when applied systemically (fig. 3.8). This strongly speaks against the idea that i.c.v. application simply represents a slow intravenous infusion (Pardridge, 2016) and instead suggests that ETX penetrates into relevant brain regions directly from the CSF (cf. fig. 3.8).

To our knowledge, the i.c.v. application of VPA has not been tested in absence epilepsy yet. However, the method was used in a model for temporal lobe epilepsy (amygdala kindling epilepsy model). This study showed that high concentrations, approximately 4.5 mg/animal, generated a significant antiepileptic effect, but were accompanied by remarkable ataxia and sedation (Serralta et al., 2006). In GAERS we found a significant reduction of SWDs after the i.c.v. application of only 0.6 mg VPA, whereas higher concentration did not result in a significant anti-absence effect. Indeed, the application of 0.3 mg appeared to exacerbate seizure incidences.

VPA has been shown to have biphasic effects on extracellular GABA levels (Biggs et al., 1992). The i.p. injection of 50 mg/kg VPA decreased GABA levels in the brain of rats compared to basal, whereas the injection of 400 mg/kg VPA drastically increased the GABA levels. Interestingly, treatment with 200 mg/kg VPA had virtually no effect on GABA levels. This may explain the pro-epileptic effects seen at low doses VPA because of increased excitability in the cortex. However, high concentrations of VPA may facilitate burst firing in the thalamus and thus triggers again SWDs (cf. Chapter 1.2), which may occlude the anti-absence effect of i.c.v. applied VPA above a specific dose.
Furthermore, it has been suggested that the action of VPA in the brain is region specific (F. Baldino and Geller, 1981). As i.c.v. treatment will likely achieve variable drug concentrations throughout the brain, the contributions of different drug effects in different relevant brain regions are hard to predict and likely occlude the interpretation of our data on the therapeutic effects of IT applied VPA. In any case, our results indicate a rather narrow therapeutic window for i.c.v. application of VPA. I.c.v. treatment with concentrations between 0.3 – 2.5 mg did not appear to have an adverse effect in the animal. This, however, has to be studied in more detail.

Interestingly, we observed a delayed onset of the therapeutic effects of approximately two hours after i.c.v. treatment for both AEDs. A considerable fraction of the therapeutics must most likely distribute through the brain's extracellular space to reach its target area. The distribution properties of any substance are affected by several factors, including the brain microenvironment, tortuous extracellular space, and the substance's physiochemical properties (Wolak and Thorne, 2013). Hence, i.c.v. application could result in a gradual drug distribution in the CNS and decelerated accumulation of the therapeutic agent in the brain's target areas within some distance from the lateral ventricle (e.g., thalamus, S1 cortex). The belated reach of therapeutic concentration in distinct brain areas could explain the delayed antiepileptic efficacy by i.c.v. applied AEDs (cf. fig. 3.12).
Richards et al. (2003), reported a similar delay in the therapeutic onset after the local injection of ETX into the thalamic VB and NRT. The authors have also attributed this effect to the distribution dynamics of ETX in brain tissue. An alternative hypothesis would be that delayed antiepileptic efficiency is caused by specific, possibly slow, mechanisms that are targeted by ETX in the thalamic brain areas. This idea would also be in line with the observation that i.c.v. application of ETX, between 2.0 – 2.5 mg, shows in contrast to systemic drug administration a more robust effect on seizure duration than on the number of seizures. These observations suggest that the therapeutic effects of

i.c.v. applied ETX may to a large degree be mediated by effects on thalamic rather than cortical structures. Such a bias regarding the site of pharmacological action could also explain why the antiepileptic efficiency does not reach a maximum of 100% seizure suppression as effects in the cortex are strongly contributing to the anti-absence effect of ETX after systemic application (Greenhill et al., 2012).
The delayed seizure suppression of i.c.v. applied ETX though was not described by the above mentioned study of van Luijtelaar et al., 2000. However, by not displaying the time-dependent variations of antiepileptic efficacy within their six-hours recordings, this effect may have been occluded.

A closer inspection of the time-window of drug action could reveal further insight into the pharmacodynamics of IT applied VPA. The systemic application of the therapeutic dose of VPA revealed an antiepileptic action of approximately two hours with an immediate onset in GAERS, which corresponds with the results from other studies (Dedeurwaerdere et al., 2011; Löscher, 2002). The short efficiency could be explained by the short half-life of the drug and by transport mechanisms that support the rapid removal of the AED from the brain (Frey and Löscher, 1978). Indeed, the i.c.v. application of VPA shows a delayed drug efficiency, however, the duration of action persists approximately until four hours after application (fig. 3.7). A possible explanation could be that the IT applied drugs are not so much affected by efflux mechanisms, though Frey and Löscher (1978) showed that the underlying transporters could also be found in the CSF-blood barrier. A further interesting aspect could be that the direct application of VPA into the CSF is to a lower extent affected by metabolism relative to systemic application, leading to a longer half-life of the AED (Misra et al., 2003). Such an increased drug half-life within the CSF could be a further advantage of IT drug application.

In conclusion, the systemic investigation on whether an IT drug application could be an alternative option for the treatment of epileptic disorders, revealed that the i.c.v. administration of ETX or VPA caused robust and dose-dependent reductions in SWDs. However, complete seizure suppression could not be achieved. Because ETX showed a prolonged and more solid anti-absence effect in GAERS compared to VPA, we suggested that ETX is a better choice for IT drug applications. Indeed, the effect of locally applied ETX was dramatically stronger than the effect after systemic application of the same drug dose, which proved that the therapeutic effect was not caused by the indirect entry of ETX into brain parenchyma via the bloodstream but rather mediated by a direct entry from the CSF. Finally, the animals showed no behavioral or motor deficits after the i.c.v.

treatment, suggesting that this application route may indeed be a feasible alternative to systemic drug application.

4.5 Tissue distribution of ETX after treatment via different application routes

The CSF fills the cerebral ventricles, cisterns, as well as the cranial and spinal subarachnoid spaces and moves within these compartments (Linninger et al., 2016). Accordingly, the CSF is engaging to a great extent with the CNS and has already been clinically used as a vehicle for drug transportation throughout the entire brain (Cook et al., 2009; Miller et al., 2013). The CSF flow dynamics, which are highly complex and not fully understood, are suggested to facilitate the drug penetration into brain tissue after IT application (João Casaca-Carreira et al., 2017; Fowler et al., 2020). To understand the mechanisms behind the therapeutic action of IT applied ETX and potentially overcome limitations of the method, we were interested in monitoring the fate of ETX after treatment using different application routes. To this end we utilized HPLC analysis and measured ETX concentration within blood plasma, CSF, and brain tissue (i.e. thalamus and S1 cortex) at different time points after treatment.

Our results show a fast exchange of ETX between CSF and bloodstream after treatment, independent of the dose, timepoint, and application method (cf. fig. 3.9). It was surprising that the i.c.v. application of ETX did not show clearly higher drug concentrations in the CSF compared to systemic treatment at any timepoint. Thus, an immediate blood-CSF exchange of ETX must appear after i.c.v. application.
However, as discussed earlier, the therapeutic effects of i.c.v. applied ETX is probably not caused by the indirect entry of ETX into the brain parenchyma via the bloodstream, but rather mediated by the direct entry from the CSF.
A plausible way of drug distribution into the brain would be via the transependymal flow close to the injection site. The transependymal flow can be defined as the motion of fluids or molecules across the ependymal layer of cells that surround the ventricles (João Casaca-Carreira et al., 2017). The CSF-brain barrier is a relatively easy way for molecules to penetrate the brain, as ependymal cells are not joined by tight junctions (Jiménez et al., 2014). Therefore, diffusion or bulk flow, which are the two suggested flow mechanisms, between CSF and brain parenchyma, is not tightly regulated. The transependymal flow, as i.c.v. drug delivery route into brain tissue, was suggested by

several previous studies (João Casaca-Carreira et al., 2017; Proescholdt et al., 1999; Westerhout et al., 2012).

Indeed, the quantification of the ETX concentration in the brain tissue, revealed similar drug levels after i.c.v. and i.v. application of the same doses in both hemispheres (fig. 3.10). These results would contradict the assumption of direct brain tissue penetration by i.c.v. applied substances close to the injection site. However, we suspect methodological errors during the brain sample preparation for HPLC analysis. The control samples, collected after vehicle injections, showed contaminations of ETX, which could not be retraced (cf. supplementary data; tab. S.2). Therefore, we evaluated the results of the measured ETX concentrations in the brain as inconclusive and further measurements utilizing an improved method would be necessary. Particularly the sample collection and preparation must be improved as these steps create the highest risk of unwanted contaminations.

To visually retrace substance distribution, throughout the CNS, we injected the dye Fast Green (FG) into the right LV of three GAERS rats and collected the brains at different time points (5min, 1h and 4h after FG administration). Although the physicochemical properties of a substance are decisive for distribution characteristics, and FG distribution dynamics can thus not be directly transferred to ETX, we believe our i.c.v. dye injections support the idea of the direct distribution of ETX in relevant brain structures. The rat brains were snap-frozen immediately after dissection. Therefore, the CSF was kept in the intracranial cavities and remained visible. The evaluation of the brain samples directly after FG injection indicates a fast distribution of FG throughout the CSF, as intensively stained CSF can be observed in all visible ventricles, i.e. in the right and left LV and the third ventricle (fig. 3.12A). The visual inspection of FG distribution across the brain supports the assumption of transependymal substance distribution. We found that FG penetration into the brain parenchyma originates at the right LV and the third ventricle. However, at the left LV, i.e. contralateral to the injection site, hardly any FG staining could be observed. FG penetration originating from the subarachnoid space (SAS) was also not obvious.

The CSF exits the LVs by bulk flow directly into the third ventricle, from where it circulates into the fourth ventricles, and finally moves via the cisterns surrounding the cerebellum into the cranial and spinal SAS (cf. fig. 1.3). However, only minimal CSF is exchanged between the two LVs via reflux mechanisms (Pardridge, 2020). Therefore, we suggest an uneven distribution of FG in the ventricular system, because the molecules

move with the CSF circulation. This is in line with the observation that FG staining of brain parenchyma was largely restricted to the side of injection. Unilateral substance distribution after i.c.v. application has already been described in other studies (Shokry et al., 2016; Yan et al., 1994). This unilateral distribution of ETX may explain the sub-total seizure suppression after i.c.v. application that we have observed. It is thus tempting to speculate, that bilateral i.c.v. administration of AEDs at low doses may achieve even more rigorous seizure suppression.
We found that the distance of penetration into brain tissue from the walls of the ventricular system at the ipsilateral site increased with time (fig. 3.12A, B, and C). Excitingly, the distribution dynamics of FG match nicely with the previously described time course of seizure suppression by i.c.v. applied AEDs. Whereas no prominent staining was detected in VB, NRT, or deep layers of somatosensory cortex immediately after dye injection, staining was prominent already after one hour in deep layers of the cortex and widespread in all structures including thalamic areas after 4 hours.

The analysis of substance distribution in the brain after i.c.v. application supported our hypothesis that substances can directly penetrate into the brain parenchyma following IT administration. However, at the same time, this route of drug distribution seems restricted to brain areas in the vicinity of the ventricular system, which narrows the CNS disorders that can be targeted by i.c.v. drug application. The distribution speed of molecules in the tortuous extracellular space probably affects the antiepileptic action of therapeutic agents (e.g. timing effects and target areas), which must be carefully considered when choosing this application route. Nevertheless, the ETX concentration in plasma and CSF after systemic administration of 100 mg/kg was more than 15 times higher than after 2 mg/animal i.c.v. treatment (fig. 3.11). Still, up to 68% seizure reduction can be achieved by low dose i.c.v. drug injection. Potentially bilateral drug injection could even enhance the anti-absence efficacy of IT applied ETX. Hence, our results clearly show that the administration of substances directly into the cerebrospinal fluid could be a potential alternative for systemic therapy within selected diseases of the CNS.

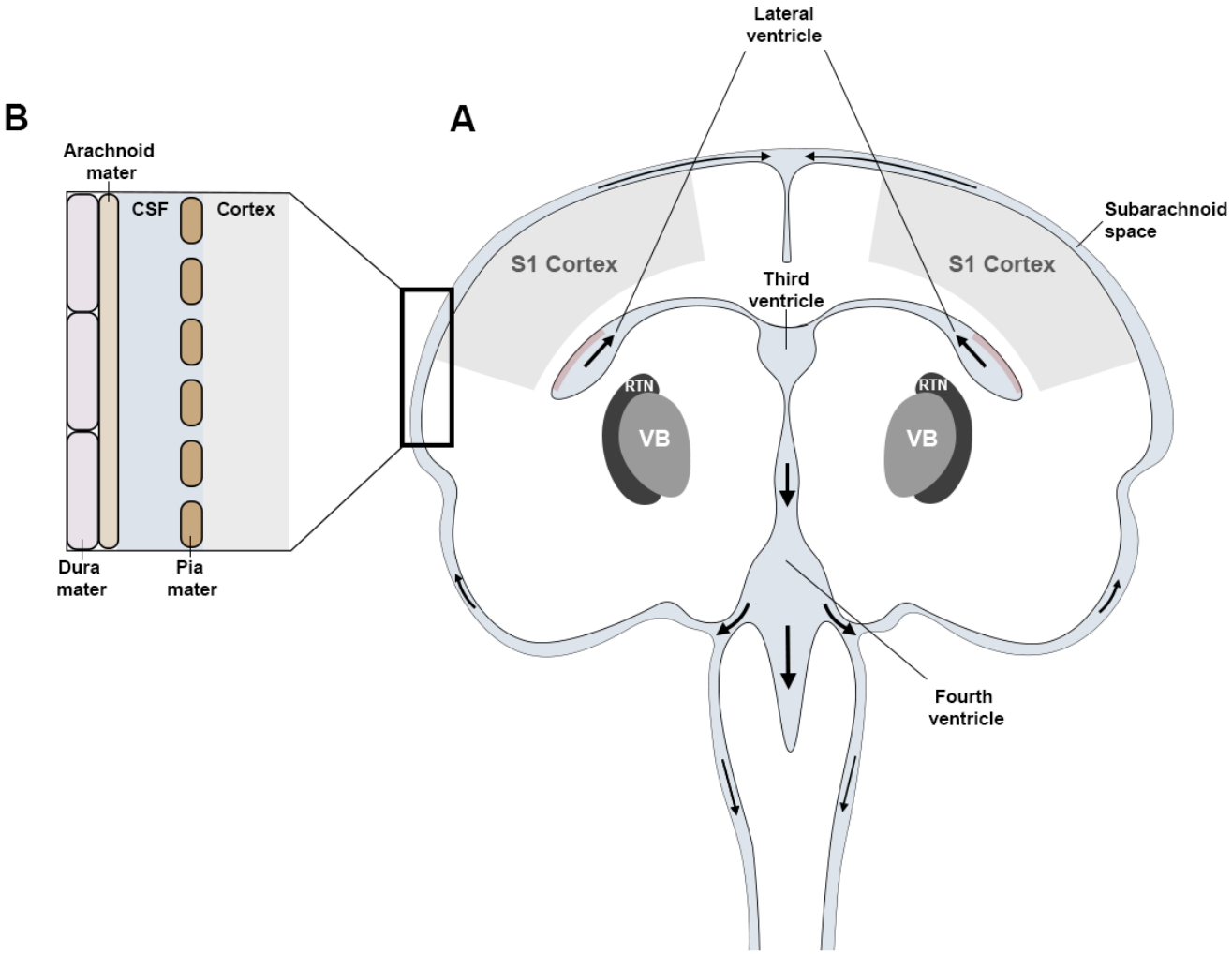

Figure 4.1: Cartoon illustrating the flow of CSF through the ventricular system and its spatial relationship with structures relevant in absence epilepsy
A) The brain areas relevant for the emergence and maintenance of SWDs are highlighted: NRT, nucleus reticularis thalami; VB, ventrobasal thalamus; S1 Cortex, primary somatosensory cortex. The arrows indicate the direction of the slow CSF circulation. B) Magnification of boxed area in A, showing the three meninges (dura mater, arachnoid mater and pia mater) and the subarachnoid space. The arachnoid mater forms the major meningeal diffusion barrier between the epidural space and the CNS.

4.6 Seizure suppressing effects of i.c.v. applied neuropeptides.

Neuropeptide Y

Due to their neuromodulating properties several neuropeptides have been suggested as potent anticonvulsant substances (Clynen et al., 2014).

The endogenous peptides show antiepileptic efficacy at extremely low doses, and they are additionally hardly affected by active elimination mechanisms in the CNS (Kovac and Walker, 2013). These properties could make neuropeptides ideal candidates for IT drug applications. One of the most studied neuropeptides in the context of epilepsy is Neuropeptide Y (NPY). NPY supposedly suppresses epileptic activity by decreasing the excitability in cortical networks. The neuromodulator can dampen excitatory activity in the brain by reducing glutamate release through the activation of presynaptic Y_2 receptors (El Bahh et al., 2005) or by increasing GABAergic neurotransmission, in cortical areas, where the Y_1 receptor is highly expressed (Bacci et al., 2002).

In 2005 the published data of Stroud et al. confirmed that i.c.v. applied NPY induces a significant anti-absence effect in GAERS. The study showed that the epileptic animals spend on average ~20% of the recorded time (90min) in seizures after vehicle injection. After i.c.v. application of NPY the rats spent only 5-10% of the recorded time in seizures, which would amount to reduction by about 50%. Moreover, the group achieved similar results by only injecting the Y_2 receptor agonists into the LV (Morris et al., 2007).

Our analysis revealed that after NPY treatment, GAERS spent equivalent time in seizures compared to the literature, though this was not different from the seizure activity after vehicle injection (fig. 3.15B; left panel). Therefore, our experiments could not confirm a seizure suppressing effect in GAERS by i.c.v. applied NPY. It is noteworthy that animals in different GAERS colonies show variations in the severity of epilepsy (Powell et al., 2014). Moreover, the experimental design working with GAERS can have a decisive effect on epileptic activity. Not only show the animals circadian variability in SWDs occurrence (fig. 3.3) but also stress factors, such as noise, handling, or the placement in a new cage that has previously hosted female rats or mice affect epileptic behavior in GAERS (Vergnes et al., 1991). These aspects could partially explain the discrepancies of baseline seizure occurrence between the GAERS rats in our experiments compared to the GAERS of the introduced study of Stroud et al. (2005).

Moreover, it has been shown that the antiepileptic action of NPY varies with brain regions: The application of NPY into the secondary somatosensory (S2) cortex significantly reduced seizure activity in GAERS. In contrast, the local injection of NPY into

the VB thalamus increased the number of SWDs (van Raay et al., 2012). Thus, how NPY distributes in the brain tissue after i.c.v. application can profoundly influence the anti-absence effect. Our evaluation of i.c.v. applied FG shows that substances can penetrate into the S2 cortex, but also into the VB thalamus after IT treatment (fig. 3.12). Provided that these distribution dynamics can be translated to NPY, the contradicting mechanisms of action in these brain areas could occlude an anti-absence effect. Finally, we cannot definitely answer the question, why our results for i.c.v. applied NPY deviate from those of Stroud et al. (2005).

Somatostatin

The neuropeptide somatostatin (SST) has also been suggested to have antiepileptic properties (Clynen et al., 2014). The receptor SST_2 most probably mediates the anticonvulsant actions of SST in rats by suppressing presynaptic glutamate release (Kozhemyakin et al., 2013). Somatostatin receptors show ubiquitous distribution throughout the brain, including the thalamus and cortex (Srikant and Patel, 1981); however, the antiepileptic actions of SST appear mainly in the hippocampus (Tallent and Qiu, 2008). Indeed, it has been demonstrated that the pharmacological modulation of hippocampal activity can also reduce the incidences of SWDs in WAG/Rij rats (Tolmacheva et al., 2012). Still, i.c.v. application of SST had no antiepileptic effects in GAERS (fig. 3.15; right panel). The IT application of SST may be a possible solution in other epilepsy types as our FG staining showed that i.c.v. applied substances can nicely distribute into the hippocampus (fig. 3.12). This assumption is line with the finding of Mazarati and Telegdy (1992), showing that the i.c.v. application of SST (1.8 nmol) decreases the severity of seizures in picrotoxin-kindled rats (a model for human temporal lobe epilepsy).

In summary our results suggest that the neuropeptides SST and NPY are unsuitable for IT treatment in absence epilepsy.

4.7 The epidural cup as alternative IT application route

The brain and the spinal cord are enclosed by three meninges: the dura mater, the arachnoid mater, and the pia mater. The thick dura mater forms the outermost barrier, whereas the pia mater directly contacts the surface of the brain. Together with the pia mater the arachnoid mater, which lies in the middle of the meninges, encloses the subarachnoid space (SAS), which contains CSF (fig. 4.1). We hypothesized that the highest drug concentration after IT application can be found in the vicinity of the injection site. Hence, drug application into the SAS might be a possibility to increase the penetration of therapeutics into cortical areas. This application route could be advantageous in absence epilepsy, as pharmacological studies showed that the injection of ETX into the S1 cortex of GAERS robustly suppresses SWDs (Manning et al., 2004). Given the relatively small size of the SAS in rats, the direct application of active agents into the CSF is challenging. An alternative application technique to distribute active agents into the SAS, respectively, into the cortex, is transmeningeal pharmacotherapy (Tanganelli et al., 1992). This approach holds the advantage that the application of solutes onto the dura mater is minimally invasive and easy to implement. However, the solute must diffuse through all meninges in order to reach the brain. While the pia and the dura mater mainly consist of collagen and elastin fibers the arachnoid mater is composed of overlapping cells with frequent tight junctions (Bernards and Hill, 1990; Nabeshima et al., 1975). Hence the arachnoid mater forms the major meningeal diffusion barrier between the epidural space and the CNS.

We tested the transmeningeal application route by implanting an epidural cup onto the dura mater (cf. Chapter 2.2; fig 2.2) and filling it with an ethosuximide solution (1 mg/animal or 2 mg/animal). The monitoring of seizures in GAERS after drug application into the cup, however, did not show any antiepileptic effect.
To reach the SAS, the ETX must cross the meninges by diffusion, in contrast, the distribution of i.c.v. applied substances into the brain parenchyma is probably facilitated by bulk flow of the CSF (João Casaca-Carreira et al., 2017). Based on Fick's law, the diffusion rate depends on the concentration differences, the strength of the barrier, the travel distance of molecules, and molecule size and solubility. Thus, we suspect that in order to enhance the diffusion rate and to reach therapeutical drug doses in the cortex, either the ETX concentration in the epidural cup has to be increased or the dura mater and arachnoid mater must be removed before applying the drug.

Although an antiepileptic effect by applying ETX on the cortex could not be demonstrated yet, we believe that further investigation of this application route would be beneficial. Regarding intracranial drug-releasing implants, a subcortical location would be surgically more accessible, less restricted by size compared to the ventricular system, and drug refill would be feasible.

4.8 Method to investigate drug releasing implants

The results from the presented study indicate that acute i.c.v. treatment with low drug dose ETX is significantly more effective in seizure suppression than systemic treatment with the same dose and would thus allow reduction of systemic drug exposure. We believe that the benefits of i.c.v. treatment may be even clearer for continuous treatment. However the permanent implantation of a ventricular catheter in humans holds a high infection risk of the CNS as the brain barriers are permanently interrupted (Chamberlain et al., 1997; Mead et al., 2014). The most common i.c.v. device in clinical use is the Ommaya reservoir, which is mostly used for intracranial chemotherapy (Sheldon and Ommaya, 1963). To widen the therapeutic spectrum of intracranial delivery of therapeutics, alternative application strategies have been investigated and the implementation of advanced biocompatible materials for IT drug delivery may be a potential improved method (Fenton et al., 2018). The demands for drug releasing materials are high as they must be biocompatible and ideally show a steady release within the therapeutic window that does not change with time (i.e zero-order release).

The methodology for i.c.v. implantation and seizure analysis in GAERS, that have been established during this study, can now be used to test drug releasing materials *in vivo*. Based on the dose-response of GAERS to i.c.v. applied ETX and VPA, the release kinetics of the implants could be directly adapted. However, it is essential to note that our knowledge concerning tissue distribution mechanisms is still limited, and a steady release could affect the therapeutic drug concentrations required.
Additionally, adverse effects of local drug exposure and material implantation in the CSF can be continuously observed by video monitoring and the introduced behavioral experiments (cf. Chapter 2.7).
However, we showed that under chloral hydrate anesthesia, the epileptic activity of GAERS was suppressed for approximately five hours. The implantation of a drug-releasing material requires that the animals are under anesthesia. Hence, to investigate the complete time course of the pharmacological effect of a drug-releasing implant, it

would be necessary to find an alternative anesthetic or to implement a material with a drug release, which only starts after more than 5-6 hours.

4.9 Conclusion

In the present study, we have examined in-depth whether the intrathecal drug delivery could in principle be an option for the treatment of epileptic disorders. To this end, we have systematically investigated the therapeutic effects of i.c.v. and subcortically applied substances in a well-validated rat model of absence epilepsy.

We found that i.c.v. administration of ETX and VPA, the classical drugs in absence epilepsy, caused robust and dose-dependent reduction of SWDs. However, ETX showed after systemic treatment and for IT application prolonged and more efficient seizure suppression in GAERS compared to VPA. Additionally, we could show that i.c.v. treatment with ETX is significantly more effective in seizure suppression than systemic treatment with the same dose.
Moreover, the localized application of the AED resulted in dramatically reduced systemic drug exposure compared to standard ETX therapy. These findings strongly argue against the idea that i.c.v. application simply represents a slow intravenous infusion (Pardridge, 2016) and instead suggests that AEDs can penetrate into relevant brain regions directly from the CSF. Indeed, the visual retracing of substance distribution throughout the CNS supported the view that i.c.v. applied drugs cross the ependymal layer surrounding the ventricles and distribute into brain tissue close to the injection site. To which extend this occurs through passive diffusion or convective transport will have to be investigated further. Though, this drug distribution route would narrow the spectrum of epileptic disorders and CNS diseases in general that can be targeted by i.c.v. drug application to those with target regions in the vicinity of the ventricular system. As our dye injections indicated that i.c.v. drug injections may only affect the ipsilateral hemisphere, we believe that the anticonvulsant effect of i.c.v. treatment with AEDs maybe enhanced with bilateral drug injections. Furthermore, the continuous localized treatment via advanced drug releasing materials or application systems, which permit regulated release and reservoir fill up with little risk of infection, could increase the therapeutic efficiency (Fenton et al., 2018). It is thus possible that i.c.v. drug application may become an alternative for systemic therapy in selected CNS disorders.

As our data suggests that IT therapy is feasible through direct transportation of substances from the CSF into the brain tissue, this application method could especially hold therapeutic potential for substances that cannot cross the BBB. Although, we could not confirm an anti-absence effect by the i.c.v. applied neuropeptides NPY and SST other substances should be tested in order to explore this possibility.

References

Abbott NJ, Pizzo ME, Preston JE, Janigro D, Thorne RG (2018). The role of brain barriers in fluid movement in the CNS: is there a 'glymphatic' system? *Acta Neuropathol. (Berl.)* 135, 387–407.

Bacci A, Huguenard JR, Prince DA, (2002). Differential modulation of synaptic transmission by neuropeptide Y in rat neocortical neurons. *Proc. Natl. Acad. Sci.* 99, 17125–17130.

Bachmann K, Jahn D, Yang C, Schwartz J (1988). Ethosuximide disposition kinetics in rats. *Xenobiotica* 18, 373–380.

Baldino F, Geller HM (1981). Sodium valproate enhancement of gamma-aminobutyric acid (GABA) inhibition: electrophysiological evidence for anticonvulsant activity. *J. Pharmacol. Exp. Ther.* 217, 445–450.

Baldino F, Geller HM (1981). Effect of sodium valporate on hypothalamic neurons in vivo and in vitro. *Brain Res.* 219, 231–237.

Baraban SC, Tallent MK (2004). Interneuron Diversity series: Interneuronal neuropeptides – endogenous regulators of neuronal excitability. *Trends Neurosci.* 27, 135–142.

Beenhakker MP, Huguenard JR (2009). Neurons that Fire Together Also Conspire Together: Is Normal Sleep Circuitry Hijacked to Generate Epilepsy? *Neuron* 62, 612–632.

Benarroch EE (2009). Neuropeptide Y: Its multiple effects in the CNS and potential clinical significance. *Neurology* 72, 1016–1020.

Bernards CM, Hill HF (1990). Morphine and Alfentanil Permeability Through the Spinal Dura, Arachnoid, and Pia Mater of Dogs and Monkeys: *Anesthesiology* 73, 1214–1219.

Biggs CS, Pearce BR, Fowler LJ, Whitton PS (1992). The effect of sodium valproate on extracellular GABA and other amino acids in the rat ventral hippocampus: an in vivo microdialysis study. *Brain Res.* 594, 138–142.

Bjorvatn B, Fagerland S, Ursin R (1998). EEG Power Densities (0.5–20 Hz) in Different Sleep–Wake Stages in Rats. *Physiol. Behav.* 63, 413–417.

Blasberg RG, Patlak C, Fenstermacher JD (1975). Intrathecal chemotherapy: brain tissue profiles after ventriculocisternal perfusion. *J. Pharmacol. Exp. Ther.* 195, 73.

Brigo F, Igwe SC, Lattanzi S (2019). Ethosuximide, sodium valproate or lamotrigine for absence seizures in children and adolescents. *Cochrane Database Syst. Rev.*

Broicher, Seidenbecher T, Meuth P, Munsch T, Meuth SG, Kanyshkova T, Pape H-C, Budde T (2007). T-current related effects of antiepileptic drugs and a Ca2+ channel antagonist on thalamic relay and local circuit interneurons in a rat model of absence epilepsy. *Neuropharmacology* 53, 431–446.

Browne T (1983). Ethosuximide (Zarontin) and other succinimides. *Epilepsy Diagn. Manag.* 215–224.

Buchanan RA, Fernandez L, Kinkel AW (1969). Absorption and elimination of ethosuximide in children. *J. Clin. Pharmacol. J. New Drugs* 9, 393–398.

Burton B (1882). On the propyl derivatives and decomposition products of ethylacetoacetate. *Am Chem J* 3, 385–95.

Casaca-Carreira João, Temel Y, Hescham S-A, Jahanshahi A (2017). Transependymal Cerebrospinal Fluid Flow: Opportunity for Drug Delivery? *Mol. Neurobiol.*

Casaca-Carreira João, Temel Y, Larrakoetxea I, Jahanshahi A (2017). Distribution and Penetration of Intracerebroventricularly Administered 2′OMePS Oligonucleotide in the Mouse Brain. *Nucleic Acid Ther.* 27, 4–10.

Chamberlain MC, Kormanik PA, Barba D (1997). Complications associated with intraventricular chemotherapy in patients with leptomeningeal metastases. *J. Neurosurg.* 87, 694–699.

Chapman AG, Riley K, Evans MC, Meldrum BS (1982). Acute effects of sodium valproate and gamma-vinyl gaba on regional amino acid metabolism in the rat brain: Incorporation of 2-[14C]glucose into amino acids. *Neurochem. Res.* 7, 1089–1105.

Chazen JL, Dyke JP, Holt RW, Horky L, Pauplis RA, Hesterman JY, Mozley DP, Verma A (2017). Automated segmentation of MR imaging to determine normative central nervous system cerebrospinal fluid volumes in healthy volunteers. *Clin. Imaging* 43, 132–135.

Chen Y, Parker WD, Wang K (2014). The Role of T-Type Calcium Channel Genes in Absence Seizures. *Front. Neurol.* 5.

Chiu C, Miller MC, Caralopoulos IN, Worden MS, Brinker T, Gordon ZN, Johanson CE, Silverberg GD (2012). Temporal course of cerebrospinal fluid dynamics and amyloid accumulation in the aging rat brain from three to thirty months. *Fluids Barriers CNS* 9, 3–3.

Clynen E, Swijsen A, Raijmakers M, Hoogland G, Rigo J-M (2014). Neuropeptides as Targets for the Development of Anticonvulsant Drugs. *Mol. Neurobiol.* 50, 626–646.

Coenen A, van Luijtelaar G, 2003. Genetic Animal Models for Absence Epilepsy: A Review of the WAG/Rij Strain of Rats. *Behav. Genet.* 33, 635–655.

Cook AM, Mieure KD, Owen RD, Pesaturo AB, Hatton J (2009). Intracerebroventricular Administration of Drugs. *Pharmacotherapy* 29, 832–845.

Coulter DA, Huguenard JR, Prince DA (1989). Characterization of ethosuximide reduction of low-threshold calcium current in thalamic neurons. *Ann. Neurol.* 25, 582–593.

Crunelli V, David F, Leresche N, Lambert RC (2014). Role for T-type Ca2+ channels in sleep waves. *Pflüg. Arch. - Eur. J. Physiol.* 466, 735–745.

Crunelli V, Leresche N (2002). Childhood absence epilepsy: Genes, channels, neurons and networks. *Nat. Rev. Neurosci.* 3, 371–382.

Cunningham M (2003). Valproate modifies spontaneous excitation and inhibition at cortical synapses in vitro. Neuropharmacology 45, 907–917.

Danober L, Deransart C, Depaulis A, Vergnes M, Marescaux C (1998). Pathophysiological mechanisms of genetic absence epilepsy in the rat. *Prog. Neurobiol.* 55, 27–57.

Davies JA (1995). Mechanisms of action of antiepileptic drugs. *Seizure* 4, 267–271.

Davis R, Peters DH, McTavish D (1994). Valproic acid. A reappraisal of its pharmacological properties and clinical efficacy in epilepsy. *Drugs* 47, 332–372.

De Gennaro L, Ferrara M (2003). Sleep spindles: an overview. *Sleep Med. Rev.* 7, 423–440.

Dedeurwaerdere S, van Raay L, Morris MJ, Reed RC, Hogan RE, O'Brien TJ (2011). Fluctuating and constant valproate administration gives equivalent seizure control in rats with genetic and acquired epilepsy. *Seizure* 20, 72–79.

Defazio R, Criado A, Zantedeschi V, Scanziani E (2015). Neuroanatomy-based Matrix-guided Trimming Protocol for the Rat Brain. *Toxicol. Pathol.* 43, 249–256.

Depaulis A, David O, Charpier S (2016). The genetic absence epilepsy rat from Strasbourg as a model to decipher the neuronal and network mechanisms of generalized idiopathic epilepsies. *J. Neurosci. Methods* 260, 159–174.

Di Chiro G (1966). Observations on the circulation of the cerebrospinal fluid. *Acta Radiol. Diagn. (Stockh.)* 5, 988–1002.

Dijk D-J, Hayes B, Czeisler CA (1993). Dynamics of electroencephalographic sleep spindles and slow wave activity in men: effect of sleep deprivation. *Brain Res.* 626, 190–199.

Drinkenburg W, Coenen A, Vossen J, Van Luijtelaar E (1991). Spike-wave discharges and sleep-wake states in rats with absence epilepsy. *Epilepsy Res.* 9, 218–224.

Dunham NW, Miya TS (1957). A Note on a Simple Apparatus for Detecting Neurological Deficit in Rats and Mice**College of Pharmacy, University of Nebraska, Lincoln 8. J. Am. *Pharm. Assoc. Sci. Ed* 46, 208–209.

El Bahh B, Balosso S, Hamilton T, Herzog H, Beck-Sickinger AG, Sperk G, Gehlert DR, Vezzani A, Colmers WF (2005). The anti-epileptic actions of neuropeptide Y in the hippocampus are mediated by Y2 and not Y5 receptors: NPY anti-epileptic effect is via Y2 not Y5 receptors. *Eur. J. Neurosci.* 22, 1417–1430.

Fenton OS, Olafson KN, Pillai PS, Mitchell MJ, Langer R (2018). Advances in Biomaterials for Drug Delivery. *Adv. Mater.* 30, 1705328.

Field KJ, White WJ, Lang CM (1993). Anaesthetic effects of chloral hydrate, pentobarbitone and urethane in adult male rats. *Lab. Anim.* 27, 258–269.

Fowler MJ, Cotter JD, Knight BE, Sevick-Muraca EM, Sandberg DI, Sirianni RW (2020). Intrathecal drug delivery in the era of nanomedicine. *Adv. Drug Deliv. Rev.* S0169409X20300120.

Frey H-H, Löscher W (1978). Distribution of valproate across the interface between blood and cerebrospinal fluid. *Neuropharmacology* 17, 637–642.

Gelfo F, De Bartolo P, Tirassa P, Croce N, Caltagirone C, Petrosini L, Angelucci F (2011). Intraperitoneal injection of neuropeptide Y (NPY) alters neurotrophin rat hypothalamic levels: Implications for NPY potential role in stress-related disorders. *Peptides* 32, 1320–1323.

Glauser TA, Cnaan A, Shinnar S, Hirtz DG, Dlugos D, Masur D, Clark PO, Capparelli EV, Adamson PC (2010). Ethosuximide, valproic acid, and lamotrigine in childhood absence epilepsy. *N. Engl. J. Med.* 362, 790–799.

Gören MZ, Onat F (2007). Ethosuximide: From Bench to Bedside. *CNS Drug Rev.* 13, 224–239.

Greenhill SD, Morgan NH, Massey PV, Woodhall GL, Jones R (2012). Ethosuximide modifies network excitability in the rat entorhinal cortex via an increase in GABA release. *Neuropharmacology* 62, 807–814.

Gülhan Aker R, Tezcan K, Carçak N, Sakalli E, Akin D, Onat FY (2010). Localized cortical injections of ethosuximide suppress spike-and-wave activity and reduce the resistance to kindling in genetic absence epilepsy rats (GAERS). *Epilepsy Res.* 89, 7–16.

Halassa MM, Acsády L (2016). Thalamic Inhibition: Diverse Sources, Diverse Scales. *Trends Neurosci.* 39, 680–693.

Hese PV, Martens JP, Boon P, Dedeurwaerdere S, Lemahieu I, Walle RV (2003). Detection of spike and wave discharges in the cortical EEG of genetic absence epilepsy rats from Strasbourg. *Phys. Med. Biol.* 48, 1685–1700.

Ho M, Beck-Sickinger AG, Colmers WF (2000). Neuropeptide Y5 Receptors Reduce Synaptic Excitation in Proximal Subiculum, But Not Epileptiform Activity in Rat Hippocampal Slices. *J. Neurophysiol.* 83, 723–734.

Holmes MD, Brown M, Tucker DM (2004). Are "Generalized" Seizures Truly Generalized? Evidence of Localized Mesial Frontal and Frontopolar Discharges in Absence. *Epilepsia* 45, 1568–1579.

Honack D, Löscher W (1995). Kindling Increases the Sensitivity of Rats to Adverse Effects of Certain Antiepileptic Drugs. *Epilepsia* 36, 763–771.

Huguenard J, Prince D (1994). Intrathalamic rhythmicity studied in vitro: nominal T-current modulation causes robust antioscillatory effects. *J. Neurosci*. 14, 5485–5502.

Huntsman MM (1999). Reciprocal Inhibitory Connections and Network Synchrony in the Mammalian Thalamus. *Science* 283, 541–543.

Jiménez AJ, Domínguez-Pinos M-D, Guerra MM, Fernández-Llebrez P, Pérez-Fígares J-M (2014). Structure and function of the ependymal barrier and diseases associated with ependyma disruption. *Tissue Barriers* 2, e28426.

Johannessen CU, Johannessen SI (2003). Valproate: Past, Present, and Future. *CNS Drug Rev*. 9, 199–216.

Jones EG (1975). Some aspects of the organization of the thalamic reticular complex. *J. Comp. Neurol.* 162, 285–308.

Kellaway P, Frost JD, Crawley JW (1980). Time modulation of spike-and-wave activity in generalized epilepsy. *Ann. Neurol.* 8, 491–500.

Kofler N, Kirchmair E, Schwarzer C, Sperk G (1997). Altered expression of NPY-Y1 receptors in kainic acid induced epilepsy in rats. *Neurosci. Lett.* 230, 129–132.

Kovac S, Walker MC (2013). Neuropeptides in epilepsy. *Neuropeptides* 47, 467–475.

Kozhemyakin M, Rajasekaran K, Todorovic MS, Kowalski SL, Balint C, Kapur J (2013). Somatostatin type-2 receptor activation inhibits glutamate release and prevents status epilepticus. *Neurobiol. Dis.* 54, 94–104.

Kwan P, Arzimanoglou A, Berg AT, Brodie MJ, Allen Hauser W, Mathern G, Moshé SL, Perucca E, Wiebe S, French J (2010). Definition of drug resistant epilepsy: consensus proposal by the ad hoc Task Force of the ILAE Commission on Therapeutic Strategies. *Epilepsia* 51, 1069–1077.

Kwan P, Schachter SC, Brodie MJ (2011). Drug-Resistant Epilepsy. *N. Engl. J. Med.* 365, 919–926.

Landisman CE, Long MA, Beierlein M, Deans MR, Paul DL, Connors BW (2002). Electrical synapses in the thalamic reticular nucleus. *J. Neurosci. Off. J. Soc. Neurosci.* 22, 1002–1009.

Lannes B, Micheletti G, Vergnes M, Marescaux Ch, Depaulis A, Warter JM (1988). Relationship between spike-wave discharges and vigilance levels in rats with spontaneous petit mal-like epilepsy. *Neurosci. Lett.* 94, 187–191.

Leresche N, Lambert RC, Errington AC, Crunelli V (2012). From sleep spindles of natural sleep to spike and wave discharges of typical absence seizures: is the hypothesis still valid? *Pflüg. Arch. - Eur. J. Physiol.* 463, 201–212.

Leresche N, Parri HR, Erdemli G, Guyon A, Turner JP, Williams SR, Asprodini E, Crunelli V (1998). On the Action of the Anti-Absence Drug Ethosuximide in the Rat and Cat Thalamus. *J. Neurosci.* 18, 4842–4853.

Li Y, Zhang B, Liu X-W, Liu M, Huang S-M (2016). An applicable method of drawing cerebrospinal fluid in rats. *J. Chem. Neuroanat.* 74, 18–20.

Liang J, Zhang Y, Wang J, Pan H, Wu H, Xu K, Liu X, Jiang Y, Shen Y, Wu X (2006). New variants in the CACNA1H gene identified in childhood absence epilepsy. *Neurosci. Lett.* 406, 27–32.

Lindberger M, Tomson T, Wallstedt L, Ståhle L (2008). Distribution of Valproate to Subdural Cerebrospinal Fluid, Subcutaneous Extracellular Fluid, and Plasma in Humans: A Microdialysis Study. *Epilepsia* 42, 256–261.

Linninger AA, Tangen K, Hsu C-Y, Frim D (2016). Cerebrospinal Fluid Mechanics and Its Coupling to Cerebrovascular Dynamics. *Annu. Rev. Fluid Mech.* 48, 219–257.

Liu Z, Vergnes M, Depaulis A, Marescaux C (1991). Evidence for a critical role of GABAergic transmission within the thalamus in the genesis and control of absence seizures in the rat. *Brain Res.* 545, 1–7.

Lockman LA (1989). Absence, Myoclonic, and Atonic Seizures. *Pediatr. Clin. North Am. 36*, 331–341.

Löscher W (2002). Basic Pharmacology of Valproate: A Review After 35 Years of Clinical Use for the Treatment of Epilepsy. *CNS Drugs* 16, 669–694.

Löscher W (2007). The Pharmacokinetics of Antiepileptic Drugs in Rats: Consequences for Maintaining Effective Drug Levels during Prolonged Drug Administration in Rat Models of Epilepsy. *Epilepsia* 48, 1245–1258.

Löscher W (1999a). The discovery of valproate, in: Löscher, W. (Ed.), Valproate. Birkhäuser Basel, Basel, pp. 1–3.

Löscher W (1999b). Valproate: a reappraisal of its pharmacodynamic properties and mechanisms of action. *Prog. Neurobiol.* 58, 31–59.

Löscher W (1978). Serum protein binding and pharmacokinetics of valproate in man, dog, rat and mouse. *J. Pharmacol. Exp. Ther.* 204, 255–261.

Löscher W, Potschka H (2005). Blood-brain barrier active efflux transporters: ATP-binding cassette gene family. *NeuroRX* 2, 86–98.

Ludvig N, Baptiste SL, Tang HM, Medveczky G, Gizycki HV, Charchaflieh J, Devinsky O, Kuzniecky RI (2009). Localized transmeningeal muscimol prevents neocortical seizures in rats and nonhuman primates: Therapeutic implications. *Epilepsia* 50, 678–693.

Ludvig N, Sheffield LG, Tang HM, Baptiste SL, Devinsky O, Kuzniecky RI (2008). Histological evidence for drug diffusion across the cerebral meninges into the underlying neocortex in rats. *Brain Res.* 1188, 228–232.

Lüttjohann A, van Luijtelaar G (2015). Dynamics of networks during absence seizure's on- and offset in rodents and man. *Front. Physiol.* 6.

Lüttjohann A, Schoffelen J-M, van Luijtelaar G (2014). Termination of ongoing spike-wave discharges investigated by cortico–thalamic network analyses. *Neurobiol. Dis.* 70, 127–137.

Macdonald RL (1989). Antiepileptic Drug Actions. *Epilepsia* 30, S19–S28.

Manning J-P, Richards DA, Bowery NG (2003). Pharmacology of absence epilepsy. *Trends Pharmacol. Sci.* 24, 542–549.

Manning J-P, Richards DA, Leresche N, Crunelli V, Bowery NG (2004). Cortical-area specific block of genetically determined absence seizures by ethosuximide. *Neuroscience* 123, 5–9.

Marescaux C, Vergnes M, Depaulis A (1992). Genetic absence epilepsy in rats from Strasbourg — A review, in: Marescaux C, Vergnes M, Bernasconi R Generalized Non-Convulsive Epilepsy: Focus on GABA-B Receptors. Springer Vienna, Vienna, pp. 37–69.
Mazarati AM, Telegdy G (1992). Effects of somatostatin and anti-somatostatin serum on picrotoxin-kindled seizures. *Neuropharmacology* 31, 793–797.

Mazarati AM, Wasterlain CG (2002). Anticonvulsant effects of four neuropeptides in the rat hippocampus during self-sustaining status epilepticus. *Neurosci. Lett.* 331, 123–127.

McCafferty C, David F, Venzi M, Lőrincz ML, Delicata F, Atherton Z, Recchia G, Orban G, Lambert RC, Di Giovanni G (2018). Cortical drive and thalamic feed-forward inhibition control thalamic output synchrony during absence seizures. *Nat. Neurosci.* 21, 744–756.

McCormick DA, Bal T (1997). Sleep and arousal: Thalamocortical Mechanisms. *Annu. Rev. Neurosci.* 20, 185–215.

McKinley MJ, Albiston AL, Allen AM, Mathai ML, May CN, McAllen RM, Oldfield BJ, Mendelsohn FA, Chai SY (2003). The brain renin–angiotensin system: location and physiological roles. *Renin-Angiotensin Syst. State Art* 35, 901–918.

McLean MJ, Macdonald RL (1986). Sodium valproate, but not ethosuximide, produces use- and voltage-dependent limitation of high frequency repetitive firing of action potentials of mouse central neurons in cell culture. *J. Pharmacol. Exp. Ther.* 237, 1001–1011.

Mead PA, Safdieh JE, Nizza P, Tuma S, Sepkowitz KA (2014). Ommaya reservoir infections: A 16-year retrospective analysis. *J. Infect.* 68, 225–230.

Meeren H, van Luijtelaar G, Lopes da Silva F, Coenen A (2005). Evolving Concepts on the Pathophysiology of Absence Seizures: The Cortical Focus Theory. *Arch. Neurol.* 62, 371.

Meeren H, Pijn J, Van Luijtelaar G, Coenen A, Lopes da Silva F (2002). Cortical Focus Drives Widespread Corticothalamic Networks during Spontaneous Absence Seizures in Rats. *J. Neurosci.* 22, 1480–1495.

Miller TM., Pestronk A, David W, Rothstein J, Simpson E, Appel SH, Andres PL, Mahoney K, Allred P, Alexander K, Ostrow LW, Schoenfeld D, Macklin EA, Norris DA, Manousakis G, Crisp M, Smith R, Bennett CF, Bishop KM, Cudkowicz ME (2013). An antisense oligonucleotide against SOD1 delivered intrathecally for patients with SOD1 familial amyotrophic lateral sclerosis: a phase 1, randomised, first-in-man study. *Lancet Neurol.* 12, 435–442.

Millership JS, Mifsud J, Collier PS (1993). The metabolism of ethosuximide. *Eur. J. Drug Metab. Pharmacokinet.* 18, 349–353.

Misra A, Ganesh S, Shahiwala A, Shah SP (2003). Drug delivery to the central nervous system: a review. *J. Pharm. Pharm. Sci. Publ. Can. Soc. Pharm. Sci. Soc. Can. Sci. Pharm.* 6, 252–273.

Morris MJ, Gannan E, Stroud LM, Beck-Sickinger AG, O'Brien TJ (2007). Neuropeptide Y suppresses absence seizures in a genetic rat model primarily through effects on Y2 receptors: NPY ameliorates absence epilepsy. *Eur. J. Neurosci.* 25, 1136–1143.

Mytinger JR, Joshi S (2012). The Current Evaluation and Treatment of Infantile Spasms Among Members of the Child Neurology Society. *J. Child Neurol.* 27, 1289–1294.

Nabeshima S, Reese TS, Landis D, Brightman MW (1975). Junctions in the meninges and marginal glia. *J. Comp. Neurol.* 164, 127–169.

Noè F, Pool A-H, Nissinen J, Gobbi M, Bland R, Rizzi M, Balducci C, Ferraguti F, Sperk G, During MJ, Pitkänen A, Vezzani A (2008). Neuropeptide Y gene therapy decreases chronic spontaneous seizures in a rat model of temporal lobe epilepsy. *Brain* 131, 1506–1515.

Oby E, Janigro D (2006). The Blood-Brain Barrier and Epilepsy. *Epilepsia* 47, 1761–1774.

Olsson I (1988). Epidemiology of Absence Epilepsy.: I. Concept and Incidence. Acta Paediatr. 77, 860–866.

Orešković D, Klarica M (2010). The formation of cerebrospinal fluid: Nearly a hundred years of interpretations and misinterpretations. *Brain Res. Rev.* 64, 241–262.

Panayiotopoulos CP (2005). Idiopathic Generalized Epilepsies: A Review and Modern Approach. *Epilepsia* 46, 1–6.

Pardridge WM (2020). Blood-Brain Barrier and Delivery of Protein and Gene Therapeutics to Brain. *Front. Aging Neurosci.* 11, 373.

Pardridge WM (2016). CSF, blood-brain barrier, and brain drug delivery. *Expert Opin. Drug Deliv.* 13, 963–975.

Pardridge WM (2005). The blood-brain barrier: Bottleneck in brain drug development. *NeuroRX* 2, 3–14.

Patel IH, Levy RH, Rapport RL (1977). Distribution Characteristics of Ethosuximide in Discrete Areas of Rat Brain. *Epilepsia* 18, 533–541.

Patsalos PN (2005). Properties of Antiepileptic Drugs in the Treatment of Idiopathic Generalized Epilepsies. *Epilepsia* 46, 140–148.

Paxinos G, Watson C (2006). The rat brain in stereotaxic coordinates: hard cover edition. Elsevier.

Pinault D, Leresche N, Charpier S, Deniau J-M, Marescaux C, Vergnes M, Crunelli V (1998). Intracellular recordings in thalamic neurones during spontaneous spike and wave discharges in rats with absence epilepsy. *J. Physiol.* 509, 449–456.

Pinault D, Smith Y, Deschênes M (1997). Dendrodendritic and axoaxonic synapses in the thalamic reticular nucleus of the adult rat. *J. Neurosci. Off. J. Soc. Neurosci.* 17, 3215–3233.

Polack P-O, Guillemain I, Hu E, Deransart C, Depaulis A, Charpier S (2007). Deep Layer Somatosensory Cortical Neurons Initiate Spike-and-Wave Discharges in a Genetic Model of Absence Seizures. J. Neurosci. 27, 6590–6599.

Polack P-O, Mahon S, Chavez M, Charpier S (2009). Inactivation of the Somatosensory Cortex Prevents Paroxysmal Oscillations in Cortical and Related Thalamic Neurons in a Genetic Model of Absence Epilepsy. *Cereb. Cortex* 19, 2078–2091.

Powell KL, Cain SM, Ng C, Sirdesai S, David LS, Kyi M, Garcia E, Tyson JR, Reid CA, Bahlo M, Foote SJ, Snutch TP, O'Brien TJ (2009). A Cav3.2 T-Type Calcium Channel Point Mutation Has Splice-Variant-Specific Effects on Function and Segregates with Seizure Expression in a Polygenic Rat Model of Absence Epilepsy. *J. Neurosci.* 29, 371–380.

Powell KL, Tang H, Ng C, Guillemain I, Dieuset G, Dezsi G, Çarçak N, Onat F, Martin B, O'Brien TJ, Depaulis A, Jones NC (2014). Seizure expression, behavior, and brain morphology differences in colonies of Genetic Absence Epilepsy Rats from Strasbourg. *Epilepsia* 55, 1959–1968.

Proescholdt MG, Hutto B, Brady LS, Herkenham M (1999). Studies of cerebrospinal fluid flow and penetration into brain following lateral ventricle and cisterna magna injections of the tracer [14C]inulin in rat. *Neuroscience* 95, 577–592.

Ramcharan EJ, Gnadt JW, Sherman SM (2000). Burst and tonic firing in thalamic cells of unanesthetized, behaving monkeys. *Vis. Neurosci.* 17, 55–62.

Rassner MP, Hebel JM, Altenmüller D-M, Volz S, Herrmann LS, Feuerstein TJ, Freiman TM (2015). Reduction of epileptiform activity through local valproate-implants in a rat neocortical epilepsy model. *Seizure* 30, 6–13.

Reubelt D, Small LC, Hoffmann M, Kapapa T, Schmitz BL (2009). MR Imaging and Quantification of the Movement of the Lamina Terminalis Depending on the CSF Dynamics. *Am. J. Neuroradiol.* 30, 199–202.

Rice AC, Floyd CL, Lyeth BG, Hamm RJ, DeLorenzo RJ (1998). Status Epilepticus Causes Long-Term NMDA Receptor-Dependent Behavioral Changes and Cognitive Deficits. *Epilepsia* 39, 1148–1157.

Richards DA, Manning J-P, Barnes D, Rombola L, Bowery NG, Caccia S, Leresche N, Crunelli V (2003). Targeting thalamic nuclei is not sufficient for the full anti-absence action of ethosuximide in a rat model of absence epilepsy. *Epilepsy Res.* 54, 97–107.

Rodgers KM, Dudek FE, Barth DS (2015). Progressive, Seizure-Like, Spike-Wave Discharges Are Common in Both Injured and Uninjured Sprague-Dawley Rats: Implications for the Fluid Percussion Injury Model of Post-Traumatic *Epilepsy. J. Neurosci.* 35, 9194–9204.

Romoli M, Mazzocchetti P, D'Alonzo R, Siliquini S, Rinaldi VE, Verrotti A, Calabresi P, Costa C (2019). Valproic Acid and Epilepsy: From Molecular Mechanisms to Clinical Evidences. *Curr. Neuropharmacol.* 17, 926–946.

Scheffer IE, Berkovic S, Capovilla G, Connolly MB, French J, Guilhoto L, Hirsch E, Jain S, Mathern GW, Moshé SL, Nordli DR, Perucca E, Tomson T, Wiebe S, Zhang Y-H, Zuberi SM (2017). ILAE classification of the epilepsies: Position paper of the ILAE Commission for Classification and Terminology. *Epilepsia* 58, 512–521.

Schlageter KE, Molnar P, Lapin GD, Groothuis DR (1999). Microvessel Organization and Structure in Experimental Brain Tumors: Microvessel Populations with Distinctive Structural and Functional Properties. *Microvasc. Res.* 58, 312–328.

Serralta A, Barcia JA, Ortiz P, Durán C, Hernández ME, Alós M (2006). Effect of intracerebroventricular continuous infusion of valproic acid versus single i.p. and i.c.v. injections in the amygdala kindling epilepsy model. *Epilepsy Res.* 70, 15–26.

Sharma AK, Rani E, Waheed A, Rajput SK (2015). Pharmacoresistant Epilepsy: A Current Update on Non-Conventional Pharmacological and Non-Pharmacological Interventions. *J. Epilepsy Res.* 5, 1–8.

Sharp P, Villano JS (2012). The laboratory rat. *CRC press.*

Sheldon P, Ommaya AK (1963). Ventricular Dilatation Masking the Presence of Cerebral Tumours. *Acta Radiol. Diagn. (Stockh.)* 1, 628–637.

Sherman SM (2001). Tonic and burst firing: dual modes of thalamocortical relay. *Trends Neurosci*. 24, 122–126.

Sherman SM, Guillery RW (1996). Functional organization of thalamocortical relays. *J. Neurophysiol.* 76, 1367–1395.

Shokry IM, Callanan JJ, Sousa J, Tao R (2016). New Insights on Different Response of MDMA-Elicited Serotonin Syndrome to Systemic and Intracranial Administrations in the Rat Brain. PLOS ONE 11, e0155551.

Sitnikova E, van Luijtelaar G (2004). Cortical control of generalized absence seizures: effect of lidocaine applied to the somatosensory cortex in WAG/Rij rats. *Brain Res.* 1012, 127–137.

Sloviter R (1987). Decreased hippocampal inhibition and a selective loss of interneurons in experimental epilepsy. *Science* 235, 73–76.

Sørensen AT, Nikitidou L, Ledri M, Lin E-J, During MJ, Kanter-Schlifke I, Kokaia M (2009). Hippocampal NPY gene transfer attenuates seizures without affecting epilepsy-induced impairment of LTP. *Exp. Neurol.* 215, 328–333.

Sorokin JM, Davidson TJ, Frechette E, Abramian AM, Deisseroth K, Huguenard JR, Paz JT (2017). Bidirectional control of generalized epilepsy networks via rapid real-time switching of firing mode. *Neuron* 93, 194–210.

Spector R, Keep RF, Robert Snodgrass S, Smith QR, Johanson CE (2015). A balanced view of choroid plexus structure and function: Focus on adult humans. *Exp. Neurol.* 267, 78–86.

Srikant CB, Patel YC (1981). Somatostatin receptors: identification and characterization in rat brain membranes. *Proc. Natl. Acad. Sci.* 78, 3930–3934.

Steriade M (1990). Spindling, Incremental Thalamocortical Responses, and Spike-Wave Epilepsy, in: Avoli, M., Gloor, P., Kostopoulos, G., Naquet, R. (Eds.), *Generalized Epilepsy. Birkhäuser Boston, Boston, MA*, pp. 161–180.

Steriade M, Contreras D (1995). Relations between cortical and thalamic cellular events during transition from sleep patterns to paroxysmal activity. *J. Neurosci. Off. J. Soc. Neurosci.* 15, 623–642.

Stroud LM, O'Brien TJ, Jupp B, Wallengren C, Morris MJ (2005). Neuropeptide Y suppresses absence seizures in a genetic rat model. *Brain Res.* 1033, 151–156.

Sun Y, Wong A, Kamel MS (2009). Classification of imbalanced data: a review. Int. J. Pattern Recognit. *Artif. Intell.* 23, 687–719.

Swank RL, Watson CW (1949). Effects of barbiturates and ether on spontaneous electrical activity of dog brain. *J. Neurophysiol*. 12, 137–160.

Tallent MK, Qiu C (2008). Somatostatin: An endogenous antiepileptic. *Mol. Cell. Endocrinol.* 286, 96–103.

Tanganelli S, Ferraro L, Bianchi C, Beani L (1992). Changes in gamma-aminobutyric acid release induced by topical administration of drugs affecting its metabolism and receptors: Studies in freely moving guinea pigs with epidural cups. *Neurochem. Int.* 21, 15–20.

Taverna S, Mantegazza M, Franceschetti S, Avanzini G (1998). Valproate selectively reduces the persistent fraction of Na+ current in neocortical neurons. *Epilepsy Res.* 32, 304–308.

Teschendorf HJ, Kretzschmar R (1985). Succinimides, in: Frey, H.-H., Janz, D. (Eds.), Antiepileptic Drugs, Handbook of Experimental Pharmacology. *Springer Berlin Heidelberg, Berlin* pp. 557–574.

Tollner K, Wolf S, Löscher W, Gernert M (2011). The Anticonvulsant Response to Valproate in Kindled Rats Is Correlated with Its Effect on Neuronal Firing in the Substantia Nigra Pars Reticulata: A New Mechanism of Pharmacoresistance. *J. Neurosci*. 31, 16423–16434.

Tolmacheva EA, Oitzl MS, van Luijtelaar G (2012). Stress, glucocorticoids and absences in a genetic epilepsy model. *Horm. Behav.* 61, 706–710.

Tu Y-K (2016). Testing the relation between percentage change and baseline value. *Sci. Rep*. 6, 23247.

Urrego JA, Greene SA, Rojas MJ (2014). Brain burst suppression activity. *Psychol. Neurosci.* 7, 531–543.

Van Luijtelaar G, Coenen A (1988). Circadian rhythmicity in absence epilepsy in rats. *Epilepsy Res.* 2, 331–336.

Van Luijtelaar G, Lüttjohann A, Makarov VV, Maksimenko VA, Koronovskii AA, Hramov AE (2016). Methods of automated absence seizure detection, interference by stimulation, and possibilities for prediction in genetic absence models. *J. Neurosci. Methods* 260, 144–158.

Van Luijtelaar G, Mishra AM, Edelbroek P, Coman D, Frankenmolen N, Schaapsmeerders P, Covolato G, Danielson N, Niermann H, Janeczko K, Kiemeneij A, Burinov J, Bashyal C,

Coquillette M, Lüttjohann A, Hyder F, Blumenfeld H, van Rijn CM (2013). Anti-epileptogenesis: Electrophysiology, diffusion tensor imaging and behavior in a genetic absence model. *Neurobiol. Dis.* 60, 126–138.

Van Luijtelaar G, van Oijen G (2020). Establishing Drug Effects on Electrocorticographic Activity in a Genetic Absence Epilepsy Model: Advances and Pitfalls. *Front. Pharmacol.* 11, 395.

Van Luijtelaar G, Wiaderna D, Elants C, Scheenen W (2000). Opposite effects of T- and L-type Ca2q channels blockers in generalized absence epilepsy 9.

Van Raay L, Jovanovska V, Morris MJ, O'Brien TJ (2012). Focal administration of neuropeptide Y into the S2 somatosensory cortex maximally suppresses absence seizures in a genetic rat model: Focal NPY Suppresses Seizures in GAERS. *Epilepsia* 53, 477–484.

Van Rijn CM, Sun MS, Deckers CL, Edelbroek PM, Keyser A, Renier W, Meinardi H (2004). Effects of the combination of valproate and ethosuximide on spike wave discharges in WAG/Rij rats. *Epilepsy Res.* 59, 181–189.

Vergnes M, Marescaux C, Boehrer A, Depaulis A (1991). Are rats with genetic absence

epilepsy behaviorally impaired? *Epilepsy Res.* 9, 97–104.

Vergnes M, Marescaux Ch, Micheletti G, Reis J, Depaulis A, Rumbach L, Warter JM (1982). Spontaneous paroxysmal electroclinical patterns in rat: A model of generalized non-convulsive epilepsy. *Neurosci. Lett.* 33, 97–101.

Viollet C, Lepousez G, Loudes C, Videau C, Simon A, Epelbaum J (2008). Somatostatinergic systems in brain: Networks and functions. *Mol. Cell. Endocrinol.* 286, 75–87.

Von Krosigk M, Bal T, McCormick D (1993). Cellular mechanisms of a synchronized oscillation in the thalamus. *Science* 261, 361–364.

Walden J, Altrup U, Reith H, Speckmann E-J (1993). Effects of valproate on early and late potassium currents of single neurons. *Eur. Neuropsychopharmacol.* 3, 137–141.

Wallace RH, Marini C, Petrou S, Harkin LA, Bowser DN, Panchal RG, Williams DA, Sutherland GR, Mulley JC, Scheffer IE, Berkovic SF (2001). Mutant GABAA receptor γ2-subunit in childhood absence epilepsy and febrile seizures. *Nat. Genet.* 28, 49–52.

Westerhout J, Ploeger B, Smeets J, Danhof M, de Lange EC (2012). Physiologically Based Pharmacokinetic Modeling to Investigate Regional Brain Distribution Kinetics in Rats. *AAPS J*. 14, 543–553.

White HS (1999). Comparative Anticonvulsant and Mechanistic Profile of the Established and Newer Antiepileptic Drugs. *Epilepsia* 40, 2–10.

Wolak DJ, Thorne RG (2013). Diffusion of Macromolecules in the Brain: Implications for Drug Delivery. *Mol. Pharm.* 10, 1492–1504.

World Health Organization (2006). Neurological disorders: public health challenges. World Health Organization.

Yan Q, Matheson C, Sun J, Radeke MJ, Feinstein SC, Miller JA (1994) Distribution of Intracerebral Ventricularly Administered Neurotrophins in Rat Brain and Its Correlation with Trk Receptor Expression. *Exp. Neurol.* 127, 23–36.

Zhan XJ, Cox CL, Sherman SM (2000). Dendritic Depolarization Efficiently Attenuates Low-Threshold Calcium Spikes in Thalamic Relay Cells. *J. Neurosci.* 20, 3909–3914.

Zimmerman FT, Burgemeister BB (1958). A new drug for petit mal epilepsy. *Neurology* 8, 769–769.

Supplementary data

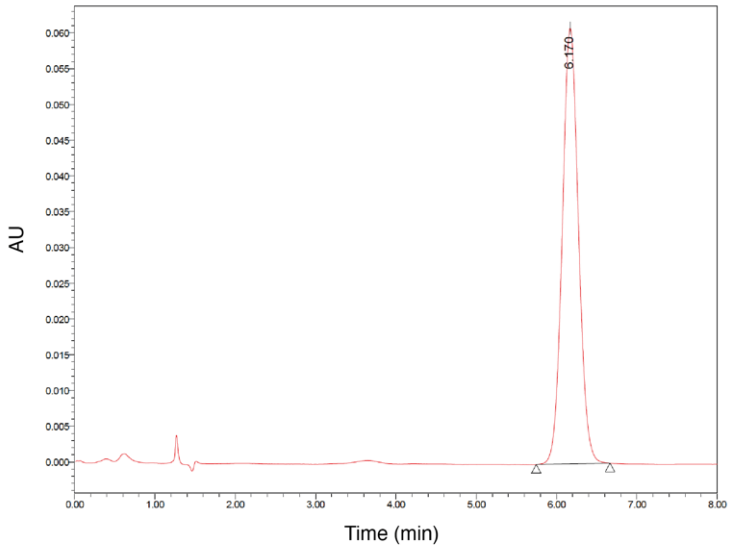

Figure S.1: HPLC calibration chromatogram, to detect ETX in brain samples after animals were treated with the AED. The concertation of 54,6 µg/ml ETX dissolved in water was injected into the apparatus (detection at 249 nm). A clear peak for ETX is visible after 6.1 minutes.

Table S.2: Reference samples for HPLC analysis – ETX concentration (µg/g) of (µg/ml) in collected samples after ICV, IP, or IV drug injection of ringer solution.

	IP(Saline)	IV(Saline)	ICV(Saline)
CSF (µg/ml)	0	0	0
Plasma (µg/ml)	0	0	0
Cortex (+) (µg/g)	0	0	6.0
Cortex (-) (µg/g)	0	0	10.0
Thalamus (+) (µg/g)	0	0	12.7
Thalamus (-) (µg/g)	0	0	3.7

Danksagung

Am Ende einer intensiven Zeit möchte ich all den Menschen danken, die mich bei meinem wissenschaftlichen Forschungsprojekt unterstützt haben und die am Gelingen dieser Arbeit beteiligt waren.
Mein besonderer Dank gilt Prof. Dr. Peer Wulff, ein großartiger Supervisor, für die wissenschaftliche und methodische Betreuung dieser Arbeit und den bereichernden und konstruktiven Austausch. Er ist nicht nur ein sehr guter Lehrer, sondern hatte auch immer ein offenes Ohr und unterstützte mich tatkräftig bei all meinen Ideen.
Ich danke Dr. Thomas Schiffelholz für die Begleitung im ersten halben Jahr. Er hat das Setup maßgeblich aufgebaut, die EEG recordings etabliert und mich so außerordentlich in der Anfangszeit unterstützt.
Meiner Arbeitsgruppe am physiologischen Institut danke ich für die anhaltende Hilfsbereitschaft und die vielen wertvollen Anregungen und Gespräche. Hervorzuheben sind Gilda Baccini, Annetrude de Mooij und Angelica Foggetti, die mir stets mit Rat und Tat zur Seite standen und aktiv bei der Durchführung der Experimente halfen. Bei ausgedehnten Mittags- und zahlreichen Kaffeepausen diskutierten wir nicht nur lautstark über Wissenschaft, sondern auch über zahlreiche andere interessante und weltbewegende Fragestellungen. Des Weiteren war Annetrude eine wunderbare Ersatzbetreuerin, die ich sehr im Labor vermissen werde. Kerstin Kronenbitter danke ich für lange Online-Shoppingtouren und der Hilfe bei der Durchführung vieler Experimente.
Bei Prof. Dr. Regina Scherließ möchte ich mich sehr herzlich für Ihre hilfsbereite Unterstützung bei der HPLC-Analyse und der wissenschaftlichen Betreuung als Zweitgutachterin bedanken. Im Besonderen gilt der Dank Hannah Göttsche für die umfangreichen fachlichen Gespräche und die angenehme Zusammenarbeit.
Allen Mitstreiter*innen des Graduiertenkollegs Materials for Brain danke ich für den intensiven wissenschaftlichen Austausch. Hier möchte ich Vivian Adamski, Igor Barg, Florian Rasch und Christina Schmitt nennen, die nicht nur tolle Kolleg*innen waren, sondern auch zu Freund*innen wurden. Mein ausdrücklicher Dank gilt Igor, der mit seiner ruhigen Art stets eine hilfsbereite Stütze war.
Ich möchte meinen engen Freund*innen danken, die mich durch Höhen und Tiefen dieser Arbeit begleiteten und trotz monatelange Distanz Verständnis für mich hatten. Swantje Falcke tausend Dank dafür, dass du die Herausforderungen dieser Arbeit stets nachvollziehen konntest und ein offenes Ohr hattest. Charlotte Irene Thompson möchte ich für alle Telefonate und tiefgehenden Impulse in den letzten Monaten danken. Rahel

Jacobs danke ich für alle hitzigen Diskussionen auf den angenehm ausgleichenden Spaziergängen. Tief verbunden und sehr dankbar bin ich meiner Freundin, Lena Holzapfel, für ihre Unterstützung, ihre Zuversicht und ihren unermüdlichen Kampf mir die deutsche Rechtschreibung und Zeichensetzung zu lehren.
Ganz herzlich möchte ich meiner Familie aus Kiel und Wiesbaden danken, die mir geduldig und fürsorglich zur Seite standen. Ulla Ellersdorfer danke ich für alle inspirierenden Gespräche, die mir sehr viel bedeuten.
Bei meinen Eltern Bettina Buschhoff, Sebastian Meyer und Wieland Buschhoff möchte ich mich ganz besonders für die liebevolle und konstruktive Unterstützung auf meinem Lebensweg bedanken.

Eidesstattliche Erklärung

Hiermit erkläre ich an Eides statt, dass ich die vorliegende Dissertation, abgesehen von der Beratung durch meinen akademischen Betreuer, nach Inhalt und Form selbstständig verfasst und keine anderen als die angegebenen Quellen und Hilfsmittel benutzt habe. Des Weiteren versichere ich, dass die Arbeit unter Einhaltung der Regeln guter wissenschaftlicher Praxis der Deutschen Forschungsgemeinschaft entstanden ist und alle Ausführungen, die anderen Schriften wörtlich oder sinngemäß entnommen wurden, kenntlich gemacht sind. Diese Dissertation wurde weder im Ganzen, noch zum Teil an anderer Stelle in einem Prüfungsverfahren vorgelegt, veröffentlicht oder zur Veröffentlichung eingereicht. Zusätzlich bekräftige ich, dass mir kein akademischer Grad entzogen wurde. Die gedruckte Form stimmt mit der elektronischen Form überein.

Kiel, den Anna-Sophia Buschhoff